Interplay Between Dbf4-Dependent Cdc7 Kinase and Polo-like Kinase Unshackles Mitotic Recombination Mechanisms by Promoting Synaptonemal Complex Disassembly

Bilge Argunhan

Thesis submitted for the degree of Doctor of Philosophy

University of Sussex

December 2015

UNIVERSITY OF SUSSEX

BILGE ARGUNHAN

THESIS SUBMITTED FOR THE DEGREE OF DOCTOR OF PHILOSOPHY
BIOCHEMISTRY

INTERPLAY BETWEEN DBF4-DEPENDENT CDC7 KINASE AND POLO-LIKE KINASE UNSHACKLES MITOTIC RECOMBINATION MECHANISMS BY PROMOTING SYNAPTONEMAL COMPLEX DISASSEMBLY

Meiotic recombination is initiated by self-inflicted DNA breaks and primarily involves homologous chromosomes, whereas mitotic recombination involves sister chromatids. Whilst the mitotic recombinase Rad51 exists during meiosis, its activity is suppressed in favour of the meiosis-specific recombinase, Dmc1, thus establishing a meiosis-specific mode of homologous recombination (HR). A key contributor to the suppression of Rad51 activity is the synaptonemal complex (SC), a meiosis-specific chromosomal structure that adheres homologous chromosomes along their entire lengths. Here, in budding yeast, we show that two major cell cycle kinases, Dbf4-dependent Cdc7 kinase (DDK) and Polo-kinase (Cdc5), collaborate to link the mode change of HR to the meiotic cell cycle by. This regulation of HR is through the SC. During prophase I, DDK is shown to maintain SC integrity and thus inhibition of Rad51. Cdc5, which is produced during the prophase I/metaphase I transition, interacts with DDK to cooperatively destroy the SC and remove Rad51 inhibition. By enhancing the interaction between DDK and Cdc5 or depleting DDK at late prophase I, meiotic DNA breaks are repaired even in the absence of Dmc1 by utilising Rad51. We propose that the interplay between DDK and Polo-kinase reactivates mitotic HR mechanisms to ensure complete repair of DNA breaks before meiotic chromosome segregation.

Acknowledgements

I would firstly like to thank by supervisor and mentor, Dr Hideo Tsubouchi. Not only did he give me the opportunity to conduct this work, but he inspired and motivated me throughout the four years that I was in his lab. Words cannot reasonably express my gratitude to him for standing as a true scientist and educator in a time when imposters roam freely. It is not an exaggeration to say that he has had an everlasting impact on my life. Thank you Sensei.

Secondly, I would like to thank all of my family and friends for the support they have given me during the last four years. I have nothing but the utmost respect and admiration for my sister and mother, who both believed in me even when my own faith waivered. I bow humbly to my wife, who happily joined me in the trenches, and thank her family for their trust and support. Salutations to my friends who made countless visits to Brighton; I hope the times we shared were as valuable to you as they were for me.

Finally, I would like to express my gratitude to my colleagues. Without your daily encouragement, the battle would likely have been lost a long time ago. For those of you that are in the thick of it, I implore you to persevere because it is well and truly worth it. I would also like to extend special thanks to Professor Antony Carr, whose guidance and advice has helped to shape my future.

Contents

Abbreviations

bp - base pairs

BSA - bovine serum albumin

dH_2O - distilled water

dNTP - deoxyribonucleotide triphosphate

dCTP - deoxycytidine triphosphate

DSB - double-strand break

dsDNA - double-stranded DNA

DTT - dithiothreitol

EDTA - ethylenediaminetetraacetic acid

HEPES - 4-(2-Hydroxyethyl)piperazine-1-ethanesulfonic acid

HU - hydroxyurea

IPTG - isopropyl beta-D-1-thiogalactopyranoside

MES - 2-(N-morpholino)ethanesulfonic acid hydrate

NaOH - sodium hydroxide

OD_{600} - optical density at 600 nm

ORF - open reading frame

PAGE - polyacrylamide gel electrophoresis

PBD - polo-box domain

PBS - phosphate-buffered saline

PEG - polyethylene glycol

PMSF - phenylmethansulfonyl fluoride

PFA - paraformaldehyde

RPM - revolutions per minute

SDS - sodium dodecyl sulphate

ssDNA - single-stranded DNA

TAE - Tris-acetate-EDTA

TBE - Tris-borate-EDTA

TCA - trichloroacetic acid

TCEP - Tris(2-carboxyethyl)phosphine

TE - Tris-EDTA

UTR - untranslated region

WT - wild type

List of Figures and Tables

Chapter 1: Introduction

Meiosis is central to the life cycle of sexually reproducing organisms. By coupling one DNA replication event to two tandem nuclear divisions, meiosis reduces the ploidy of a parent cell by exactly half. Consequently, for diploids such as humans, the resulting daughter cells have only one full set of chromosomes i.e., are haploid. Following fertilisation, the ploidy level is restored to the diploid state and the zygote is able to grow mitotically to give rise to a new individual. Upon reaching reproductive maturity, this new individual will then produce haploid gametes via meiosis.

The first division of meiosis, meiosis I, is called a reductional division. During meiosis I, homologous chromosomes are separated to opposite poles of the cell. The second division of meiosis, meiosis II, is called an equational division. Meiosis II is mechanistically similar to mitosis in that sister chromatids are separated. Although the DNA content is halved during both divisions, the reduction in ploidy takes place in meiosis I.

There are numerous specialised processes during meiosis I that facilitate the reduction of ploidy (Petronczki et al., 2003). Firstly, reciprocal recombination between nonsister chromatids of homologous chromosomes leads to the formation of physical linkages known as chiasmata. Ultimately, this reshuffling of chromosomal content generates genetic diversity upon which natural selection can act, but the immediate benefit of this recombination is that homologous chromosome pairs (homologues) act as a single unit and are able to align correctly on the metaphase plate during metaphase I. Secondly, the kinetochores of sister chromatids attach to spindles from the same pole through a process known as monoorientation. Conversely, the kinetochores of

homologues attach to spindles from opposite poles of the cells (i.e., they undergo biorientation). Thus, homologous chromosomes as opposed to sister chromatids come under tension during meiosis I, as spindles tug on maternal and paternal chromosomes. Thirdly, arm cohesion but not centromeric cohesion is destroyed at the onset of anaphase I. When combined with the resolution of chiasmata as crossover or noncrossover products, this liberates homologues from one another and leads to their separation in anaphase I (Youds & Boulton, 2011). Importantly, centromeric cohesin is maintained until the onset of anaphase II, where its destruction allows for the separation of sister chromatids. Thus, meiosis prevents the number of chromosome sets from doubling upon fertilisation and maintains the ploidy of a species with each successive generation (**Figure 1.1**).

Homologous recombination (HR) is integral to the aims of meiosis. In comparison to the recombination that takes place in mitotic cells, meiotic HR occurs in the context of a meiosis-specific proteinaceous structure known as the synaptonemal complex (SC). The SC adheres homologues along their lengths and components of the SC promote HR specifically between homologous chromosomes as opposed to sister chromatids (Lao & Hunter, 2010). Meiotic HR is induced in early prophase I by self-inflicted DNA double-strand breaks (de Massy, 2013). It is paramount that all double-strand breaks (DSBs) are repaired before chromosomes migrate to the metaphase plate and segregate at anaphase I, since any acentric chromosomal fragments will not segregate correctly, leading to the production of gametes lacking potentially essential genetic material (Gerton & Hawley, 2005). The existence of a so-called recombination checkpoint (also known as the pachytene checkpoint) enforces

Figure 1.1. Meiosis is a specialised cell division that generates unique cells with half the complement of chromosomes.

From left to right. The nucleus of a diploid cell in the G1 phase of the cell cycle is shown. **(1)** By the end of S phase, chromosomes are replicated and organised as closely associated sister chromatids. During mitosis, identical sister chromatids undergo biorientation and are pulled to opposite poles of the cell **(2)**; thus, the partitioning of two identical sets of chromosomes results in daughter cells that are genetically identical to the mother cell. In contrast, meiosis consists of two tandem divisions. Prior to the first division, homologous chromosomes pair and exchange genetic material, resulting in the monoorientation of sister chromatids and separation of homologous chromosomes **(3)**. During the mitosis-like second division, sister chromatids undergo biorientation and are pulled to opposite poles of the cell **(4)**. As a consequence of the genetic exchange and specialised mode of chromosome separation, meiosis produces four haploid cells with unique DNA content.

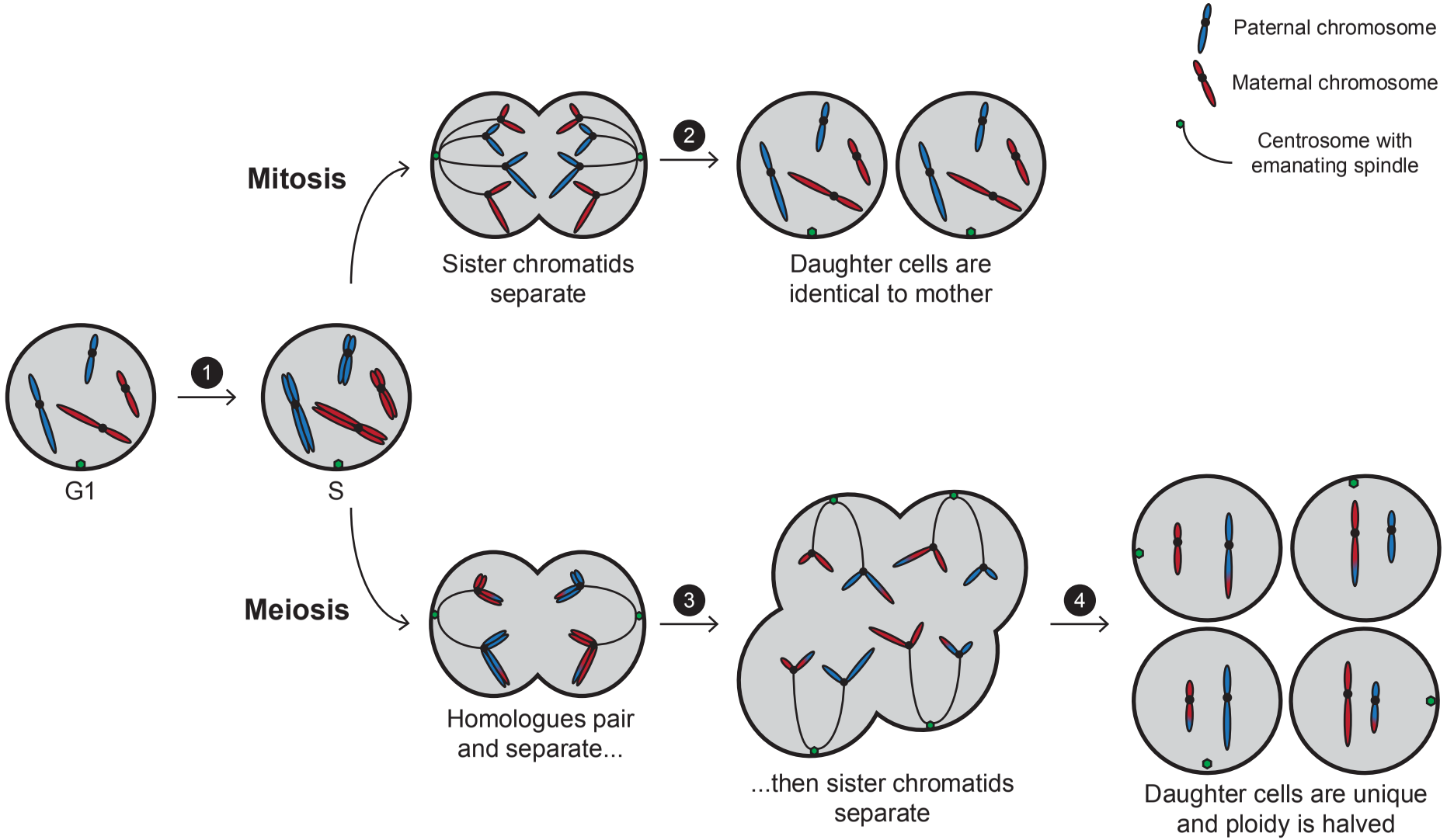
Paternal chromosome
Maternal chromosome
Centrosome with emanating spindle
Mitosis
Sister chromatids separate
Daughter cells are identical to mother
G1
S
Meiosis
Homologues pair and separate...
...then sister chromatids separate
Daughter cells are unique and ploidy is halved
1
2
3
4

cell cycle arrest at the end of the pachytene stage of prophase I in cells with unrepaired DSBs, thus coordinating HR with the meiotic cell cycle.

Throughout this chapter, I will introduce the concepts and summarise the literature that is key to understanding the logic of the experiments and interpretation of the results presented herein. It is beyond the scope of this introduction to describe in detail all of the key contributors to the unique chromosome segregation pattern seen in meiosis I, which were briefly summarised above. Instead, this introduction will focus mainly on the events that occur during prophase I, which is where the SC is formed and HR takes place.

Prophase I is substantially longer than prophase II or mitotic prophase. Hence, prophase I can be subdivided into five stages: leptotene, zygotene, pachytene, diplotene, diakinesis. The first four stages are of particular interest to this thesis and are associated with the following phenomena (Gerton & Hawley, 2005):

- Leptotene - HR is initiated through self-inflicted DSB formation
- Zygotene - the developing SC structure becomes cytologically detectable
- Pachytene - the SC structure is fully mature and stable recombination intermediates form
- Diplotene - the SC is destroyed and chiasmata become visible

For simplicity, leptotene/zygotene will be referred to interchangeably as early prophase I and pachytene/diplotene will be referred to interchangeably as mid/late prophase I throughout this thesis. In the interests of the reader, **Table 1** provides a list of budding yeast proteins and their homologues.

Table 1. Homologues of proteins relevant to this study.

Homologues based on protein function are listed for proteins involved in cell cycle regulation, homologous recombination or meiosis. *It is not possible to study meiosis using conventional human tissue culture techniques. More commonly, the mouse is utilised as a model for studying meiosis in higher eukaryotes. Thus, for numerous proteins, the mouse homologue has been included instead of the human homologue. *Hs*, *Homo sapien* protein. *Mm*, *Mus musculus* protein. Question mark indicates possible homology.

Table 1

	Budding yeast	**Fission yeast**	**Higher eukaryote***
***S. cerevisiae* biological function**	***S. cerevisiae***	***S. pombe***	***Homo sapien / Mus musculus***
DDK regulatory subunit	Dbf4	Dfp1	ASK1, *Hs*
DDK catalytic subunit	Cdc7	Hsk1	CDC7, *Hs*
Polo-like kinase	Cdc5	Plo1	PLK1, *Hs*
Meiotic DSB induction	Spo11	Rec12	SPO11, *Mm*
Meiotic DSB induction	Ski8	Rec14	WDR61, *Mm*
Meiotic DSB induction	Rec102	-	-
Meiotic DSB induction	Rec104	-	-
Meiotic DSB induction	Rec114	Rec7	REC114, *nt*
Meiotic DSB induction	Mei4	Rec24	MEI4, *Mm*
Meiotic DSB induction	Mer2	Rec15	-
Synaptonemal complex	Hop1	Hop1	HORMAD1, *Mm*
Synaptonemal complex	Mek1	Mek1	MAP2K1?, *Hs*
Synaptonemal complex	Red1	Rec10	SYCP2/SYCP3?, *Mm*
Synaptonemal complex	Zip1	-	SYCP1, *Mm*
DSB end resection	Sae2	Ctp1	CtIP, *Hs*
3'-5' Exonuclease	Mre11-Rad50-Xrs2	Mre11-Rad51-Nbs1	MRE11-RAD50-NBS1, *Hs*
5'-3' Exonuclease	Exo1	Exo1	EXO1
ssDNA binding protein	RPA	RPA	RPA
Mitotic recombinase	Rad51	Rad51	RAD51, *Hs*
Meiotic recombinase	Dmc1	Dmc1	DMC1, *Hs*
Meiotic HR protein	Hed1	-	-
Meiotic HR protein	Hop2	-	HOP2, *Mm*
Meiotic HR protein	Mnd1	Mcp7?	MND1, *Mm*
Meiotic HR protein	Mei5	Sfr1	SFR1, *Mm*
Meiotic HR protein	Sae3	Swi5	SWI5, *Mm*
Crossover protein	Mer3	-	HFM1, *Hs*
Crossover protein	Msh4	-	MSH4, *Mm*
Crossover protein	Msh5	-	MSH5, *Mm*
Crossover protein	Zip2	-	-
Crossover protein	Zip3	-	-
Crossover protein	Zip4	-	-
Checkpoint protein	Rad17	Rad9	RAD9, *Hs*
Checkpoint protein	Rad24	Rad17	RAD17, *Hs*
Checkpoint protein	Mec1	Rad3	ATR, *Hs*
Checkpoint protein	Tel1	Tel1	ATM, *Hs*
Meiotic transcription factor	Ndt80	-	-
AAA ATPase	Pch2	-	TRIP13, *Mm*
Endonuclease complex	Mus81-Mms4	Mus81-Eme1	MUS81-EME1, *Hs*

1.1 Initiation of homologous recombination and the meiotic cell cycle

Genome instability is a major cause of diseases such as premature aging and cancer (Hoeijmakers, 2001). The DNA of clonally dividing cells is subjected to constant assault from both exogenous (e.g., UV rays from the sun) and endogenous (e.g., production of free radicals from cellular metabolism) sources. It is likely due to the existence of an armamentarium of DNA repair pathways that the majority of humans do not suffer the consequences of DNA damage until old age. The very existence of these pathways, and their conservation amongst vastly diverged species, highlights the selection pressure and hence the importance of maintaining genome stability (Aguilera & Gómez-González, 2008). Thus, the idea of inducing ~150 self-inflicted DSBs across the genome seems preposterous, yet this is precisely how meiotic HR is initiated in a variety of species, including the budding yeast *Saccharomyces cerevisiae* and mice (de Massy, 2013). The risk associated with this programmed HR initiation in meiotic cells is a testament to the importance of chiasmata formation.

Programmed DSB formation initiates HR during early prophase I, once DNA has been replicated. The catalytic component of the DSB forming machinery is Spo11, a meiosis-specific type II topoisomerase-like enzyme (Keeney et al., 1997). Befitting of its central role in meiotic DSB formation, *SPO11* was one of the first genes identified as being essential for DSB formation (Klapholz et al., 1985). During the process of DSB formation, Spo11 forms a phosphodiester linkage with the phosphodiester backbone of the DNA, occupying the 5' strands at the break site and releasing the 3' strands that eventually act as substrates for the HR reaction (Keeney et al., 1997).

Since the discovery and biochemical characterisation of Spo11, numerous accessory proteins required for DSB formation have been identified in *S. cerevisiae*. Although the Mre11-Rad50-Xrs2 (MRX) complex has well characterised and highly conserved roles in DNA end resection (Bernstein & Rothstein, 2009), it was shown to be required for DSB formation in meiosis (Usui et al., 1998). Interestingly, the MRX complex is not the only member of the DSB formation machinery with established roles in other molecular processes. In addition to its roles in RNA metabolism, Ski8 was shown to interact with Spo11, and in the absence of Ski8, spore viability was reduced to <1% (>95% in wild type), likely due to an inability to stabilise the Spo11-DNA complex (Arora et al., 2004). In addition to Ski8, Rec102 was shown to coimmunoprecipitate with both Rec104 and Spo11 (Jiao et al., 2003), and combining hypomorphic alleles of *REC102* and *SPO11* lead to a synergistic reduction in DSB formation (Kee & Keeney, 2002). Consistent with the notion that Rec102 and Rec104 are required for DSB formation, both proteins were shown to localise to meiotic chromosomes at or before leptotene, which is when DSB formation is initiated (Kee et al., 2004). Despite these findings, the precise role of the Rec102-Rec104 complex in DSB formation remains to be determined.

In addition to the MRX, Spo11-Ski8, and Rec102-Rec104 complexes, Rec114, Mei4, and Mer2 were shown to coimmunoprecipitate as a complex that is also essential for DSB formation (Li et al., 2006). Mer2 foci was shown to peak during the leptotene stage of prophase I, with ~60% of each individual complex component showing colocalisation with the other two components (Li et al., 2006). Intriguingly, the localisation of this complex to meiotic

chromosomes was shown to be independent of other DSB forming proteins (Li et al., 2006).

It is paramount that DSBs are not induced before the completion of premeiotic DNA replication, as such DNA damage would massively compromise the fidelity of DNA replication. The first evidence that such regulation takes place was provided by specifically deleting the three major origins of replication on the left arm of chromosome III and measuring DSB formation on both arms (Borde et al., 2000). The authors showed by two-dimensional gel electrophoresis that replication of the left arm, which occurs due to a replication fork that traverses the centromere, was delayed; importantly, there was an equivalent delay in DSB formation only on the left arm. This result was confirmed by artificially delaying replication through the ectopic integration of a telomeric sequence (Borde et al., 2000). A notable conclusion of this study is the finding that DNA replication is linked to DSB formation locally, not globally i.e., the entire genome does not need to be replicated before DSB formation is induced.

As in mitotic DNA replication, the only cyclin-dependent kinase (CDK) in budding yeast, Cdc28 (homologue of human CDK1), is essential for premeiotic DNA replication (Benjamin et al., 2003). Since Borde et al. (2000) showed that DNA replication and meiotic DSB formation are linked, the possibility that Cdc28 activity itself is required for DSB formation was explored. Indeed, Cdc28 was shown to phosphorylate Mer2 primarily on Ser30 but also to some extent on Ser271 (Henderson et al., 2006). In the absence of this phosphorylation, meiotic DSBs were virtually non-existent, similar to the phenotype of the *mer2Δ* mutant. These findings raised the possibility that Mer2 is a prime candidate for

coordinating DNA replication with DSB formation. Similarly to Cdc28, the cell cycle regulator Dbf4-dependent Cdc7 kinase (DDK), which is also required for DNA replication in mitotic cells, is required for premeiotic replication (Valentin et al., 2006). Whereas the conditional depletion of DDK activity by the Tet-off system before induction into meiosis permitted premeiotic DNA replication, the resulting meiosis was massively defective, with ~60% of cells failing to complete nuclear divisions (Valentin et al., 2006). In contrast, when DDK activity was depleted at later time points (e.g., 2 hours into meiosis), both premeiotic DNA replication and meiosis were unaffected. These findings suggested that DDK activity is required for early meiotic events, with more activity being required than for premeiotic replication.

Consistent with the work of Valentin et al. (2006), DDK was later shown to be essential for meiotic DSB formation (Sasanuma et al., 2008; Wan et al., 2008). Interestingly, DDK phosphorylates Mer2 on Ser29, adjacent to the Cdc28 target Ser30; phosphorylation of both sites is essential for DSB formation and spore viability (Sasanuma et al., 2008; Wan et al., 2008). When combined with its essential role in meiotic DSB formation, the regulation of Mer2 function by the cell cycle kinases Cdc28 and DDK suggests that Mer2 may be a key protein in coordinating DNA replication with meiotic DSB formation. In agreement with this possibility, Mer2 formed chromatin associated foci even before meiotic entry (Henderson et al., 2006). A model was proposed in which Cdc28 and DDK are recruited to a given chromatin associated Mer2 molecule(s) only after the replication fork has passed it, resulting in phosphorylation of Mer2 and subsequent induction of meiotic DSB formation (Murakami & Keeney, 2008). This model postulates that, due to the cyclic

nature of Dbf4 production, DDK activity increases throughout the cell cycle, starting in S-phase and peaking in meiosis. As such, the progression of replication forks coincides with increasing DDK activity, so that chromatin associated Mer2 is only likely to be phosphorylated after the replication fork has passed. However, there was little empirical data to verify this hypothesis. Two key experiments have since provided mechanistic insight to support this model (Murakami & Keeney, 2014). First, by utilizing the system created by Borde et al. (2000) where deletion of the origins on the left arm of chromosome III delays replication of the left arm and is accompanied by an equivalent delay in local DSB formation, Murakami and Keeney (2014) showed that increasing DDK activity by overexpression of both subunits eliminated the delay in DSB formation. Second, Dbf4 was shown to weakly coimmunoprecipitate with Tof1, a component of replisomes, raising the possibility that the Dbf4-Tof1 interaction is important for the coordination of DNA replication and meiotic DSB formation. In support of this, deletion of *TOF1* eliminated the difference in meiotic DSB formation between the originless left arm and the WT right arm, despite retaining the delay in replication. The in-frame fusion of Dbf4 with Cdc45, another replisome component, partially rescued the coordination of replication with DSB formation in the absence of Tof1, suggesting that the recruitment of DDK to replication forks is essential for this coordination.

1.2 Homologous recombination and the synaptonemal complex

DSBs are crucial for the initiation of meiotic HR. In addition to the discussed proteins, which are considered to be part of the DSB formation machinery, several structural elements of meiotic chromosomes are essential for WT levels

of DSB formation. Hop1, Red1, and Mek1 interact to form the cores of meiotic chromosome axes (Hollingsworth et al., 1990; Smith & Roeder, 1997; Bailis & Roeder, 1998). Referred to as axial elements, these structures are called lateral elements once they are incorporated into the SC (Page & Hawley, 2004). Interestingly, meiotic DSB formation was shown to be reduced by varying degrees in the absence of any of the three proteins (Xu et al., 1997; Woltering et al., 2000). Thus, chromosomal structure is crucial for supporting WT levels of meiotic DSB formation.

The basic model of DSB repair by HR has remained mostly unchanged over the last ~30 years (Szostak et al., 1983). Following DSB formation, DSB ends are resected in a 5' to 3' direction (Sun et al., 1991). As in mitotic cells, meiotic end resection is dependent on the combined activities of MRX and Exo1 (Tsubouchi & Ogawa, 1998; Tsubouchi & Ogawa, 2000). Unlike DNA ends that arise as a consequence of spontaneous DSB formation, scheduled DSB formation in meiosis results in DNA ends that are covalently bound to Spo11, which must be removed before resection can take place (Keeney et al., 1997). The removal of Spo11 is achieved through nicking of the covalently attached DNA, resulting in the release of Spo11-oligo fragments (Neale et al., 2005). Importantly, the release of these Spo11-oligo fragments is dependent on Sae2 (Neale et al., 2005), which is likely involved in eliciting a dsDNA endonuclease activity from the MRX complex (Cannavo & Cejka 2014), with subsequent resection proceeding bidirectionally through the coordinated activities of Mre11 and Exo1 (Garcia et al., 2011).

Following DSB end resection, the resulting 3' single-stranded tails are coated with replication protein A (RPA) and recombinases (enzymes that

catalyse strand exchange), of which there are two in meiosis: Rad51 and Dmc1 (Krogh & Symington, 2004). Whereas Rad51 is required for both mitotic and meiotic recombination, Dmc1 is only produced in meiosis and hence is only required for meiotic recombination (Bishop et al., 1992; Shinohara et al., 1992). Following strand invasion into the donor DNA molecule, structures known as single-end invasions are detectable and can lead to the formation of double Holliday junctions, or joint molecules, which are eventually resolved as noncrossovers or crossovers (Schwacha & Kleckner, 1995; Hunter & Kleckner, 2001). The molecular process of HR is depicted in **Figure 1.2**. A germane aspect of HR in meiosis is that these recombination events occur preferentially between homologous chromosomes (homologues) as opposed to sister chromatids (Schwacha & Kleckner, 1994), a phenomenon often referred to as the interhomologue recombination bias.

The question of why two recombinases are required for meiotic recombination is still unanswered. In the absence of Dmc1, cells arrest with unrepaired DSBs despite the presence of Rad51 (Bishop et al., 1992), pointing towards the existence of an inhibitory mechanism acting on Rad51. Axiomatically, these cells fail to form any detectable joint molecules or crossovers (Schwacha & Kleckner, 1997; Shinohara et al., 1997). In contrast, cells lacking Rad51 form interhomologue crossovers, although the appearance of these crossovers is delayed and their numbers are reduced compared to WT (Shinohara et al., 1997). In agreement with this, the numbers of interhomologue joint molecules relative to intersister joint molecules is reduced ~9-fold compared to WT (Schwacha & Kleckner, 1997), indicating that Rad51 is essential for interhomologue recombination. Additionally, both Dmc1 and Rad51

Figure 1.2. Homologous recombination during meiosis can yield crossover or noncrossover products.

Following arrows from left to right. A meiotic DSB is induced on the blue DNA duplex by Spo11 during leptotene. DSB formation also requires Ski8, Rec102-Rec104, Rec114-Mei4-Mer2, Mre11-Rad50-Xrs2 (MRX) and the combined activities of cyclin-dependent kinase and Dbf4-dependent Cdc7 kinase. During zygotene, homologous DNA molecules undergo extensive interactions. In combination with Sae2, MRX is able to remove covalently attached Spo11, and with the contribution of Exo1, 5'-3' end resection occurs, yielding 3' ssDNA overhangs. These overhangs are coated with RPA to remove any secondary structure, which would be inhibitory for homology searching. Rad51 and Dmc1 are able to displace RPA with assistance from Rad55-Rad57 and Mei5-Sae3, respectively, leading to the formation of the nucleoprotein filament, which invades an intact homologous DNA duplex and displaces the non-complementary strand. The resultant structure is referred to as a displacement loop (D-loop). Although not shown here, Rad52 is essential for the localisation of Rad51 to ssDNA. Following D-loop formation, further displacement of the non-complementary strand occurs due to the activities of Rad54, Rdh54 and Mer3, which facilitates extension of the invading 3' strand by DNA synthesis by the end of pachytene. **1)** The invading 3' strand undergoes some extension and re-anneals to the ssDNA at the opposite side of the DSB on the original DNA duplex. This is known as synthesis-dependent strand annealing. **2)** The invading strand undergoes extensive extension, allowing the displaced strand to capture the second-end of the DSB, leading to extension of the second 3' strand and formation of a double Holliday Junction (dHJ). Following exit from pachytene, the dHJ is resolved through the combined activities of Mus81-Mms4 and Yen1. These proteins are regulated by Cdc5. **3)** The left and right junctions are cleaved at the black scissors, leading to a noncrossover product. **4)** The left junction is cleaved at the black scissors and the right junction is cleaved at the green scissors, leading to a crossover. If only one junction is cleaved at the green scissors, a single crossover results. If both junctions are cleaved at the green scissors, a double crossover results.

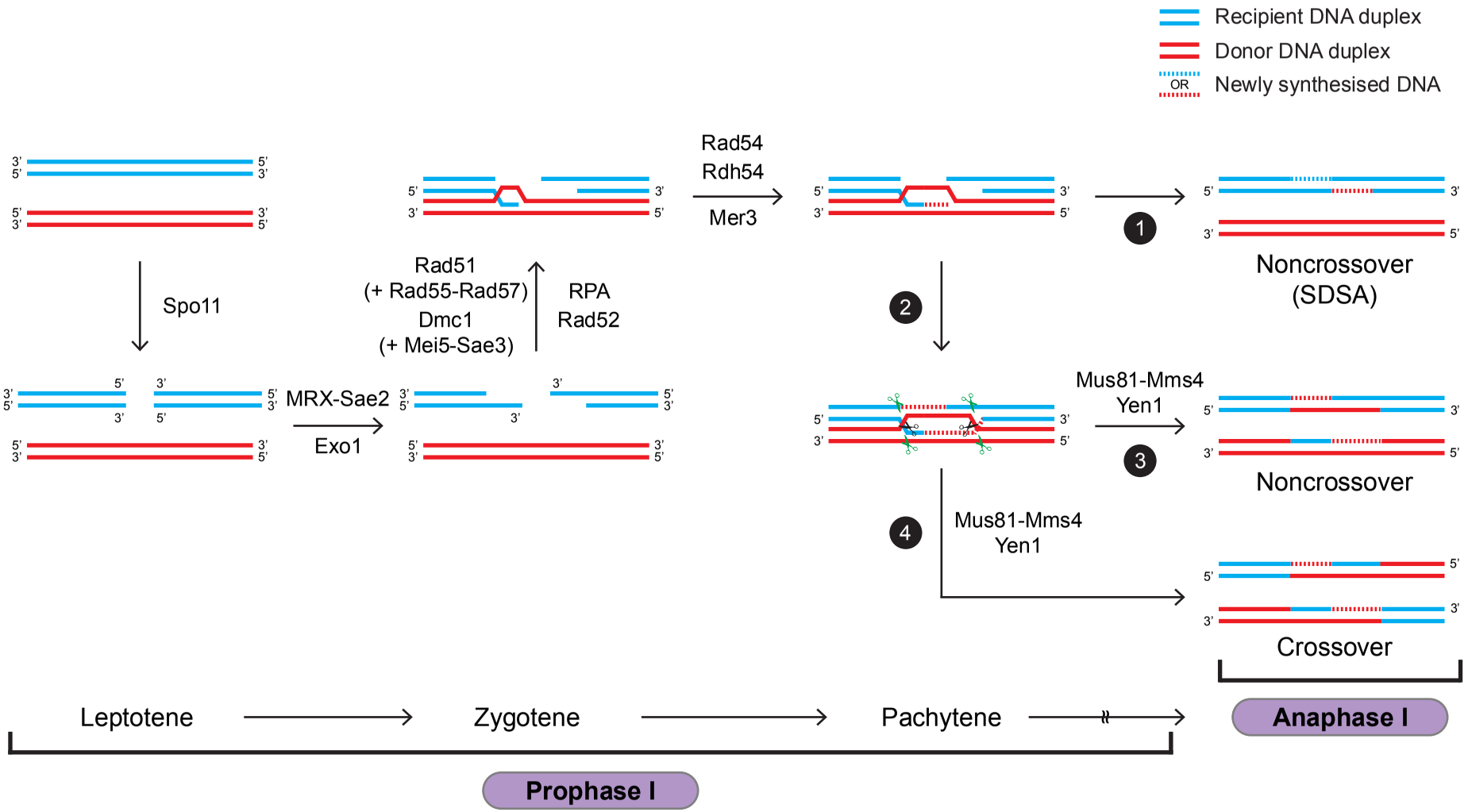
Recipient DNA duplex
Donor DNA duplex
OR
Newly synthesised DNA
Spo11
MRX-Sae2
Exo1
Rad51
(+ Rad55-Rad57)
Dmc1
(+ Mei5-Sae3)
RPA
Rad52
Rad54
Rdh54
Mer3
1
Noncrossover
(SDSA)
2
Mus81-Mms4
Yen1
3
Noncrossover
4
Mus81-Mms4
Yen1
Crossover
Leptotene
Zygotene
Pachytene
Prophase I
Anaphase I

are required for the early interactions between homologous chromosomes that lead to homologue pairing (Rockmill et al., 1995).

The differences in the meiotic phenotypes of *dmc1Δ* and *rad51Δ* strains has lead to the idea that the two recombinases play mechanistically distinct roles in meiotic HR, with Dmc1 preferentially catalysing interhomologue and Rad51 preferentially catalysing intersister recombination (Masson & West, 2001). The detection of Dmc1 foci by immunostaining was shown to be hampered by the absence of Rad51, such that Dmc1 foci were fainter without Rad51, whereas the formation of Rad51 foci was unaffected by the absence of Dmc1 (Bishop, 1994; Dresser et al., 1997; Shinohara et al., 1997). This finding suggests that Rad51 might play a supporting role in meiotic HR by targeting Dmc1 to sites of DSBs (Sheridan & Bishop, 2006), but any such targeting would likely be dependent on another protein(s) that interacts with both Dmc1 and Rad51, since Dresser et al. (1997) failed to detect any interaction between Dmc1 and Rad51 via yeast two-hybrid. Recent evidence has emerged supporting this model. Through separation-of-function analysis, it has been possible to generate a *RAD51* allele, referred to as *rad51-II3A*, encoding a recombinase that can bind DNA but is mostly defective for catalysis of strand invasion (Cloud et al., 2012). The authors showed that, while the formation of interhomologue joint molecules was severely reduced in the *rad51Δ* strain, they formed at WT levels in the *rad51-II3A* strain, suggesting that the catalytic activity of Rad51 is dispensable for meiotic HR. However, despite this evidence, it is pertinent to note that the Rad51-II3A protein retained some catalytic activity in vivo (Cloud et al., 2012) and the *rad51-II3A* strain had reduced spore viability (~87% compared to ~99% in WT), suggesting that Rad51-II3A is not

catalytically dead but still confers a reduction in spore viability. These findings point towards a catalytic role for Rad51 in meiotic HR. Consistently, it has been shown that overproduction of Rad51 can compensate for the spore inviability seen in *dmc1Δ* (Tsubouchi & Roeder, 2003), suggesting that Rad51 is able to catalytically compensate for the loss of Dmc1. Thus, the precise requirement for two recombinases in meiotic HR is still under scrutiny.

A novel mechanism of preferentially driving Dmc1-dependent HR was discovered relatively recently. *HED1* was identified as a multicopy suppressor of the spore inviability seen in *red1-22* mutants (Tsubouchi & Roeder, 2006). Deletion of *HED1* was shown to suppress the meiotic arrest and spore inviability of the *dmc1Δ* mutant, a phenotype that is reminiscent of Rad51 overproduction (Tsubouchi & Roeder, 2003). Importantly, the authors showed that *dmc1Δ hed1Δ* cells repaired their meiotic DSBs in a Rad51-dependent fashion to yield interhomologue crossovers, indicating that the meiosis-specific inhibition towards Rad51 had been lost in the absence of Hed1 (Tsubouchi & Roeder, 2006). Additionally, by abrogating the interaction between Rad51 and Rad54, Hed1 was shown to ablate the synergistic increase in activity of both Rad51 and Rad54 (Busygina et al., 2008). Interestingly, the interactions of Hed1 with itself and Rad51 were shown to be crucial in its ability to inhibit Rad51 activity in meiosis (Busygina et al., 2012). Thus, the discovery and characterisation of Hed1 has yielded compelling evidence that Hed1 is essential for enforcing the interhomologue recombination bias that exists in meiosis.

Meiotic HR is further complicated by the possibility of nonhomologous chromosomes synapsing, which could lead to missegregation of chromosomes and loss of genetic information. Importantly, meiosis-specific factors exist to

prohibit such interaction between nonhomologous chromosomes and promote Dmc1-dependent interhomologue HR. Hop2 was identified as a meiosis-specific protein that is essential for meiotic HR (Leu et al., 1998); in its absence, DSBs accumulate with hyperresected ends and superfluous recombinases are recruited to this ssDNA (Tsubouchi & Roeder, 2003; Henry et al., 2006). However, despite the localisation of both Rad51 and Dmc1 to chromosomes, DSBs are not repaired in *hop2Δ*, likely due to the fact that chromosome pairing is mostly between nonhomologous chromosomes (Tsubouchi & Roeder, 2003). One possible explanation for this is that due to the accumulation of recombinases in the absence of Hop2, promiscuous recombination between nonhomologous DNA sequences is initiated, leading to nonhomologous pairing. In support of this, Tsubouchi & Roeder (2003) showed that homologue pairing in *hop2Δ* is improved when it is combined with either *dmc1Δ* or *rad51Δ*. These functions of Hop2 are performed in complex with Mnd1 (Tsubouchi & Roeder, 2002).

In addition to Hop2-Mnd1, Mei5 and Sae3 have been shown to function in the Dmc1 pathway of HR (Tsubouchi & Roeder, 2004; Hayase et al., 2004). However, whereas Dmc1 is epistatic to Hop2-Mnd1, Mei5 and Sae3 are thought to function at the same stage of HR as Dmc1. In vitro experiments have shown that Rad55 and Rad57 function as a hetrerodimer to overcome the inhibitory presence of RPA on ssDNA to allow Rad51-dependent strand exchange (Sung, 1997). In an analogous manner, the Mei5-Sae3 heterodimer has been shown to perform the same function for Dmc1-dependent strand exchange (Ferrari et al., 2009). Thus, the complexities of meiotic HR are addressed by the activity of specialised, meiosis-specific HR machinery.

Meiotic chromosome structure is a key consideration when thinking about HR in meiosis. As chromatin condenses during early prophase I, chromosome become visible as individual entities and sister chromatids are organised together along axial elements. Following DSB formation, early interactions between homologous DNA sequences brings the axial elements of homologous chromosomes into close proximity to form axial associations (Page & Hawley, 2004). These interactions lead to the pairing of homologous chromosomes and the incorporation of the axial elements into the early SC structure as lateral elements (Page & Hawley, 2004). Lateral element proteins Hop1, Red1, and Mek1 play a crucial role in enforcing the interhomologue recombination bias in meiosis (Page & Hawley, 2004).

Hop1 was shown to be required for the formation of WT levels of crossovers but not for intrachromosomal recombination (Hollingsworth & Byers, 1989). Furthermore, phosphorylation of Hop1 was shown to be required for the formation of interhomologue crossovers (discussed later) (Carballo et al., 2008). Consistent with the notion that lateral element proteins are essential for interhomologue recombination, in the absence of Red1, interhomologue joint molecule formation was drastically reduced (Schwacha & Kleckner, 1997). More recently, it was shown that *red1Δ* cells display a proportional increase in intersister joint molecules, suggesting that the role of Red1 in enforcing the meiotic recombination bias is in converting the intersister recombination bias operating in mitotic cells into the interhomologue recombination bias that is characteristic of meiosis (Kim et al., 2010). Moreover, evidence exists to suggest that, in the absence of either Red1 or Mek1, the meiotic mode of HR is not established and the mitotic mode of HR predominates during meiosis (Hong

et al., 2013). This mitotic mode of HR is not only dependent on Rad51 activity, but also on Rad55 and Rad57, two accessory factors that promote Rad51-dependent strand exchange during mitotic HR (Hong et al., 2013).

Since *MEK1* was identified as encoding a meiosis-specific kinase (Rockmill & Roeder, 1991), an approach utilising conditional mutants that specifically abrogate the kinase activity of Mek1 has been employed. It is possible to enlarge the ATP-binding pocket of kinases by mutation of a residue, resulting in a kinase that irreversibly binds ATP analogues without hydrolysis and is thus deactivated. Importantly, in the absence of the analogue, these proteins can hydrolyse ATP and are otherwise WT. The alleles encoding these proteins are referred to as *-as* alleles (analogue sensitive). In the absence of Dmc1, cells undergo meiotic arrest with unrepaired DSBs, despite the presence of Rad51 (Bishop et al., 1992). However, if Mek1-as is inactivated through the addition of ATP analogue to the culture, *dmc1Δ* cells are able to repair their DSBs and complete meiosis (Wan et al., 2004). Furthermore, this DSB repair is dependent on Rad54, a protein that functions with Rad51 to repair DSBs using the sister chromatid as a template (Arbel et al., 1999; Niu et al., 2005). In support of a role for Mek1 in enforcing the interhomologue recombination bias, Rad54 was shown to be phosphorylated by Mek1 in meiosis, resulting in reduced Rad54-Rad51 complex formation and reduced Rad51 activity (Niu et al., 2009), thus contributing to the preferential usage of Dmc1.

The Hop1-dependent dimerization of Mek1 is thought to be required for autophosphorylation and subsequent activation of Mek1 (Niu et al., 2005). By GST-tagging Mek1, it is possible to artificially promote dimerization through the GST moiety of the protein, bypassing the requirement for Hop1 in Mek1

dimerization (Niu et al., 2005). In theory, Mek1 fused with GST should be more active than Mek1 alone. In support of this, GST-tagged Mek1 shows a specific reduction in the formation of intersister joint molecules, whereas interhomologue joint molecules are formed in comparable numbers to the untagged Mek1 strain (Wu et al., 2010). Taken together, these findings highlight the importance of lateral element proteins in establishing and enforcing the interhomologue recombination bias.

The central element of the SC is composed mainly of Zip1, a highly conserved coiled-coil protein (Sym et al., 1993; Sym & Roeder, 1995). In the absence of Zip1, there is no chromosome synapsis, resulting in a substantial reduction in the formation of crossovers despite WT levels of DSB formation (Sym et al., 1993; Xu et al., 1997). Interestingly, cells that lack Zip1 are still able to correctly pair homologous chromosomes (Rockmill et al., 1995), suggesting that the axial associations that take place before SC formation are sufficient to prevent nonhomologous chromosome pairing. Due to the requirement for Zip1 in the structural association of homologues, it is not yet known whether Zip1 contributes to the interhomologue recombination bias seen in meiosis, as deletion of *ZIP1* spatially discourages interhomologue interactions.

Zip1 belongs to a group of proteins known as ZMM, all of which are required for meiotic crossing over. ZMM proteins have been subdivided into three subgroups based on functional criteria (Lynn et al., 2007). Subgroup 1 consists of Mer3, Msh4 and Msh5. Mer3 is a helicase that is required for the progression of DSBs into crossovers (Nakagawa & Ogawa, 1999), with a role implicated in stimulating heteroduplex extension by Rad51 (and presumably Dmc1) (Mazina et al., 2004). Despite being identified as MutS homologues,

Msh4 and Msh5 were shown to be essential for reciprocal recombination in meiosis but dispensable for mismatch repair (Ross-Macdonald & Roeder, 1994) (Hollingsworth et al., 1995). Subgroup 2 consists of Zip2, Zip3 and Zip4. In early prophase, Zip1 is detectable as punctate foci and forms more continuous, linear staining elements as prophase progresses; these early foci show colocalisation with Zip2 and Zip2 is required for the development of linear Zip1 staining (Chua & Roeder, 1998). This finding raised the possibility that Zip2 is required for the initiation of synapsis. Although Zip3 colocalises with Zip2 and early Zip1 foci, defects in SC development are relatively mild in *zip3Δ* when compared to *zip2Δ* (Agarwal & Roeder, 2000). Furthermore, Zip3 shows some colocalisation and interacts with Mre11, suggesting that, in early prophase, Zip1, Zip2 and Zip3 all localise to certain DSBs to initiate SC formation. Zip4 colocalises with Zip2 and is also required for the transition of punctate Zip1 foci into linear Zip1 staining (Tsubouchi et al., 2006). Subgroup 3 consists solely of Zip1, which has been discussed above. In summary, ZMM proteins are all required for crossover formation and are thought to constitute synapsis initiation complexes that nucleate Zip1 assembly.

Relatively little is known about disassembly of the SC. As cells complete pachytene and enter the diplotene stage of prophase I, the SC disassembles and homologues remain connected only at chiasmata (Page & Hawley, 2004). It is crucial that this disassembly of the SC precedes chromosome segregation at anaphase I, as the proteinaceous SC structure could compromise the physical separation of chromosomes, potentially resulting in the formation of aneuploid gametes. A key advancement in our knowledge of SC disassembly was provided when the Ndt80-dependent induction of Cdc5, the only polo kinase in

budding yeast, was shown to be sufficient to disassemble the SC structure from meiotic chromosomes (Sourirajan & Lichten, 2008). Sourirajan & Lichten (2008) also showed that inhibition of Cdc28 activity leads to a small delay in SC breakdown, suggesting that perhaps CDK is also required to some extent for SC disassembly. It is not currently known how this process is regulated and whether other Ndt80-independent factors are involved.

1.3 The recombination checkpoint

Having discussed the importance of coordinating premeiotic DNA replication with the induction of DSBs, it is pertinent to discuss the coordination of DSB repair with the meiotic cell cycle. Early indications that a mechanism exists for this coordination came from the discovery that the mitotic checkpoint genes *RAD17*, *RAD24* and *MEC1* are required for the arrest of *dmc1Δ* cells (Lydall et al., 1996). Importantly, mutations that reduce/abolish DSB formation (e.g., *spo11Δ*) also allow *dmc1Δ* cells to sporulate, strongly suggesting that the checkpoint monitors the status of HR and/or chromosome synapsis (Roeder, 1997). In order to rule out the possibility that mutation of these checkpoint genes disrupts meiotic DSB formation, which would act in favour of cell cycle progression by reducing the amount of detectable damage, Lydall et al. (1996) showed by Southern blotting and immunofluorescence microscopy that *dmc1Δ* cells with mutations in *RAD17/RAD24/MEC1* accumulate DSBs and progress through meiosis without repairing these DSBs.

Interestingly, the mitotic components of the recombination checkpoint cooperate with meiosis-specific proteins to promote the meiotic mode of HR. The lateral element protein Hop1 was shown to be phosphorylated by the

checkpoint kinases Mec1 and Tel1 (Carballo et al., 2008). By mutating the relevant Ser/Thr residues to nonphosphorylatable Ala residues, the authors showed that, whereas phosphorylation was dispensable for meiotic DSB formation, it was critical in preventing Dmc1-independent DSB repair (Carballo et al., 2008). As expected, this Dmc1-independent DSB repair resulted in a substantial reduction of crossovers. Additionally, since phosphorylation of Hop1 was shown to be essential for inhibiting Dmc1-independent DSB repair, Hop1 phosphorylation is critical for checkpoint-enforced cell cycle arrest (Carballo et al., 2008). Thus, the meiotic mode of HR is enforced by a complex network of mitotic and meiotic factors that are regulated by the recombination checkpoint.

Early insight into how the recombination checkpoint is able to cause cell cycle arrest revealed the importance of canonical cell cycle regulators such as Cdc28. Phosphorylation of Cdc28 on Tyr19 is known to inhibit Cdc28 activity, and the only kinase known to phosphorylate this residue in budding yeast is the Swe1 kinase (Lew & Kornbluth, 1996). Whereas the *hop2Δ* mutant undergoes tight pachytene arrest with ~2% sporulation, the *hop2Δ swe1Δ* double mutant shows ~60% sporulation (Leu & Roeder, 1999). Consistent with the notion that deletion of *SWE1* leads to a loss of coordination between DSB repair and cell cycle progression, *hop2Δ swe1Δ* cells complete meiosis with unrepaired DSBs, leading to the production of inviable spores (Leu & Roeder, 1999). Interestingly, Leu et al. (1999) also showed that hyperphosphorylated Swe1 accumulates in the absence of Hop2. These findings suggest that 1) inhibitory phosphorylation of Cdc28 is required for a functional recombination checkpoint in meiosis and 2) phosphorylation of Cdc28 is mediated by Swe1, which itself is activated by phosphorylation in response to checkpoint activation. Taken together, these

data indicate that mechanisms regulating the DNA damage checkpoint in mitotic cells are conserved in meiotic cells.

In addition to sharing components with the mitotic checkpoint, the recombination checkpoint also comprises meiosis-specific elements. Commitment to meiosis is regulated by Ndt80, a meiosis-specific transcription factor that upregulates ~200 genes upon exit from pachytene (Xu et al., 1995; Chu & Herskowitz, 1998). In WT cells, Ndt80 is robustly upregulated upon pachytene exit, resulting in irreversible commitment to meiosis (Tsuchiya et al., 2014). However, in checkpoint arrested cells such as *hop2Δ*, the levels of Ndt80 are substantially lower (Tung et al., 2000). Moreover, Tung et al. (2000) showed that Ndt80 from WT cells is phosphorylated, whereas checkpoint arrested cells contain mostly unphosphorylated Ndt80. These findings suggest that Ndt80, the master regulator of meiotic commitment, is under the control of the recombination checkpoint. Only once the checkpoint has been deactivated is Ndt80 upregulated and subsequently phosphorylated.

Ndt80 is only one example of a meiosis-specific protein that regulates cell cycle progression. Another notable example is the Pch2 protein, which was initially isolated as a meiosis-specific protein that is required to maintain the arrest of cells lacking Zip1, Zip2 or Dmc1 (San-Segundo & Roeder, 1999). Cells lacking Pch2 or Rad17 exhibit a delay in the cell cycle that is dependent on Rad17 or Pch2, respectively, as the *pch2Δ rad17Δ* double mutant completes the first meiotic division faster than WT and at the same rate as *spo11Δ* (Wu & Burgess, 2006), in which the checkpoint is not activated due to the absence of DSBs. This finding suggests that Pch2 is capable of delaying cell cycle progression independently of the recombination checkpoint per se. However,

caution must be exercised when interpreting this data since recent evidence suggests that Pch2 is required for WT levels of DSB formation (Farmer et al., 2012), so the accelerated cell cycle progression seen in *pch2Δ rad17Δ* could be partially explained by reduced DSB formation in the absence of Pch2.

In comparison to our knowledge of meiotic DSB formation, relatively little is known about how this process, once initiated, is regulated. More recently, evidence has emerged indicating that the recombination checkpoint participates in the regulation of DSB formation. Whereas the Mec1 branch of the DNA damage checkpoint was shown to downregulate DSB formation, the Tel1 branch was shown to upregulate DSB formation specifically on larger chromosomes (this thesis: (Argunhan et al., 2013))(Gray et al., 2013). Moreover, an essential component of the DSB formation machinery, Rec114, was shown to be phosphorylated in a DSB- and Mec1/Tel1-dependent manner (Carballo et al., 2013). Interestingly, cells expressing the phosphomimetic Rec114-8D protein showed a reduction in DSB formation, whereas cells expressing the nonphosphorylatable Rec114-8A protein showed a mild increase in DSB formation (Carballo et al., 2013), suggesting that the checkpoint can downregulate or upregulate DSB formation by phosphorylating or dephosphorylating Rec114, respectively.

Whereas Mec1 is thought to respond primarily to resected DSB ends, Tel1 is thought to respond to unresected DSB ends (Lydall et al., 1996; Usui et al., 2001). Thus, it is relevant to note that the effects on DSB formation reported by Carballo et al. (2013) were mostly lost when the background was switched from *sae2Δ*, which accumulates unresected DSB ends, to *dmc1Δ*, which accumulates hyperresected DSB ends. This consideration raises the possibility

that regulation of DSB formation through Rec114 might occur predominantly by Tel1. Although these emerging roles in regulating meiotic DSB formation have contributed to our knowledge of the recombination checkpoint, there is still much to be learned about how the checkpoint regulates different aspects of meiotic HR and synapsis, with some suggestions that these phenomena are detected by different branches of the checkpoint or by different checkpoints altogether (Hochwagen & Amon, 2006).

1.4 Meiotic roles of Dbf4-dependent Cdc7 kinase (DDK)

DDK is composed of two subunits, both of which are essential in budding yeast: Dbf4 and Cdc7. The relationship between Dbf4 and Cdc7 has been compared to that between cyclins and CDKs, due to the relatively constant levels of the catalytic subunit (Cdc7/CDK) and the cyclic production of the regulatory subunit (Dbf4/cyclin) (Sclafani, 2000). Here, I will briefly introduce the essential role of DDK in mitotic growth before discussing what is known about the meiotic roles of DDK.

Both Dbf4 and Cdc7 subunits are essential for the G1-S transition and overproduction of Dbf4 can supress cell cycle arrest in the temperature sensitive *cdc7-1* mutant but not in the *cdc7Δ* mutant (Kitada et al., 1992). In support of the notion that Dbf4 regulates Cdc7 activity, DDK immunoprecipitated from yeast cultures expressing the temperature sensitive Dbf4-1 protein was shown to have substantially less kinase activity than DDK with WT Dbf4 only when the assay was performed at the restrictive temperature (Jackson et al., 1993). These studies indicated that DDK activity is required for the transition from G1 to S phase of the cell cycle.

The first indication that DDK is required for the initiation of DNA replication came from the finding that Dbf4 interacts with origins of replication (Dowell et al., 1994). Consistently, *CDC7* alleles with mutations in conserved kinase residues were shown to prevent DNA replication, suggesting that DDK activity is required for DNA replication (Ohtoshi et al., 1997). Accordingly, the presence of Cdc7 was shown to be required for the formation of a stable prereplicative complex, which includes the hexameric MCM helicase that is required for DNA unwinding (Sheu & Stillman, 2006). Moreover, the in vivo function of the Mcm4 subunit was shown to be dependent on DDK-dependent phosphorylation of the Mcm4 N-terminus (Sheu & Stillman, 2006). In addition to Mcm4, there is evidence that Mcm6, and to a lesser extent Mcm2, are also phosphorylated by DDK (Francis et al., 2009). Although the precise requirement for this phosphorylation remains unknown, there is evidence to suggest that the phosphorylation of Mcm4 by DDK alleviates an intrinsic property of Mcm4 that is counterproductive for DNA replication (Sheu & Stillman, 2010).

In contrast to its well established roles in initiating DNA replication, relatively little is known about the meiotic roles of DDK. The catalytic activity of DDK has been known to be essential for both mitosis and meiosis for ~25 years (Buck et al., 1991). As in mitotic cells, DDK was shown to be crucial for premeiotic DNA replication (Valentin et al., 2006). The role of DDK in regulating DSB formation was discussed in section **1.1** and, in the interests of brevity, will not be discussed here. In addition to DSB formation, DDK has a crucial role in ensuring monoorientation of sister chromatids at the first meiotic division (Marston, 2009). In the absence of DDK activity, meiosis results in the formation

of two diploid spores as opposed to four haploid spores due to a failure to separate homologous chromosomes during meiosis I (Matos et al., 2008).

In contrast to previous reports (Lo et al., 2008; Lo et al., 2012), Matos et al. (2008) showed that DDK is not essential for Ndt80 production or meiotic progression. One possible explanation for this difference is in the methods used to deplete the cells of DDK activity. Matos et al. (2008) utilised temperature sensitive alleles of *DBF4/CDC7* or deletions of *DBF4/CDC7* in conjunction with the *bob1* suppressor mutation that bypasses the requirement for DDK in replication (Hardy et al., 1997). In contrast, Lo et al. (2008, 2012) utilised the conditional *cdc7-as* allele (analogue sensitive) encoding a version of Cdc7 with an enlarged ATP binding pocket that renders the protein inactive only in the presence of an ATP analogue (Wan et al., 2006). Due to these discrepancies, the role of DDK as a transcriptional regulator of *NDT80* or members of the *NDT80* regulon requires further investigation. Evidence presented later in this thesis provides support for the findings of Matos et al. (2008) i.e., DDK is dispensable for the production of Ndt80 and commitment to meiosis.

A role for DDK in the removal of meiotic cohesin has also been demonstrated. Phosphorylation of Rec8, the meiosis-specific paralogue of cohesin subunit Scc1, is essential for the removal of sister chromatid cohesion (Lee & Amon, 2003). This phosphorylation event was shown to redundantly depend on DDK and Hrr25, the casein kinase in yeast (Katis et al., 2010), and Cdc5 (Attner et al., 2013). Thus, the major roles of DDK during meiosis are in initiating DSB formation during prophase I, establishing monoorientation of sister chromatids at metaphase I, and facilitating the removal of sister chromatid cohesion during anaphase I.

1.5 Meiotic roles of Cdc5, the budding yeast polo kinase

Like many of the cell division cycle genes, Cdc5 was identified in a screen for mutations that disrupt the cell cycle (Hartwell et al., 1973). Since then, Cdc5 has been shown to be the only polo kinase in budding yeast and is the homologue of PLK1 in mammals, which have at least three other paralogues of Cdc5 (Barr et al., 2004; Lee et al., 2005). The polo family of kinases are characterised by the presence of a polo-box domain (PBD), which is involved in substrate recognition (Barr et al., 2004). Cdc5 was first suggested to have roles in M phase when temperature sensitive *CDC5* alleles were shown to confer an increase in the loss of chromosomes, even when heterozygous with the WT gene (Hartwell & Smith, 1985). As with DDK, the mitotic roles of Cdc5 predominate the literature, thus they will be introduced briefly before discussing the importance of Cdc5 during meiosis. Cdc5 was shown to promote the full activation of the anaphase promoting complex (APC) before being targeted for destruction by the APC itself (Charles et al., 1998; Shirayama et al., 1998). Cdc5 is also required for exit from mitosis (Saunders, 2002). The separation of sister chromatids during mitosis is dependent on the cleavage of cohesin, which otherwise acts to maintain sister chromatid cohesion (Uhlmann et al., 1999). Crucially, Cdc5 is required for phosphorylation of the cohesin subunit Scc1, without which budding yeast separase Esp1 cannot efficiently cleave chromosomal cohesin to permit separation of sister chromatids during mitosis (Alexandru et al., 2001).

Interestingly, the role of Cdc5 in promoting destruction of chromosomal cohesin is conserved in meiotic cells, where Esp1 drives efficient cleavage of phosphorylated Rec8 (Lee & Amon, 2003). However, in meiotic cells,

centromeric cohesin is protected from the effects of Cdc5-dependent phosphorylation via the recruitment of phosphatases that negate the effect of Cdc5, resulting in the cleavage of cohesin located along chromosome arms only during anaphase I, whereas cleavage of centromeric cohesin occurs in anaphase II (Gregan et al., 2008). In essence, this stepwise removal of cohesin contributes to the establishment of the meiosis I-specific chromosome segregation pattern (Gregan et al., 2008).

Since Cdc5 production depends on Ndt80 (Chu & Herskowitz, 1998), which itself is produced as cells commit to pachytene exit and entry into metaphase I (Xu et al., 1995), there is no biological role for Cdc5 during or before pachytene. In WT cells, induction of Ndt80 is followed by resolution of double Holliday junctions into crossovers (and noncrossovers) and disappearance of SC; neither takes place in meiotic cells depleted for Cdc5, indicating that Cdc5 is required for the maturation of recombination intermediates into products and disassembly of the SC (Clyne et al., 2003). Accordingly, the induction of Cdc5 alone in *ndt80Δ* cells was shown to be sufficient to promote resolution of double Holliday junctions and SC disassembly (Sourirajan & Lichten, 2008).

The mechanism by which Cdc5 drives double Holliday junction resolution was recently elucidated (Matos et al., 2011). By purifying the Mus81-Mms4 endonuclease at numerous points throughout a meiotic time course experiment, Matos et al. (2011) showed that the maximal activity of the Mus81-Mms4 endonuclease in an in vitro resolution assay coincides with Cdc5 production. Furthermore, the authors showed that Cdc5-dependent phosphorylation of Mms4 was required for maximal activity of the Mus81-Mms4 endonuclease.

Finally, Matos et al. (2011) identified the sites of phosphorylation on Mms4 and mutated them to nonphosphorylatable alanines; the resultant Mus81-Mms4 endonuclease showed very little resolution activity compared to the WT endonuclease and was impervious to the production of Cdc5. These studies present compelling evidence that, in addition to facilitating the destruction of arm cohesin in meiosis I, Cdc5 plays a crucial role in promoting resolution of double Holliday junctions as cells commit to meiosis I.

Since Cdc5 is critical for numerous meiosis I processes, Attner et al. (2013) set out to determine whether it is also required during meiosis II. By employing an inducible allele of *NDT80*, it is possible to increase the synchrony in cultures as cells arrest at the end of pachytene and can be induced to undergo a highly synchronous meiosis (Benjamin et al., 2003). When combined with the *cdc5-as* allele (analogue sensitive), which can be conditionally inactivated through the addition of an ATP analogue (Snead et al., 2007), it becomes possible to inactivate Cdc5-as at a given time after cells commit to meiosis I. When cells were released from their pachytene arrest through induction of Ndt80, and Cdc5-as was inactivated one hour after Ndt80 induction, cells remained arrested in a metaphase I-like state. In contrast, when Cdc5-as was inactivated 1 hour 15 minutes after release from pachytene, cells remained arrested in anaphase I. Finally, when Cdc5-as was inactivated 1 hour 30 minutes after pachytene release, there was only a subtle delay in the completion of meiosis compared to cultures expressing WT Cdc5 with ATP analogue (Attner et al., 2013). Taken together, these data suggest that while Cdc5 is essential for meiosis I, it is dispensable for meiosis II. Alternatively, it is possible that although the kinetics of meiosis are only mildly affected in *cdc5-as*

cells and there are no cytologically detectable differences with WT, spores that form as a result of such meioses have reduced viability, which would suggest that Cdc5 might have some roles in meiosis II.

1.6 Interactions between Dbf4 and Cdc5

An interesting genetic finding pointed at the existence of an interaction between Dbf4 and Cdc5. The *dbf4-1* temperature sensitive mutant has a similar terminal phenotype as the *dbf4Δ* mutant, which arrests with unreplicated DNA (Kitada et al., 1993; Sclafani, 2000). However, overexpression of *CDC5* was shown to suppress the arrest phenotype of *dbf4-1* cells (Kitada et al., 1993).

In evidence of the genetic data implicating an interaction between Dbf4 and Cdc5, Cdc5 was shown to immunoprecipitate with Dbf4 (Hardy & Pautz, 1996). Moreover, Hardy et al. (1996) presented in vitro evidence to suggest that Cdc5 phosphorylates Dbf4. In support of this finding, Dbf4 immunoprecipitated from yeast cells blocked in M phase and subjected to immunoblotting was present as a doublet, with the upper band corresponding to phosphorylated Dbf4, whereas Dbf4 immunoprecipitated from cells blocked in S phase existed as a single band (Ferreira et al., 2000). This data is consistent with the possibility that Cdc5 phosphorylates Dbf4 in vivo, since Cdc5 protein levels were shown to increase following S phase and peak during M phase (Hardy & Pautz, 1996).

Dbf4 and Cdc5 have also been shown to interact in meiotic cells (Matos et al., 2008). In fact, Cdc5 was also shown to immunoprecipitate with Cdc7, the catalytic partner of Dbf4, but this interaction is most likely indirect, since it requires the presence of Dbf4 and the PBD of Cdc5 (Matos et al., 2008). As in

mitotic cells, a Cdc5-dependent low mobility species of Dbf4 was seen in meiotic cells, although no evidence was presented to suggest that this higher molecular weight Dbf4 corresponded to phosphorylated Dbf4 (Matos et al., 2008). Taken together, there is substantial evidence that Cdc5 interacts with and phosphorylates Dbf4 in both mitotic and meiotic cells.

Cdc5 is not the only protein capable of phosphorylating Dbf4. When recombinant Dbf4 was purified and incubated with recombinant Cdc7, both Dbf4 and Cdc7 were shown to be phosphorylated; this phosphorylation was dependent on the catalytic activity of Cdc7 (Weinreich & Stillman, 1999). This finding strongly suggests that DDK is capable of autophosphorylation. The biological relevance of Dbf4 phosphorylation, either by Cdc5 or DDK itself, remains unknown. Evidence also exists to suggest that DDK phosphorylates the PBD of Cdc5, but even less is known about the significance of this phosphorylation event (Miller et al., 2009).

Interestingly, production of a truncated version of Dbf4 that is unable to interact with Cdc5 was able to partially suppress the growth defect of *cdc5-1* cells at the restrictive temperature (Miller et al., 2009), suggesting that the interaction between Dbf4 and Cdc5 is at least partially responsible for the terminal phenotype associated with insufficient Cdc5 activity. Consistent with the notion that Dbf4 negatively regulates Cdc5 in mitosis, expression of Dbf4-E86K, a Dbf4 mutant that shows an enhanced interaction with Cdc5, exacerbated the growth defect of *cdc5-1* cells (Chen & Weinreich, 2010). These studies provide evidence that Dbf4 interacts with and limits Cdc5 kinase activity in mitosis, potentially to regulate mitotic exit. Taken together, there is an abundance of genetic and biochemical evidence indicating that DDK and Cdc5

interact during both mitosis and meiosis, although the biological significance of this interaction is yet to be determined. Additionally, there is some evidence to suggest that Dbf4 is phosphorylated by Cdc5, although even less is known about the nature or purpose of this phosphorylation event.

1.7 Preface to results

In order to better understand the coordination between meiotic HR and meiotic cell cycle progression, previous members of our lab employed mutant strains that are defective in meiotic HR and undergo a tight pachytene arrest to screen for genes whose overproduction allows such mutants to complete meiosis. This screen identified *DBF4* as a multicopy suppressor of pachytene arrest. The thesis presented here describes the characterisation of this suppression phenotype and subsequent elucidation of the underlying mechanism that allows Dbf4 to promote unscheduled cell cycle progression in meiotic HR mutants. The following chapters will reveal that the ability of Dbf4 to regulate meiotic progression is dependent on its interaction with and subsequent phosphorylation by Cdc5. Dbf4-Cdc5 interaction strength shows a strong positive correlation with the efficiency of Cdc5-driven SC destruction/disassembly (used interchangeably from hereon), which results in ablation of the Rad51 inhibition operating in meiosis. Consequently, DSBs are repaired by Rad51 in the absence of Dmc1 and the recombination checkpoint is deactivated, resulting in progression of the meiotic cell cycle. Importantly, the phosphorylation status of Dbf4 shows a strong positive correlation with the efficiency of Cdc5-driven SC destruction. Moreover, DDK is shown to play an active role in promoting SC destruction, as depletion of DDK activity confers a

reduction in the ability of Cdc5 to destroy the SC. Furthermore, in the absence of Cdc5, DDK is shown to be required for maintaining SC integrity and upholding the inhibition to Rad51 within prophase I, indicating that DDK plays dual roles in regulating the SC. Finally, the checkpoint kinases Mec1 and Tel1 are shown to downregulate and upregulate DSB formation, respectively, while Cdc5 is identified as being able to prohibit DSB formation when it is ectopically expressed in early prophase. Thus, by preserving SC integrity, DDK maintains the meiotic mode of HR by enforcing inhibition of Rad51. However, the robust upregulation of Cdc5 at the end of pachytene, a time by which interhomologue joint molecules have formed, results in Dbf4 phosphorylation; this phosphorylation is key in driving efficient destruction of the SC. As a result, Rad51 is unshackled from its meiotic inhibition and the meiotic mode of HR is abrogated to ensure complete repair of all DSBs before chromosome segregation at anaphase I. In parallel, Cdc5 prohibits any further DSB formation after prophase I, which would cause catastrophic missegregation of chromosomes. Additionally, the dynamic process of DSB formation during prophase I is subjected to fine-tuning by different components of the recombination checkpoint.

Chapter 2: Materials and Methods

For recipes of media and other solutions/buffers, please advance to section **2.7** (page 46). For abbreviations, please refer to page I. For a list of all strains used in this study, please refer to **Appendix 1** (page 133).

2.1 General yeast techniques

2.1.1 Storage and growth of yeast

All equipment and media were sterilised by autoclaving and procedures were performed under aseptic conditions. Yeast strains were stored in 40% glycerol at -80 ˚C. Growth of yeast on plates (solid medium) and sporulation on plates was always conducted at 30 ˚C. Growth of yeast in culture (liquid medium) and sporulation in culture was always conducted at 30 ˚C, 250 RPM.

2.1.2 Mating for diploid formation

Approximately equal amounts of cells from two strains were mixed on rich media (YPADU) and incubated at 30 ˚C for 5 hours. Mating was confirmed by monitoring cells using a Nikon ECLIPSE E200 light microscope (this microscope was used for all light microscopy) and identifying those with a characteristic zygote morphology. For BR1919 strains, cells from the mass mating plate were streaked onto a fresh YPADU plate and putative zygotes were picked with a tetrad dissection microscope (Singer MSM 400) and allowed to form single colonies, before confirming that candidates were non-maters. For SK1 strains, single colonies were streaked from the mass mating plate and colonies with a characteristic diploid morphology were identified.

2.1.3 Genetic crosses

Mating was performed as in **2.1.3**. Cells were then transferred to a sporulation media (SPM) plate and allowed to sporulate for >24 hours. Sporulation was confirmed by light microscopy. Tetrads were dissected (see **2.1.4**) and colonies with the desired markers were identified by replica plating onto selective plates.

2.1.4 Tetrad dissection

A small amount of cells from an SPM plate were resuspended in 50 µL of 1 M sorbitol and gently mixed following the addition of 3 µL of zymolyase (10 mg/mL; this stock concentration was maintained throughout this study). This mixture was incubated at 30 ˚C for 30 minutes, before adding 100 µL of dH_2O and gently mixing. 8 µL of this cell suspension was loaded onto a YPADU plate and tetrads were dissected. The same tetrad dissection microscope was used throughout this study (Singer MSM 400).

2.1.5 Genetic manipulation of yeast

Yeast were transformed according to the lithium acetate/single-stranded carrier DNA/polyethylene glycol method (Gietz & Woods, 2002). Briefly, a single colony was inoculated in 2 mL YPADU overnight, before being introduced into 25 mL YPADU for 4 hours. After washing with dH_2O, cells were pelletized and resuspended in premixed 240 µL 50% PEG 3350, 36 µL 1 M lithium acetate, 50 µL single-stranded salmon sperm DNA (2 mg/mL) and DNA of interest. After heat-shock treatment at 42 ˚C for 45 minutes, cells were briefly pelletized again, before being resuspended in dH_2O and spread on the desired plate.

2.1.6 Preparation of genomic DNA

A small amount of yeast cells were resuspended in 100 µL of sorbitol solution (0.9 M sorbitol, 0.1 M Tris (pH 8), 0.1 M EDTA (pH 8)) and treated with 0.2 µL beta-mercaptoethanol and 0.4 µL of zymolyase at 30 ˚C for 30 minutes. Cells were gently centrifuged (845 *g*, 2 minutes) and resuspended in 100 µL 50:20 TE (50 mM Tris-20 mM EDTA), before mixing with 10 µL of 10% SDS and storing at 65 ˚C for 20 minutes. Cell suspensions were then supplemented with 40 µL of 5 M potassium acetate and stored on ice for at least 30 minutes. Once firmly pelletized (20000 *g*, 5 minutes), DNA was purified by ethanol precipitation.

2.1.7 Plasmid extraction from yeast

Plasmid containing transformants were scraped off the selective plate and resuspended in 200 µL of breaking buffer. This suspension was mixed with an equal volume of 0.5 mm zirconia/silica beads (Bio Spec Products), before adding 200 µL of phenol-chloroform-isoamyl alcohol mixture (25:24:1, Sigma). Cells were then lysed using a ribolyser and centrifuged (20000 *g*, 5 minutes) to yield aqueous DNA, which was then amplified by bacterial transformation (see **2.2.2**).

2.2 General molecular biology techniques

2.2.1 Polymerase chain reaction (PCR)

All PCR reagents were stored at -20 ˚C. PCR was performed using either DreamTaq (Fermentas) or Primestar GXL (Takara) polymerases with a T3000

Thermocycler (Biometra). A stock containing 2 mM of each dNTP was prepared from 100 mM stocks of each individual dNTP (Roche). Listed below are the conditions for each polymerase. Primers were used from a stock concentration of 4 µM. (mins - minutes, secs - seconds).

DreamTaq

Total volume	30 µL	Cycling conditions
dH_2O	18 µL	1. 94 ˚C 2 mins
Buffer	3 µL	2. 94 ˚C 30 secs
dNTPs	3 µL	3. 55 ˚C 30 secs
Primer 1	3 µL	4. 70 ˚C 3 mins (steps 2-4, 35 cycles)
Primer 2	3 µL	5. 72 ˚C 5 mins
Enzyme	0.3 µL	
Template DNA	1 µL	

Primestar GXL

Total volume	50 µL	Cycling conditions
dH_2O	30 µL	1. 98 ˚C 5 mins
Buffer	10 µL	2. 98 ˚C 10 secs
dNTPs	5 µL	3. 60 ˚C 15 secs
Primer 1	2.5 µL	4. 68 ˚C 3 mins (steps 2-4, 35 cycles)
Primer 2	2.5 µL	5. 68 ˚C 5 mins
Enzyme	0.8 µL	
Template DNA	1 µL	

When required, PCR products were purified and concentrated using silica spin columns (QIAquick PCR Purification Kit, Qiagen).

2.2.2 Transformation of *Escherichia coli*

XL1-Blue competent *E. coli* were purchased from Agilent Technologies and stored at -80 ˚C. To amplify plasmid DNA, a 100 µL aliquot was thawed on ice and mixed with DNA. After a further 5 minutes on ice, this mixture was transferred to 42 ˚C for 45 seconds. Upon addition of 0.5 mL lysogeny broth (LB), this mixture was agitated at 37 ˚C for 45 minutes, before finally spreading on an LA (lysogeny broth agar) supplemented with desired antibiotics.

2.2.3 Plasmid extraction from *E. coli*

Colonies growing on selective plates were resuspended in 2 mL of LB supplemented with desired antibiotics and left to grow overnight at 37 ˚C with agitation. Plasmid DNA was extracted from cells using a QIAprep Spin Miniprep Kit (Qiagen).

2.2.4 Restriction enzyme digestion of DNA

All enzymes used in this study were supplied by New England Biolabs. Cutting of DNA using restriction enzymes was performed according to the manufacturers guidelines.

2.2.5 Agarose gel electrophoresis

DNA was separated with 0.8% agarose gels in 0.5x TAE buffer using a Mupid-exU mini-gel system (Eurogentec).

2.2.6 DNA sequencing

All DNA sequencing was by Sangar sequencing (GATC Biotech).

2.3 Meiotic time course experiments

2.3.1 Measuring sporulation on a plate

Single colonies grown on YPADU or selective media were patched onto SPM plates and incubated at 30 ˚C for 48 hours (SK1) or 72 hours (BR1919). Cells from different patches were viewed with a light microscope. The formation of dyads/triads/tetrads was scored as sporulation.

2.3.2 Meiotic induction (BR1919)

A single colony grown on YPADU was resuspended in 2 mL of liquid YPADU and grown overnight with agitation. This was supplemented with 5 mL of fresh YPADU and grown for a further 8 hours before centrifuging, washing with water, and resuspending in 50 mL of 2% potassium acetate (liquid SPM). Cells were harvested from liquid SPM at the desired time points after induction.

2.3.3 Synchronous meiotic induction (SK1)

A single colony grown on YPADU was resuspended in 10 mL of liquid YPADU and grown for 24 hours. These cells were centrifuged and resuspended in 100 mL of pre-sporulation media (BYTA) so as to yield an OD_{600} of 0.5. After a further 12 hours of growth, cells were centrifuged, washed twice with 25 mL of dH_2O, and resuspended in either 100 mL or 200 mL of liquid SPM, so as to yield an OD_{600} of 1.9. Time zero samples were taken from BYTA. Cells were harvested from liquid SPM at the desired time points after induction.

2.3.4 Measuring sporulation in a culture

0.5 mL of cells were harvested from a sporulating culture and fixed with an equal volume of 100% ethanol before storing at -20 ˚C. 200 µL of fixed cells were mixed with 0.4 µL of DAPI (1 mg/mL) and left for 5 minutes, before centrifuging (20000 *g*, 3 minutes) and washing with 0.5 mL dH_2O. Cell pellets were then resuspended in 30 µL of 90% glycerol 10% PBS and loaded onto a regular microscope slide, spread with a coverslip, and sealed with nail varnish. Slides were stored at -20 ˚C until use. DNA was visualised and the number of nuclei were determined using a Nikon ECLIPSE E400 microscope. Data was analysed using GraphPad Prism 5.0. Two independent cultures were averaged to yield the graphical results, error bars represent standard error of the mean.

2.3.5 Inducible Cdc5 production

This method of protein induction has been previously characterised (Benjamin et al., 2003). Briefly, the *GAL1* promoter was cloned onto the *CDC5* ORF with 312 bp of the 3'-UTR to yield plasmid p1211. This plasmid was digested with NotI then self-ligated, followed by linearization with NcoI and integration at the *URA3* locus. Diploids were constructed so that one *URA3* locus was occupied by P_{GAL1}-*CDC5* and the other was occupied by a fusion of *GAL4* and the estradiol receptor (GAL-ER). In this background, the addition of beta-estradiol (1 mM in BR1919 and 5 mM in SK1 strains) to a culture leads to the induction of Cdc5.

2.3.6 Anchor-away technique

The anchor-away system was utilised as previously described (Haruki et al., 2008). Briefly, proteins of interest were tagged at their C-termini with FRB in a background where the yeast ribosomal protein Rpl13A is fused to two copies of the human FKBP12 protein, *TOR1* is mutated to *tor1-1*, and *FPR1* is deleted. Target proteins were depleted from the nucleus by adding rapamycin (Sigma) to cultures at a final concentration of 1 µg/mL.

2.4 Protein analysis

2.4.1 TCA preparation of yeast proteins

All of the following was performed on ice. Cell pellets were resuspended with 1 mL of ice-cold dH_2O and mixed with 150 µL 1.85 M NaOH-7.5% beta-mercaptoethanol before leaving on ice for 15 minutes. 150 µL of 55% TCA was added and thoroughly mixed, followed by a further 10 minute incubation on ice. Samples were centrifuged (20000 *g*, 10 minutes) and supernatants were discarded. Samples were centrifuged again to remove residual supernatant and the pellets were solubilised in HU buffer supplemented with 200 mM Tris and 100 mM DTT at 70 ˚C, before storing at -20 ˚C until use.

2.4.2 SDS-PAGE and Western blotting of yeast proteins

Proteins were separated on 8% polyacrylamide gels with an acrylamide-to-bisacrylamide ratio of 29:1. Following separation, proteins were transferred to methanol-activated PVDF membranes (Immobilon-P 0.45 µm, Fisher Scientific) overnight at 4 ˚C. Membranes were then stained with Ponceau S (Sigma-

Aldrich), imaged, and incubated in 0.1% Tween 20-PBS supplemented with 5% milk powder for 1 hour; all incubations were performed with gentle agitation. The milk solution was replaced with fresh milk solution containing the primary antibody of interest, and membranes were incubated for 1 hour. The primary antibody solution was removed, membranes were washed three times for 5 minutes with 0.1% Tween 20-PBS, and fresh milk solution containing the secondary antibody was added to membranes for 1 hour. The secondary antibody solution was removed and membranes were washed as before. Following 5 minutes of incubation in WesternBright Quantum enhanced chemiluminescence solution (Advansta), membranes were imaged using a CCD camera (ImageQuant LAS 4000, GE Healthcare).

2.4.3 Identification of Dbf4 phosphosites

An allele of *DBF4* encoding a protein in which 54 out of 114 serines/threonines were mutated to nonphosphorylatable alanines was synthesised; these residues were highly conserved amongst numerous species of the *Saccharomyces* genus (*cerevisiae*, *bayanus*, *mikatae*, *paradoxus*, *castellii*, *kluyveri*). This allele, referred to as *dbf4-np* (nonphosphorylatable), resulted in a complete loss of phosphorylation, as determined by western blotting (data not shown). To identify the residues that are modified, numerous chimeric combinations of *dbf4-np* and *DBF4* were constructed, and the resultant proteins were examined for modification by western blotting. Eventually, a chimeric construct encoding only 10 serine/threonine to alanine mutations (*dbf4-10A*) was identified as being equivalent to *dbf4-np* regarding protein modification. The *dbf4-10A* allele encoded mutations of the following residues to alanine:

274, 280, 303, 318, 319, 328, 350, 361, 374, 375. A further reduction in the number of mutations to four led to the identification of the *dbf4-4A* allele, which showed a partial reduction in phosphorylation. The *dbf4-4A* allele encoded mutations of the following residues to alanine: 350, 361, 374, 375. This screening was performed by Hideo Tsubouchi.

2.4.4 Protein purification in *E. coli*

A fragment of *CDC5* encoding the PBD (residue 357 to C-terminus) was cloned at the XhoI and BamHI sites of pGEX-6P-1 (GE Healthcare) to yield plasmid p1351. Rosetta2 (DE3) competent cells were transformed with p1351 and GST-CDC5-PBD was induced with 0.3 mM IPTG overnight at 18 ˚C. Following protein induction, cells were sonicated in lysis buffer (50 mM Tris-Cl (pH 7.5), 10% glycerol, 0.5 mM EDTA, 250 mM NaCl, 0.01% igepal (Sigma), 1 mM beta-mercaptoethanol and 100 µg/mL PMSF). The lysate was cleared by centrifugation (100000 *g*, 1 hour) and the GST-CDC5-PBD protein was captured on glutathione agarose beads (Qiagen), before eluting with elution buffer (25 mM Tris-Cl (pH 7.5), 10% glycerol, 0.5 mM EDTA, 250 mM NaCl, 0.01% igepal (Sigma), 1 mM beta-mercaptoethanol and 20 mM glutathione). The eluate was fractionated in a gel filtration column (Superdex S200, GE Healthcare) with column buffer (20 mM HEPES (pH 7.5), 10% glycerol, 5 mM EDTA, 250 mM NaCl and 0.5 mM TCEP (Sigma)). Peak fractions were amalgamated and concentrated using a microconcentrator (Vivaspin-30, Sartorius). The concentrated protein solution was used immediately in the fluorescence polarisation assay.

2.4.5 Fluorescence polarisation assay

Peptides were synthesised by Peptide Protein Research (Fareham, UK). The following peptides were used (mutations are underlined):

wild type Flu-GGEKKRARIERARSIEGAVQVSKGTG

R83E Flu-GGEKKRARIERAESIEGAVQVSKGTG

E86K Flu-GGEKKRARIERARSIKGAVQVSKGTG

E86V Flu-GGEKKRARIERARSIVGAVQVSKGTG

(Flu, Fluorescein. Two glycines were placed between Flu and the peptides as a linker).

Peptides at 100 nM were incubated at room temperature with increasing concentrations of Cdc5-PBD in polarisation buffer (20 mM HEPES (pH 7.5), 10% glycerol, 5 mM EDTA, 250 mM NaCl, 0.5 mM TCEP (Sigma) and 0.05% tween 20), with a total volume of 50 µL per sample. The sample mixtures were then transferred to a black 96-well polypropylene plate for measurement of fluorescence polarisation in a POLAR star Omega multimode microplate reader (BMG LABTECH). Having set excitation and emission wavelengths of 485 nm and 520 nm, respectively, emission signals from 50 flashes were collected and averaged in endpoint mode for each well, with either parallel of perpendicular polarisers in-line. Background fluorescence in samples carrying only peptides was subtracted from the averaged values. Data was analysed using GraphPad Prism 5.0 by non-linear fitting with a one-site total binding model. Non-specific binding component was then subtracted for presentation purposes. All data represent the mean of three independent experiments and error bars represent one standard deviation.

2.5 Immunofluorescence microscopy

5-10 mL of a sporulating culture was harvested and pelletized. Cells were resuspended in 1% potassium acetate-1M sorbitol solution, before gently mixing with 8 µL 1 M DTT and 8 µL zymolyase. Cells were incubated at 30 ˚C with gentle agitation for 25 minutes, before centrifuging (250 *g*, 2 minutes) and resuspending in 1 M sorbitol-1x MES. Following further centrifugation (250 *g*, 2 minutes), pellets were resuspended with premixed PFA-1x MES (350 µL 3.7% PFA with 100 µL 1x MES) and spread onto microscopy slides (Superfrost, Thermo Scientific). After semi-drying, these slides were washed twice with 0.4% Photoflo (Kodak) and allowed to fully dry. Slides were then stored in -20 ˚C until required. To immunostain, slides were incubated with 5% BSA-PBS for 30 minutes in a moist environment, before incubating overnight at 4 ˚C with 5% BSA-PBS supplemented with primary antibody. Slides were then washed by submerging in PBS-filled coplin jars, before incubating for 3 hours at room temperature with 5% BSA-PBS supplemented with secondary antibody. Slides were washed as before and allowed to dry. 30 µL of mounting media was added to each slide and spread with a cover slip before sealing. All slides were viewed and images captured using the Deltavision IX70 system (Applied Precision) and *softWoRx* software. Deconvolved z-slices were projected together to form the processed images displayed in this study. Graphs were drawn using GraphPad Prism 5.0 and Microsoft Excel. Where errors bars are shown, they represent the standard error of the mean (n = 2).

2.6 Detection of meiotic DSBs

This procedure was performed as previously described (Farmer et al., 2011; Farmer et al., 2012), with specifics detailed below.

2.6.1 Sample preparation

30 mL of a sporulating culture was harvested, washed with 125 mM EDTA and stored at -80 ˚C. This cell pellet was resuspended in 100 µL 125 mM EDTA supplemented with 7 µL zymolyase, 3 µL 1 M DTT, and 2 µL 30 mg/mL RNase A, before mixing with 200 µL of low melting-point agarose (InCert Agarose, Lonza) dissolved in 125 mM EDTA (2.8 mg agarose per 200 µL). Following rapid mixing, the samples were pipetted into 50-well moulds and allowed to set on an ice-cold metal surface. Plugs were then incubated at 37 ˚C for 3 hours, before leaving overnight in 1 mL of 10 mM Tris 500 mM EDTA supplemented with 10 mg N-Lauroylsarcosine sodium salt and 2 mg proteinase K (both from Sigma). This solution was discarded and plugs were washed 3 times with 1.5 mL of 10 mM Tris 500 mM EDTA at 4 ˚C, before storing in the same solution at 4 ˚C until use.

2.6.2 Pulsed-field gel electrophoresis

Agarose-embedded genomic DNA was separated on a 1% gel in 0.5x TBE buffer using the CHEF DR-II system from BIO-RAD. Running conditions are as follows: 24 hours at 14 ˚C, with an initial switching time of 20 seconds and a final switching time of 60 seconds, at a voltage of 6 V. Following electrophoresis, the gel was stained with ethidium bromide to visualise DNA.

2.6.3 Southern blotting

The gel was treated with 120 mJ/cm^2 of ultraviolet energy, before incubating for 15 minutes in 0.25 M hydrochloric acid, washing briefly with dH_2O, and then incubating twice with 0.4 M sodium hydroxide for 15 minutes. DNA was transferred overnight to a nylon membrane (Hybond-XL, GE Healthcare) by capillary action.

2.6.4 Probe hybridisation and washing

DNA was crosslinked with 70 mJ/cm^2 of ultraviolet energy and incubated in hybridisation buffer at 65 ˚C for 45 minutes. A chromosome II probe was prepared by mixing PCR-amplified chromosome II-specific DNA with the Rediprime II labelling kit (GE Healthcare) and incubating in the presence of P^{32}-dCTP (Perkin Elmer) at 37 ˚C for 30 minutes. This probe was then denatured by heating to 95 ˚C for 3 minutes, quenched on ice for 3 minutes, and added to the membrane with fresh hybridisation buffer before incubating overnight at 65 ˚C. Unbound radiolabel was removed by washing the membrane 5 times for 5 minutes with Southern wash buffer at 65 ˚C.

2.6.5 Exposure and imaging

Radiolabelled membranes were exposed to a phosphor screen in complete darkness for 24 hours. The screen was then imaged using a Fujifilm FLA-5000 phosphorimager.

2.6.6 Data analysis

Southern blots were analysed using AIDA Image Analyser (Raytest) and GraphPad Prism 5.0. Samples were normalised by subtracting the signal at time zero from each corresponding time point. Graphs represent averages of at least two independent cultures, error bars represent standard error of the mean. In order to calculate estimates of the number of breaks per chromosome, a previously established method relying on partial observation was used (Toyoizumi & Tsubouchi, 2012).

2.7 Recipes

2.7.1 Solid media

All solid media was made up to 600 mL using dH_2O, autoclaved, and stored at room temperature until required. pH adjustments were only made where indicated.

YPADU

Yeast extract	6 g
Tryptone	12 g
Glucose	12 g
Adenine	67 mg
Uracil	13 mg
Agar	12 g

SPM

Yeast extract	1.2 g
Glucose	0.6 g
Potassium acetate	12 g
Synthetic complete mix	75 mg
Agar	12 g

Selective media

Genetic modifications that involved resistance to hygromycin, cloNAT or G418 were selected for by supplementing YPADU with 300, 100 and 200 µg/mL, respectively. Auxotrophic selection was performed by utilising the following media, with a different synthetic complete mix for each selection marker (e.g., synthetic complete mix without uracil to select for genetic modifications that restore the ability to synthesise uracil). This media was set to pH 5.6.

Yeast nitrogen base	4 g
Glucose	12 g
Synthetic complete mix	0.3 g
Agar	12 g

LA

LA was melted in a microwave, allowed to cool to hand-hot, then supplemented with ampicillin and chloramphenicol at final concentrations of 50 µg/mL and 34 µg/mL, respectively.

Yeast extract	6 g

Tryptone	12 g
NaCl	6 g
Agar	7.2 g

2.7.2 Liquid media

All liquid media was made up to 1 L using dH_2O, autoclaved, and stored at room temperature until required. BYTA was prepared fresh and stored in the dark until use. pH adjustments were only made where indicated.

YPADU

Yeast extract	10 g
Tryptone	20 g
Glucose	20 g
Adenine	112 mg
Uracil	22 mg

SPM (pH 6.5)

Potassium acetate	20 g

BYTA

Yeast extract	10 g
Tryptone	20 g
Potassium acetate	10g
Potassium phthalate monobasic	10.2 g

LB

LB was supplemented with ampicillin and chloramphenicol at final concentrations of 50 µg/mL and 34 µg/mL, respectively.

Yeast extract	10 g
Tryptone	20 g
NaCl	10 g

2.7.3 Other solutions and buffers

Where dH_2O is shown in brackets, this denotes that once solutes were dissolved in approximately half the total volume of dH_2O, further dH_2O was added until the solution reached the desired volume as determined using a measuring cylinder.

10 mg/mL zymolyase (1 mL)

Zymolyase	10mg
Tris-Cl (pH 7.5)	10 µL
Glycerol	500 µL
dH_2O	480 µL

Breaking buffer (100 mL)

Triton X-100	2 mL
10% SDS	10 mL
5 M NaCl	2 mL
2 M Tris-Cl (pH 8.0)	500 µL

500 µM EDTA (pH 8.0)	200 µL
(dH_2O)	

2x MES (200 mL) (pH 6.4)

MES hydrate	7.8 g
500 µM EDTA (pH 8.0)	0.8 mL
1 M MgCl2	200 µL
(dH_2O)	

3.7% PFA (10 mL)

1 M KOH	28 µL
PFA	0.37 g
dH_2O	9.972 mL

Mounting media (10 mL)

p-Phenylenediamine	10 mg
Glycerol	9 mL
PBS	1 mL

HU buffer (200 mL)

Urea	96.1 g
SDS	10 g
1 M Tris-Cl (pH 6.8)	40 mL
500 µM EDTA (pH 8.0)	0.4 mL
Bromophenol blue	0.02 g

50x TAE (500 mL)

Tris base	242 g
Glacial acetic acid	57.1 mL
500 μM EDTA (pH 8.0)	100 mL
(dH_2O)	

10x TBE (1 L)

Tris base	108 g
Boric acid	55 g
500 μM EDTA (pH 8.0)	40 mL
(dH_2O)	

Hybridisation buffer (1 L)

*1 L of 1 M sodium phosphate solution (pH 6.5) is made by mixing 684 mL of 1 M sodium phosphate dibasic (Na_2HPO_4) with 316 mL of 1 M sodium phosphate monobasic (NaH_2PO_4).

SDS	70 g
500 μM EDTA (pH 8.0)	2 mL
*1 M sodium phosphate solution	500 mL
(dH_2O)	

Southern wash buffer (800 mL)

SDS	8 g
500 μM EDTA (pH 8.0)	1.6 mL

1 M sodium phosphate solution	32 mL
(dH_2O)	

Chapter 3: Dbf4 and Cdc5 Interact to Regulate Prophase I Exit

The coordination of HR with the meiotic cycle is crucial, since repair of the self-inflicted DSBs in prophase I must be complete before commencing homologue alignment at metaphase I and chromosome segregation at anaphase I (Roeder & Bailis, 2000). In order to learn more about the coordination of HR with the meiotic cell cycle, previous lab members conducted a multicopy suppressor screen to identify genes whose overexpression allows the *zip1-4LA* mutant to sporulate. *zip1-4LA* encodes a mutant version of Zip1, the SC central element protein, that was previously characterised as a recessive nonnull allele that confers an extremely tight checkpoint-dependent arrest in the pachytene stage of prophase I (Mitra & Roeder, 2007). *DBF4* was identified as a gene whose expression from a multicopy plasmid, but not a single copy plasmid, could suppress the *zip1-4LA* arrest. Subsequently, the Dbf4-E86V mutation was identified as a single copy suppressor of *zip1-4LA* arrest. This chapter details the genetic and biochemical characterisation of this suppression phenotype.

3.1 The arrest of meiotic recombination mutants is suppressed by overproducing Dbf4 or producing Dbf4-E86V

The *zip1-4LA* arrest can be suppressed by deletion of the *SPO11* gene (Mitra & Roeder, 2007), which encodes the conserved endonuclease that induces programmed DSBs in early prophase I (Keeney et al., 1997), suggesting that *zip1-4LA* arrest is associated with the consequent recombination events that occur following DSB formation. To test the possibility that Dbf4-dependent suppression occurs in other strains with defects in meiosis-specific HR factors, I employed the *hop2Δ* mutant to determine if Dbf4 overproduction or Dbf4-E86V

could suppress this pachytene arrest. Hop2 is a component of the Dmc1-dependent recombination pathway, and in its absence, cells show a tight pachytene arrest due to the accumulation of resected DSB ends (Tsubouchi & Roeder, 2002; Tsubouchi & Roeder, 2003). *hop2Δ* cells were transformed with the indicated plasmids and assayed for their ability to sporulate (**Figure 3.1**). As with *zip1-4LA* cells, overproduction of Dbf4 or production of Dbf4-E86V was able to suppress the pachytene arrest of *hop2Δ* cells, thus identifying Dbf4 as playing a role in pachytene exit.

3.2 Dbf4-E86V interacts with Cdc5 more strongly than Dbf4

The 86th residue of Dbf4 constitutes part of the motif that was identified as binding to Cdc5 (Chen & Weinreich, 2010), the only polo-like kinase in *S. cerevisiae* (PLK1 in humans) (Barr et al., 2004; Lee et al., 2005), raising the possibility that the effect exerted by Dbf4 in promoting meiotic progression in HR mutants involves an interaction with Cdc5. To determine whether the Dbf4-Cdc5 interaction is altered by the Dbf4-E86V mutation, I GST-tagged and purified the region of Cdc5 that contains the PBD (**Figure 3.2A**) and synthesised peptides representing WT Dbf4 and Dbf4-E86V for use in the fluorescence polarisation (FP) assay. In addition, two previously characterised mutant peptides were also synthesised: the Dbf4-R83E mutation abolishes the Dbf4-Cdc5 interaction, whereas the Dbf4-E86K mutant protein shows an enhanced interaction with Cdc5 (**Figure 3.2B**) (Chen & Weinreich, 2010).

The FP assay relies on the tumbling of molecules in solution. Any given molecule has the propensity to tumble in solution. The degree of tumbling is inversely proportional to the molecular volume of the species, with more

Figure 3.1. Overproduction of Dbf4 or production of Dbf4-E86V suppresses *hop2Δ* arrest.

Sporulation was monitored by phase contrast microscopy in wild type (WT) cells or *hop2Δ* cells transformed with multicopy plasmid (vector), multicopy plasmid carrying wild type *DBF4* (multi *DBF4-WT*), single copy plasmid carrying wild type *DBF4* (single *DBF4-WT*), or single copy plasmid carrying wild type dbf*4-E86V* (single E86V). Error bars ±SEM, n = 3.

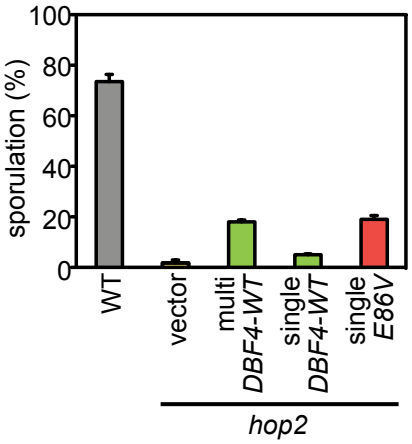
100
80
60
40
20
0
sporulation (%)
WT
vector
multi DBF4-WT
single DBF4-WT
single E86V
hop2

Figure 3.2. Dbf4-E86V shows an enhanced interaction with Cdc5's polo-box domain.

A GST-Cdc5-PBD was purified to homogeneity for use in the fluorescence polarisation (FP) assay and 1 µg of protein was run on a polyacrylamide gel, which was then stained with InstantBlue coomassie stain. **B** Schematic of the Dbf4 motif that binds Cdc5. **C** K_D values for the interaction between the indicated Dbf4 peptides and Cdc5-PBD were calculated from the FP data and plotted. Error bars ±SD, n = 3. **D** Polarisation data from the FP assay (y-axis) at different concentrations of Cdc5-PBD (x-axis) for the indicated Dbf4 peptides was plotted.

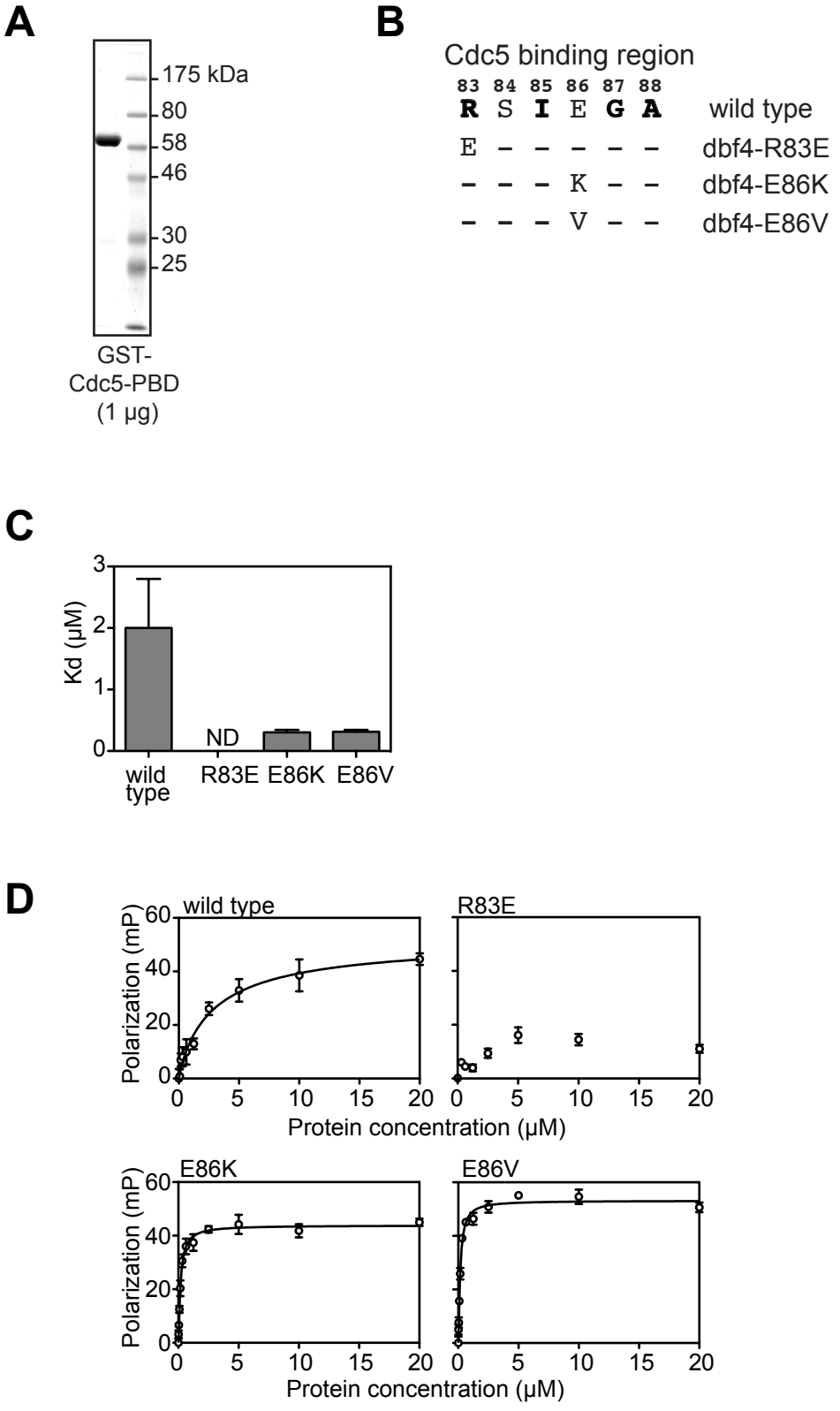
A
175 kDa
80
58
46
30
25
GST-
Cdc5-PBD
(1 μg)
B
Cdc5 binding region
83 84 85 86 87 88
R S I E G A
wild type
E – – – – – dbf4-R83E
– – – K – – dbf4-E86K
– – – V – – dbf4-E86V
C
Kd (μM)
3
2
1
0
ND
wild type
R83E
E86K
E86V
D
wild type
R83E
E86K
E86V
Polarization (mP)
60
40
20
0
0
5
10
15
20
Protein concentration (μM)

tumbling seen for smaller species. Importantly, when a stationary fluorophore is excited by plane-polarised light, no more than 60% of the emitted light will remain in the same plane (Rossi & Taylor, 2011). However, if the fluorophore tumbles more, then less of the emitted light will remain polarised. Thus, if a small, rapidly tumbling, fluorescent ligand interacts with a large, mostly stationary protein, the tumbling of the ligand is drastically reduced due to its interaction with the bulkier protein. As a result, the fluorophore covalently attached to the ligand emits a higher proportion of light that remains polarised. Thus, the stronger the ligand interacts with the protein, the more efficiently it transitions from emitting de-polarised to polarised light. Hence, a lower concentration of protein is needed to substantially retard the tumbling of the ligand. For this experiment, the Cdc5-PBD fragment serves the role of the large protein and the synthesised peptides, which have the fluorophore fluorescein covalently attached to them, serve the role of the ligand.

In agreement with previous data (Chen & Weinreich, 2010), the WT peptide showed an interaction with Cdc5 with a K_d value of ~2 μM (**Figure 3.2C**). As expected, the Dbf4-E86K peptide yielded a K_d value of ~0.3 μM, indicating an interaction with Cdc5 that is of higher affinity than WT Dbf4. Likewise, the Dbf4-E86V peptide's interaction with Cdc5 yielded a K_d value of ~0.3 μM. In contrast, a K_d value could not be calculated for the Dbf4-R83E peptide because the relevant polarisation data was not above background levels (**Figure 3.2D**), indicating an absence of interaction, as was reported by Chen & Weinreich (2010). These data suggest that mutation of Dbf4's 86th residue to valine enhances its interaction with Cdc5.

3.3 Enhanced interaction between Dbf4 and Cdc5 suppresses the pachytene arrest of meiotic recombination mutants

To better investigate whether the Dbf4-Cdc5 interaction regulates meiotic progression in HR mutants, the chromosomally located *DBF4* gene was mutated to encode the E86V substitution. Strains carrying the Dbf4-R83E and Dbf4-E86K mutations were also generated. These strains were constructed in the *zip1-4LA* and *hop2Δ* mutant backgrounds, as well as the *zip2Δ zip3Δ* double mutant background, which displays defects in meiotic HR and consequently shows a pachytene arrest (Tsubouchi et al., 2006). Following meiotic induction, both the *DBF4-E86V* and *DBF4-E86K* mutations allowed sporulation to be completed in all three mutant backgrounds (**Figure 3.3A**), strongly suggesting that the Dbf4-Cdc5 interaction regulates prophase I exit in cells that are defective in meiotic recombination.

To better monitor the progression phenotype, the BR1919 background was substituted with the SK1 strain background. In the SK1 background, a cell population can be induced to undergo highly efficient meiosis in a synchronous fashion, allowing for the accurate assessment of molecular changes at the population level. In SK1 meiosis, the *dmc1Δ* mutant shows a robust pachytene arrest (Bishop et al., 1992), and as such, was combined with the various *DBF4* mutations. To characterise the kinetics of cell cycle progression, protein markers such as the meiosis-specific transcription factor Ndt80 can be employed. The upregulation of Ndt80 at the end of pachytene is a landmark event for prophase I exit and can be detected by western blotting (Xu et al., 1995; Chu & Herskowitz, 1998; Tung et al., 2000). The same is true for proteins that are under Ndt80's control, such as Cdc5. In addition, nuclear divisions were

Figure 3.3. Enhancing the interaction between Dbf4 and Cdc5 leads to unscheduled cell cycle progression in *dmc1Δ* cells.

A Sporulation was monitored in the *hop2Δ*, *zip1-4LA*, and *zip2Δ zip3Δ* strains with homozygous *DBF4* (*DBF4-WT*), *dbf4-E86K* (*E86K*), *dbf4-R83E* (*R83E*) or *dbf4-E86V* (*E86V*) at the native locus. Error bars ±SEM, n = 3. **B** *dmc1Δ* strains with the indicated *DBF4* allele homozygous at the native locus were synchronously introduced into meiosis and protein extracts were subjected to immunoblotting. Ponceau stained membranes were included as a loading control (total). **C** Cell cycle progression in the same cultures from **B** was scored by fluorescent microscopy of DAPI stained cells. Error bars ±SEM, n = 2.

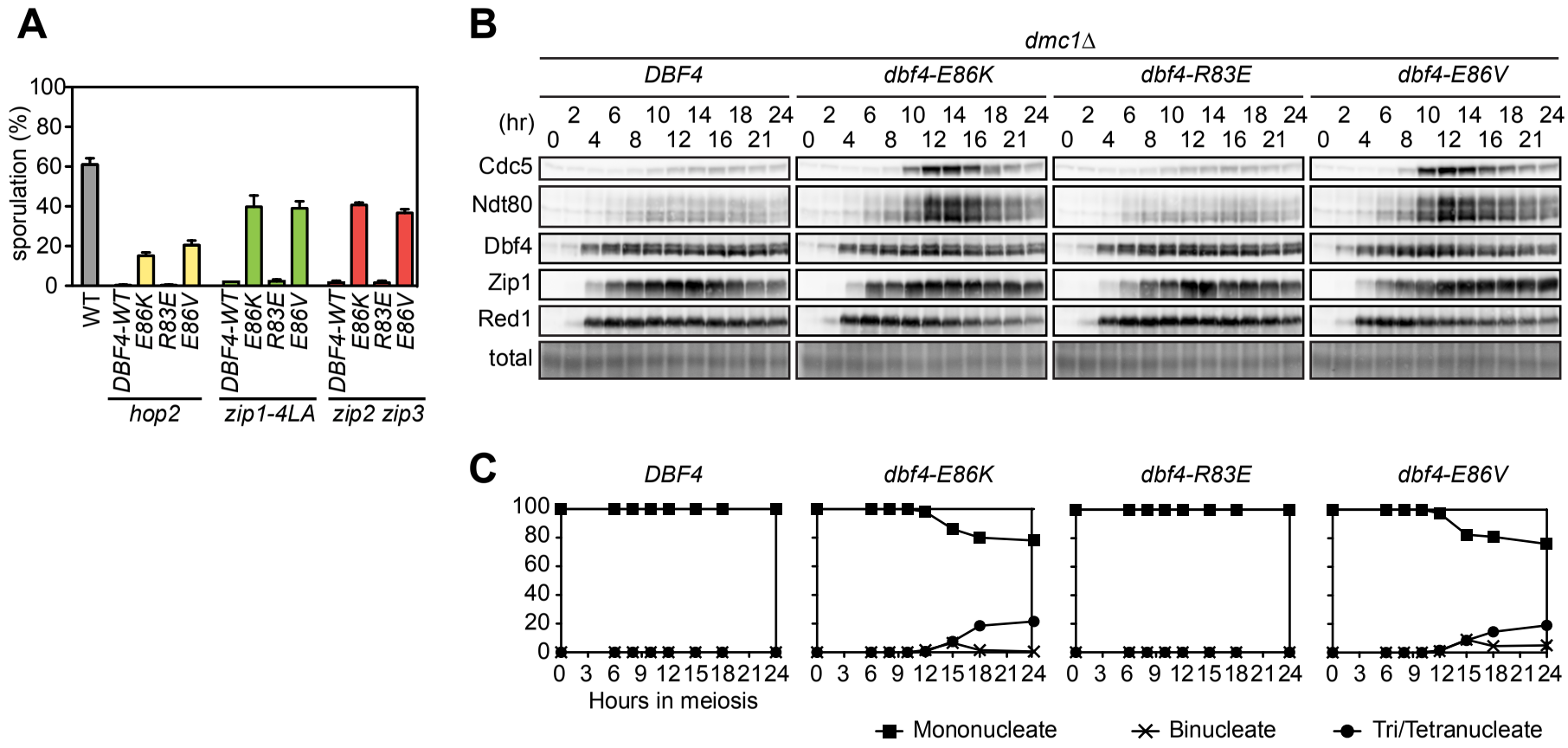
A
sporulation (%)
100
80
60
40
20
0
WT
DBF4-WT
E86K
R83E
E86V
DBF4-WT
E86K
R83E
E86V
DBF4-WT
E86K
R83E
E86V
hop2
zip1-4LA
zip2 zip3
B
dmc1Δ
DBF4
dbf4-E86K
dbf4-R83E
dbf4-E86V
(hr)
0 2 4 6 8 10 12 14 16 18 21 24
Cdc5
Ndt80
Dbf4
Zip1
Red1
total
C
DBF4
dbf4-E86K
dbf4-R83E
dbf4-E86V
100
80
60
40
20
0
0 3 6 9 12 15 18 21 24
Hours in meiosis
Mononucleate
Binucleate
Tri/Tetranucleate

monitored by staining cells with DAPI, a fluorescent dye that intercalates with DNA. Entry into meiosis was examined by blotting for proteins that are produced in early prophase: all strains showed similar levels of Dbf4, Red1 and Zip1 at the early time points (2 hours and 4 hours) (**Figure 3.3B**), indicating that the meiotic programme was initiated in a consistent manner across strains. Although a general increase in both Ndt80 and Cdc5 was seen across all four strains, the robust induction of these proteins was only seen in the *DBF4-E86K/V* mutants (**Figure 3.3B**, peak at ~ 12 hours), suggesting that the enhanced interaction between Dbf4 and basal levels of Cdc5 leads to pachytene exit through production and activation of Ndt80. In conjunction with this, binucleate cells (i.e., those that have completed meiosis I) could be seen at the 12 and 15 hour time points (**Figure 3.3C**). By the 24 hour time point, ~20% of *dbf4-E86K/V* cells had managed to exit pachytene and progress through the cell cycle to form triads/tetrads. These data suggest that Dbf4 interacts with Cdc5 to exert its effect on meiotic progression.

3.4 The Cdc5-Dbf4 fusion can suppress the meiotic cell cycle arrest of the *dmc1Δ* mutant

It is possible that the effect brought about by the Dbf4-E86K/V mutation is independent of its biochemical interaction with Cdc5. For example, it is formally possible that these mutations in particular reduce Dbf4's ability to activate Cdc7, resulting in reduced DDK activity. Since DDK is required for meiotic DSB formation (Sasanuma et al., 2008; Wan et al., 2008), reduction in DDK activity could lead to a reduction in DSBs, which would act in favour of cell cycle progression by reducing the amount of damage available for detection by the

checkpoint. To rule out such possibilities, I reasoned that, if the enhanced interaction between Dbf4 and Cdc5 is the reason for meiotic progression, then pachytene arrested meiotic HR mutants expressing a fusion protein of Dbf4 and Cdc5 should be able to sporulate. In this scenario, Dbf4's Cdc5 interaction motif is irrelevant since the two proteins are artificially kept within close proximity by covalent linkage. To test this possibility, the ORFs of *CDC5* and *dbf4-R83E* were fused together, with a five residue alanine linker placed in between. Dbf4-R83E was used to construct the chimera to prevent potential inter-chimera interactions that might promote cell cycle progression. The chimeric construct was placed under the control of the *DBF4* promoter (P_{DBF4}-*CDC5-dbf4-R83E*) and integrated at the *URA3* locus in the *dmc1Δ* mutant background, with *DBF4* or *dbf4-R83E* at the native *DBF4* locus. The *dbf4-R83E* background was included to exclude the possibility that any potential cell cycle progression was a consequence of interactions between Dbf4 and the Cdc5-Dbf4-R83E chimera. Encouragingly, the chimera allowed *dmc1Δ* cells to complete meiosis in both *DBF4* and *dbf4-R83E* backgrounds (**Figure 3.4B**). Compared to *dmc1Δ dbf4-E86V*, the production of Ndt80 and Cdc5, and subsequent progression through meiosis was delayed in cells expressing the chimera (**Figure 3.4A, B**). Nonetheless, these data suggest that enforcing the interaction between Dbf4 and Cdc5 via covalent linkage is also able to suppress the cell cycle arrest of *dmc1Δ* cells.

Overproduction of Cdc5 was previously reported to promote cell cycle progression of meiotic HR mutants in the BR1919/BR2495 backgrounds (Acosta et al., 2011). Thus, it is possible that production of the Cdc5-Dbf4-R83E chimera promotes cell cycle progression through only the Cdc5 component of

Figure 3.4. The Cdc5-Dbf4 chimera can suppress the meiotic arrest of *dmc1Δ* cells.

A, B, C The indicated strains carrying a transgene at the *URA3* locus (ectopic) were synchronously introduced into meiosis and proteins extracts were subjected to immunoblotting (panels) and cell cycle progression was monitored by fluorescent microscopy of DAPI stained cells (graphs). Error bars ±SEM, n = 2. **D** Sporulation was monitored in the indicated strains after 48 hours of incubation on an SPM plate. The top row of the x-axis label denotes the allele at the native *DBF4* locus and the bottom row denotes the transgene integrated at *URA3*. Error bars ±SEM, n = 3.

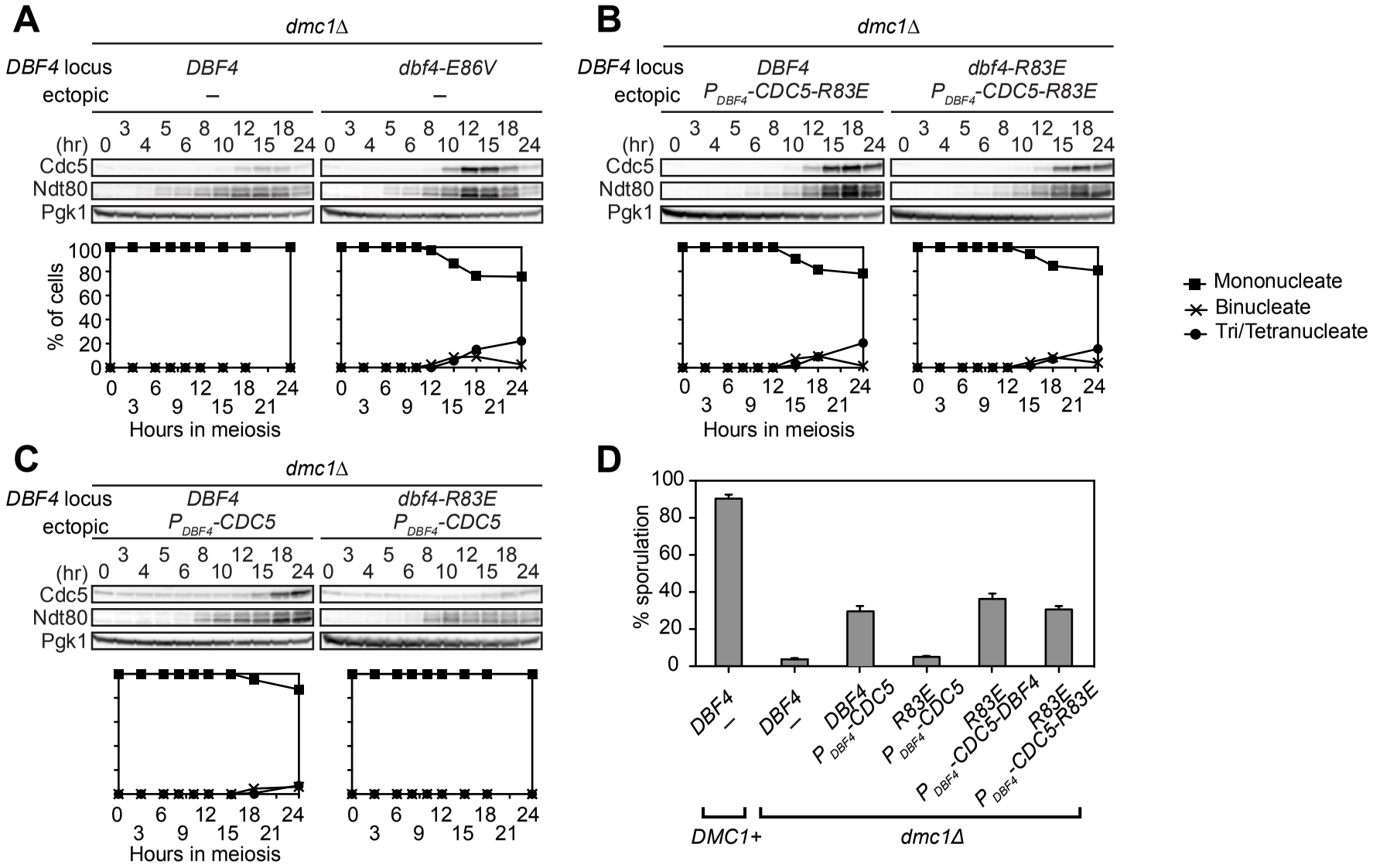
A
dmc1Δ
DBF4 locus
ectopic
DBF4
–
dbf4-E86V
–
(hr)
Cdc5
Ndt80
Pgk1
% of cells
Hours in meiosis
B
dmc1Δ
DBF4 locus
ectopic
DBF4
P DBF4 -CDC5-R83E
dbf4-R83E
P DBF4 -CDC5-R83E
Hours in meiosis
C
dmc1Δ
DBF4 locus
ectopic
DBF4
P DBF4 -CDC5
dbf4-R83E
P DBF4 -CDC5
Hours in meiosis
D
% sporulation
DBF4 –
DBF4 –
DBF4 P DBF4 -CDC5
R83E P DBF4 -CDC5
R83E P DBF4 -CDC5-DBF4
R83E P DBF4 -CDC5-R83E
DMC1+
dmc1Δ
Mononucleate
Binucleate
Tri/Tetranucleate

Figure 3.4 (continued). The Cdc5-Dbf4 chimera can suppress the meiotic arrest of *dmc1Δ* cells.

E Meiotic chromosomes from synchronously sporulating strains were examined by pulsed-field gel electrophoresis followed by Southern blotting (panel). The percentage of signal corresponding to broken chromosomes was plotted (graph). Error bars ±SEM, n = 2. **F** The indicated strains were synchronously introduced into meiosis and proteins extracts were subjected to immunoblotting. Black arrowheads designate the presence of a slow migrating band that reacts to Cdc5/Dbf4 antibodies and is only seen in strains carrying the *CDC5-DBF4* or *CDC5-DBF4-R83E* chimera at *URA3*. Overexposed images are included to better display this band.

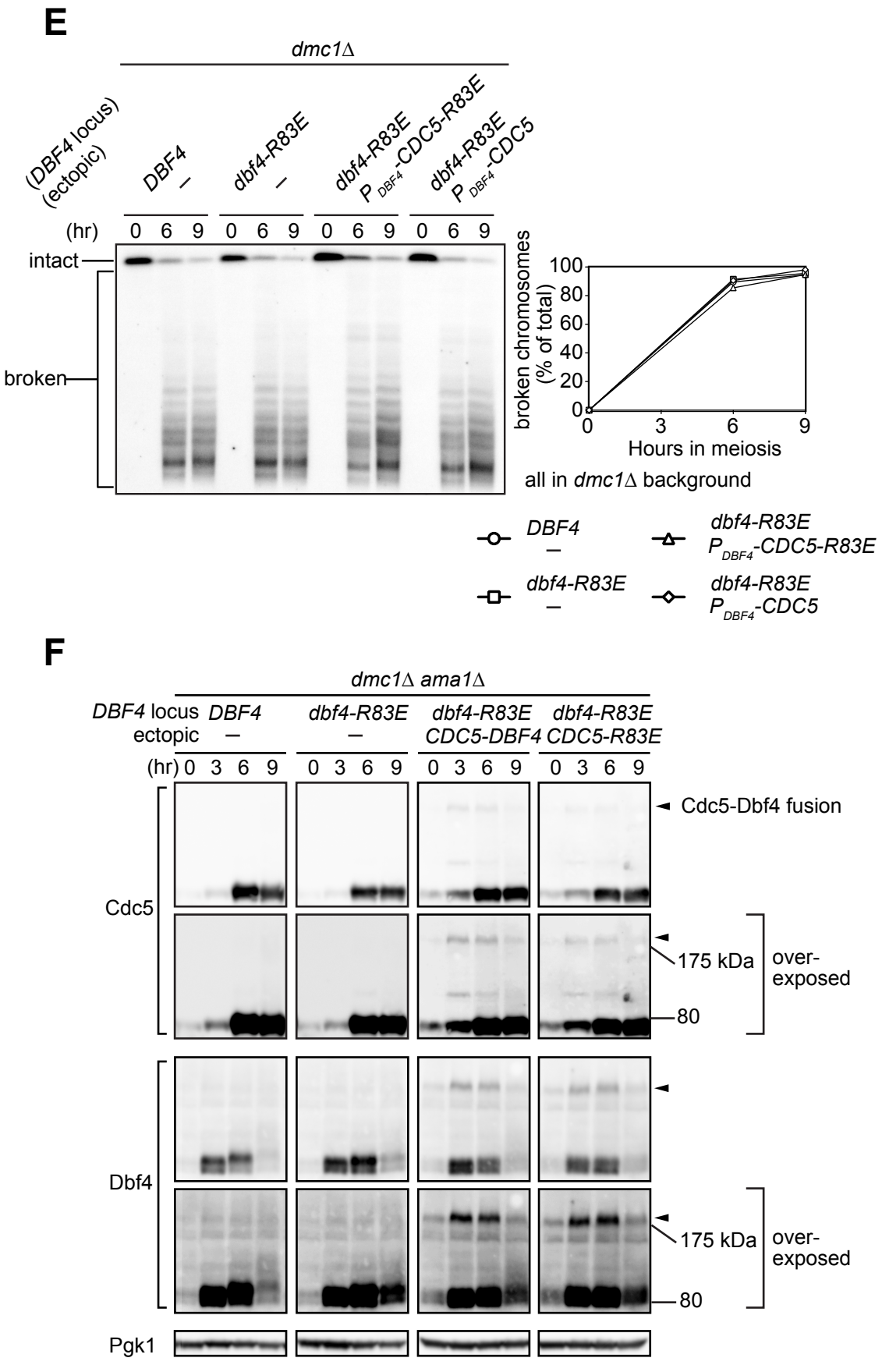
E
dmc1Δ
(DBF4 locus)
(ectopic)
DBF4
—
dbf4-R83E
—
dbf4-R83E
P DBF4-CDC5-R83E
dbf4-R83E
P DBF4-CDC5
(hr)
0 6 9 0 6 9 0 6 9 0 6 9
intact
broken
broken chromosomes
(% of total)
100
80
60
40
20
0
0 3 6 9
Hours in meiosis
all in dmc1Δ background
DBF4
—
dbf4-R83E
P DBF4-CDC5-R83E
dbf4-R83E
—
dbf4-R83E
P DBF4-CDC5
F
dmc1Δ ama1Δ
DBF4 locus
ectopic
DBF4
—
dbf4-R83E
—
dbf4-R83E
CDC5-DBF4
dbf4-R83E
CDC5-R83E
(hr) 0 3 6 9 0 3 6 9 0 3 6 9 0 3 6 9
Cdc5
Cdc5-Dbf4 fusion
175 kDa
80
over-
exposed
Dbf4
175 kDa
80
over-
exposed
Pgk1

the fusion construct. To test this possibility, P_{DBF4}-*CDC5* was integrated at the *URA3* locus in the *dmc1Δ* mutant, with *DBF4* or *dbf4-R83E* at the native *DBF4* locus. As expected, Cdc5 could be detected throughout early time points at levels that are lower than when Ndt80 is induced but higher than that seen in the corresponding strains without any insertion at *URA3* (**Figure 3.4A, C**). As with the cell cycle progression seen in the cells expressing the chimera, upregulation of Ndt80 and Cdc5 was delayed relative to the *dbf4-E86V* strain, but triads and tetrads could eventually be detected, albeit at lower levels (**Figure 3.4C**, graphs). However, in the *dbf4-R83E* counterpart, there was no robust upregulation of Ndt80 and Cdc5, and no dyads/triads/tetrads could be seen by the 24 hour time point, suggesting that cells remained in pachytene. This difference is more clearly demonstrated when sporulation was monitored after 48 hours on an SPM plate (**Figure 3.4D**). Firstly, these data suggest that the cell cycle progression seen in the chimera strains is due to the fusion of Dbf4 and Cdc5, and not due solely to the Cdc5 component of the chimera. Secondly, this data suggests that the previously reported role of Cdc5 in promoting cell cycle progression in meiotic HR mutants (Acosta et al., 2011) requires its interaction with Dbf4.

It is formally possible that the presence of the chimera in *dmc1Δ* cells disrupts DSB formation, which would act in favour of cell cycle progression. To address this possibility, the indicated strains were introduced into meiosis and their chromosomes were monitored through a combination of pulsed-field gel electrophoresis and Southern blotting with a chromosome II probe (**Figure 3.4E**). This technique exploits the difference in electrophoretic mobility between large DNA molecules and small DNA molecules. A large intact chromosome will

migrate slowly through an agarose gel. However, once this large molecule suffers a DSB, it is smaller and thus better able to navigate the gel and migrates further through it. This DNA can subsequently be transferred to a membrane and hybridised with a radioactive probe that anneals to the ends of a particular chromosome's arms. Thus, the kinetics of DSB formation/repair can be monitored. In comparison to strains that did not show cell cycle progression, the chimera strain accumulated almost identical amounts of DSBs (**Figure 3.4E**), arguing against the possibility that chimera-dependent progression is due to a reduction in DSBs.

The relative delay in the chimera-dependent pachytene exit was intriguing. In theory, the covalent linkage of Dbf4 with Cdc5 should result in a more robust phenotype than simply enhancing the non-covalent interaction between Dbf4 and Cdc5; this is not the case. In fact, the progression phenotype is milder in cells expressing the chimera. Combined with the fact that the chimeric construct could not be detected on a western blot with Cdc5 antibodies (data not shown), these discrepancies suggest that the chimera could be unstable. There are two reasons why this might be the case. Firstly, Dbf4 contains a D-box that is recognised by the APC/C and utilised for Dbf4 destruction (Ferreira et al., 2000). Secondly, Cdc5 has been shown to also be targeted for destruction in a manner that is dependent on the APC/C activator Ama1 (Okaz et al., 2012). Since each chimera molecule contains both of these motifs, it is likely targeted for destruction through both pathways. To test this possibility, *AMA1* was deleted and western blotting was performed with both anti-Cdc5 and anti-Db4 antibodies. A band that matches the approximate size of the chimera (~160 kDa) and reacts to both antibodies was seen only in the

strains expressing the chimera in the absence of Ama1 (**Figure 3.4F**), suggesting that the levels of the chimera in the presence of Ama1 are not detectable by western blotting. This goes some way to explaining why the chimera confers a relatively mild progression phenotype.

3.5 Conclusions

Having confirmed that *DBF4* is a multicopy suppressor of the pachytene arrest seen in meiotic HR mutant, I went on to show that this suppression involves an interaction with Cdc5. More specifically, I showed that arrest could be suppressed by enhancing or enforcing the interaction between Dbf4 and Cdc5. Taken together, the data presented in this chapter provides strong evidence that Dbf4 and Cdc5 interact at the end of pachytene to regulate cell cycle progression in meiotic HR mutants.

Chapter 4: Enhanced Dbf4-Cdc5 Interaction Promotes Cell Cycle Progression Through Rad51-Dependent DSB Repair

There are two possible explanations for the cell cycle progression seen in meiotic HR mutants expressing Dbf4-E86K/V. One possibility is that enhancing the interaction between Dbf4 and Cdc5 disrupts the recombination checkpoint's ability to enforce cell cycle arrest, leading to cells with persisting DSBs exiting pachytene and progressing through meiosis. Alternatively, it is possible that when Dbf4 and Cdc5 interact with increased affinity, DSBs are repaired independently of the meiotic recombination machinery, leading to exit from pachytene. This chapter describes how these two possibilities were explored.

4.1 *dbf4-E86K/V* cells enter metaphase I without DSBs in the absence of Hop2

I employed Rad51 as a marker for DNA damage and used spindle morphology to determine the stage of the meiotic cell cycle that a particular cell was in (Lydall et al., 1996). Thus, by spreading meiotic nuclei and performing immunofluorescence microscopy with antibodies for Rad51 and tubulin, it is possible to determine whether cells are progressing to metaphase I with unrepaired DSBs. The BR1919 background was used as it is more receptive to spreading of nuclei. A true defect in the checkpoint will lead to cells displaying the characteristic metaphase I spindle with Rad51 foci; this is seen when the checkpoint gene *RAD17* is deleted in the *hop2Δ* background (**Figure 4.1A**) (Lydall et al., 1996). As expected, all cells from the *hop2Δ* single mutant displayed prophase I spindle morphology with robust Rad51 staining 28 hours into meiosis, as did the *hop2Δ dbf4-R83E* strain; this is indicative of pachytene

Figure 4.1. *hop2Δ dbf4-E86K/V* cells enter metaphase I without cytological signs of DNA damage.

A *hop2Δ* strains carrying the indicated *DBF4* alleles were introduced into meiosis and cells were harvested at 28 hours, except for the *hop2Δ rad17Δ* strain, for which cells were harvested at 22 hours. Harvested cells were lysed and chromosomes were surface-spread and analysed by immunofluorescence microscopy. **B** Summary of data presented in **A**. 150 nuclei were scored.

A

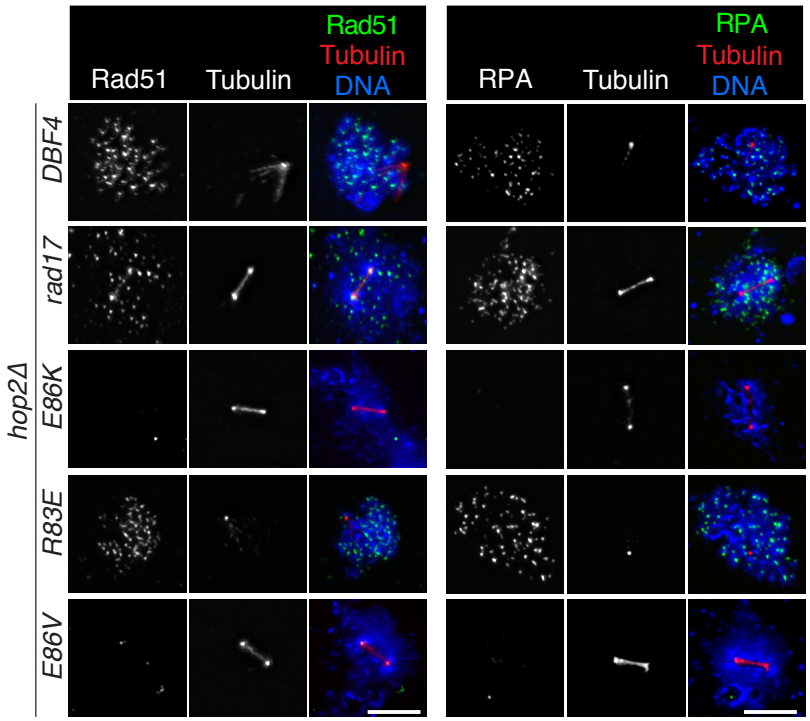

B

Genotype	% with metaphase spindle	% with metaphase spindle and damage marker
Rad51 staining		
hop2Δ DBF4	0.0	NA
hop2Δ rad17	20.0	100
hop2Δ dbf4-E86K	14.7	0
hop2Δ dbf4-R83E	0.0	NA
hop2Δ dbf4-E86V	15.3	0
RPA staining		
hop2Δ DBF4	0.0	NA
hop2Δ rad17	23.3	100
hop2Δ dbf4-E86K	14.0	0
hop2Δ dbf4-R83E	0.0	NA
hop2Δ dbf4-E86V	12.0	0

arrest with unrepaired DSBs (**Figure 4.1A**). In contrast, ~15% of *dbf4-E86K/V* cells at the same time point had metaphase I spindles, indicating meiotic progression; strikingly, none of these cells contained Rad51 foci, suggesting that DSBs are repaired before cells progress to metaphase I (**Figure 4.1A, B**). To confirm these results, the experiment was repeated with replication protein A (RPA) as the damage marker. As with Rad51, RPA signal indicates the presence of ssDNA, which arises due to resection following DSB formation (Krogh & Symington, 2004). Spreads were immunostained with antibodies against tubulin and Rfa1, a subunit of RPA (Brill & Stillman, 1991); the results mirror that which was seen when Rad51 was employed as the damage marker (**Figure 4.1A, B**). These results indicate that cell cycle progression to metaphase I is only seen in *dbf4-E86K/V* and the cells that do progress lack any cytological signs of DNA damage, suggesting that cell cycle progression is caused by DSB repair.

4.2 Enhancing the Dbf4-Cdc5 interaction promotes Rad51-dependent repair of meiotic DSBs

To directly examine the possibility that Dbf4 and Cdc5 interact to regulate meiotic DSB repair, the kinetics of meiotic DSB repair was monitored in the SK1 background. In *dmc1Δ* cells, there was little sign of DSB repair even at the 18 hour time point (**Figure 4.2A**). In contrast, the smear corresponding to broken chromosomes was noticeably reduced at the 18 hour time point in *dmc1Δ dbf4-E86V* cells. Moreover, the band corresponding to intact chromosomes reappeared in these cells, indicating that the broken chromosomal fragments were reassembled into intact chromosomes.

Figure 4.2. DSBs in *dmc1Δ dbf4-E86V* cells are repaired by Rad51.

A *dmc1Δ* cells with *DBF4* or *dbf4-E86V* at the native *DBF4* locus were synchronously introduced into meiosis and meiotic chromosomes were examined by pulsed-field gel electrophoresis followed by Southern blotting (panels). The percentage of signal corresponding to broken chromosomes was plotted (graph). Error bars ±SEM, n = 2. **B** Meiotic chromosomes from *rad51Δ dmc1Δ dbf4-E86V* cells were examined as in **A**.

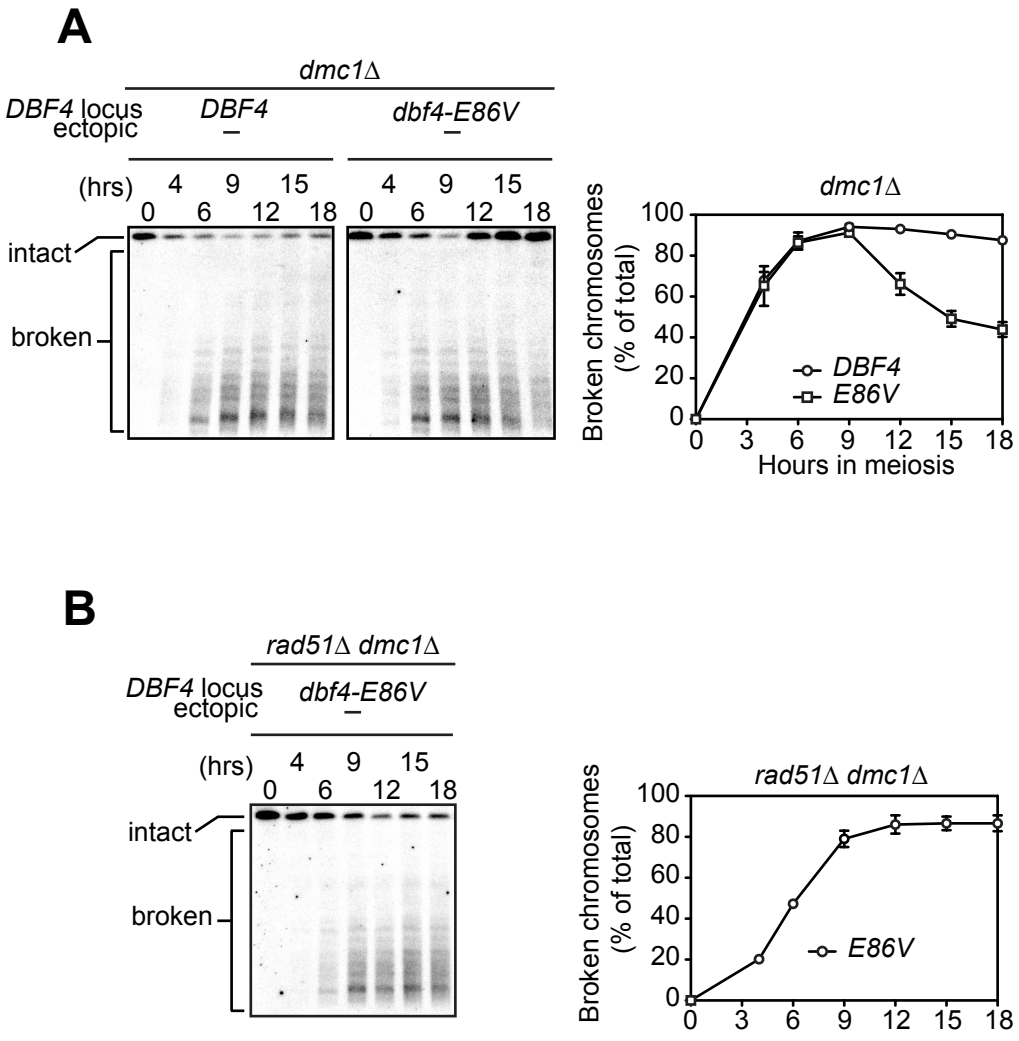
A
dmc1Δ
DBF4 locus
ectopic
DBF4
dbf4-E86V
(hrs)
4 9 15 4 9 15
0 6 12 18 0 6 12 18
intact
broken
dmc1Δ
Broken chromosomes (% of total)
100
80
60
40
20
0
DBF4
E86V
0 3 6 9 12 15 18
Hours in meiosis
B
rad51Δ dmc1Δ
DBF4 locus
ectopic
dbf4-E86V
(hrs)
4 9 15
0 6 12 18
intact
broken
rad51Δ dmc1Δ
Broken chromosomes (% of total)
100
80
60
40
20
0
E86V
0 3 6 9 12 15 18

Despite Rad51 being present in meiotic cells, its activity is suppressed by multiple pathways to promote Dmc1-dependent strand exchange, which is thought to occur preferentially between homologous chromosomes as opposed to sister chromatids (Neale & Keeney, 2006). Hence, even in the absence of Dmc1, Rad51 is unable to repair DSBs, as shown in **Figure 4.2A**. One possible explanation for the DNA repair seen in the *dbf4-E86V* strain is that Rad51 inhibition is ablated when the interaction between Dbf4 and Cdc5 is enhanced. To determine if this is true, the *RAD51* gene was deleted and DSB repair was monitored. Unlike in the *dmc1Δ dbf4-E86V* strain, the *dmc1Δ rad51Δ dbf4-E86V* strain showed no signs of DSB repair by the 18 hour time point (**Figure 4.2B**), indicating that the repair seen in the *dmc1Δ dbf4-E86V* strain is dependent on Rad51. These findings suggest that, when the interaction between Dbf4 and Cdc5 is enhanced, Rad51 is freed from its inhibition and is able to repair meiotic DSBs independently of Dmc1.

4.3 Efficient DSB repair is likely not associated with the formation of interhomologue crossovers

Meiotic DSBs can be repaired through sister chromatids or homologous chromosomes, but only the latter has the potential to facilitate faithful chromosome segregation. Although *dmc1Δ* cells show a very low level of sporulation (~1%), Tsubouchi & Roeder (2006) managed to demonstrate that the viability of these spores is severely reduced (~1%). In this case, spore inviability is likely a combination of unrepaired DSBs and chromosome missegregation. However, in the *spo11Δ* mutant where meiotic DSBs are not induced, spore inviability is solely the consequence of gross chromosome

missegregation (Klapholz et al., 1985). Thus, it is impossible to separate these two possibilities in the *dmc1Δ dbf4-E86V* mutant where DSB repair is incomplete i.e., any spore inviability may be a consequence of persisting DNA damage and/or chromosome missegregation. Since overproduction of WT Dbf4 phenocopied the normal production of Dbf4-E86V with regards to suppression of pachytene arrest, I hypothesised that the suppression phenotype, and hence DSB repair, could be further improved by the overproduction of Dbf4-E86V. Thus, an additional copy of the *dbf4-E86V* allele with 3'- and 5'-UTRs was integrated at an ectopic location in each parent haploid so that the diploid strain would have two extra copies of *dbf4-E86V*, with the idea that this would exaggerate the repair phenotype. This strain will be referred to as the double dosage strain hereafter.

The double dosage strain was induced into meiosis and meiotic DSBs were analysed as before. Encouragingly, the extent of DSB repair was substantially increased compared to the regular *dbf4-E86V* strain; by the 18 hour time point, broken chromosomal fragments were barely detectable (**Figure 4.3A**). In addition, suppression of *dmc1Δ* arrest was drastically improved in the double dosage strain. Whereas *dmc1Δ* cells with WT *DBF4* showed 1% sporulation after 48 hours, *dbf4-E86V* and double dosage cells showed 18% and 52% sporulation, respectively. Consistent with the previous result, the DSB repair seen in the double dosage strain was also shown to be Rad51-dependent (**Figure 4.3B**).

DSB repair in the double dosage strain is nearly complete by the 18 hour time point (**Figure 4.3A**). Thus, cells were sporulated on a plate for 48 hours and tetrads were dissected. Although *dbf4-E86V* seemed to marginally improve

Figure 4.3. DSB repair conferred by *dbf4-E86V* does not suppress the inviability of *dmc1Δ* spores.

A *dmc1Δ* cells with *dbf4-E86V* at the native locus and homozygous *dbf4-E86V* integrated at the *URA3* locus were introduced synchronously into meiosis and chromosomes were examined by pulsed-field gel electrophoresis followed by Southern blotting (panel). The percentage of signal corresponding to broken chromosomes was plotted (graph). Error bars ±SEM, n = 2. **B** Meiotic chromosomes from *rad51Δ dmc1Δ dbf4-E86V* cells with homozygous *dbf4-E86V* integrated at the *URA3* locus were examined as in **A**. **C** Spore viability in the indicated strains was determined by tetrad dissection (40 tetrads dissected).

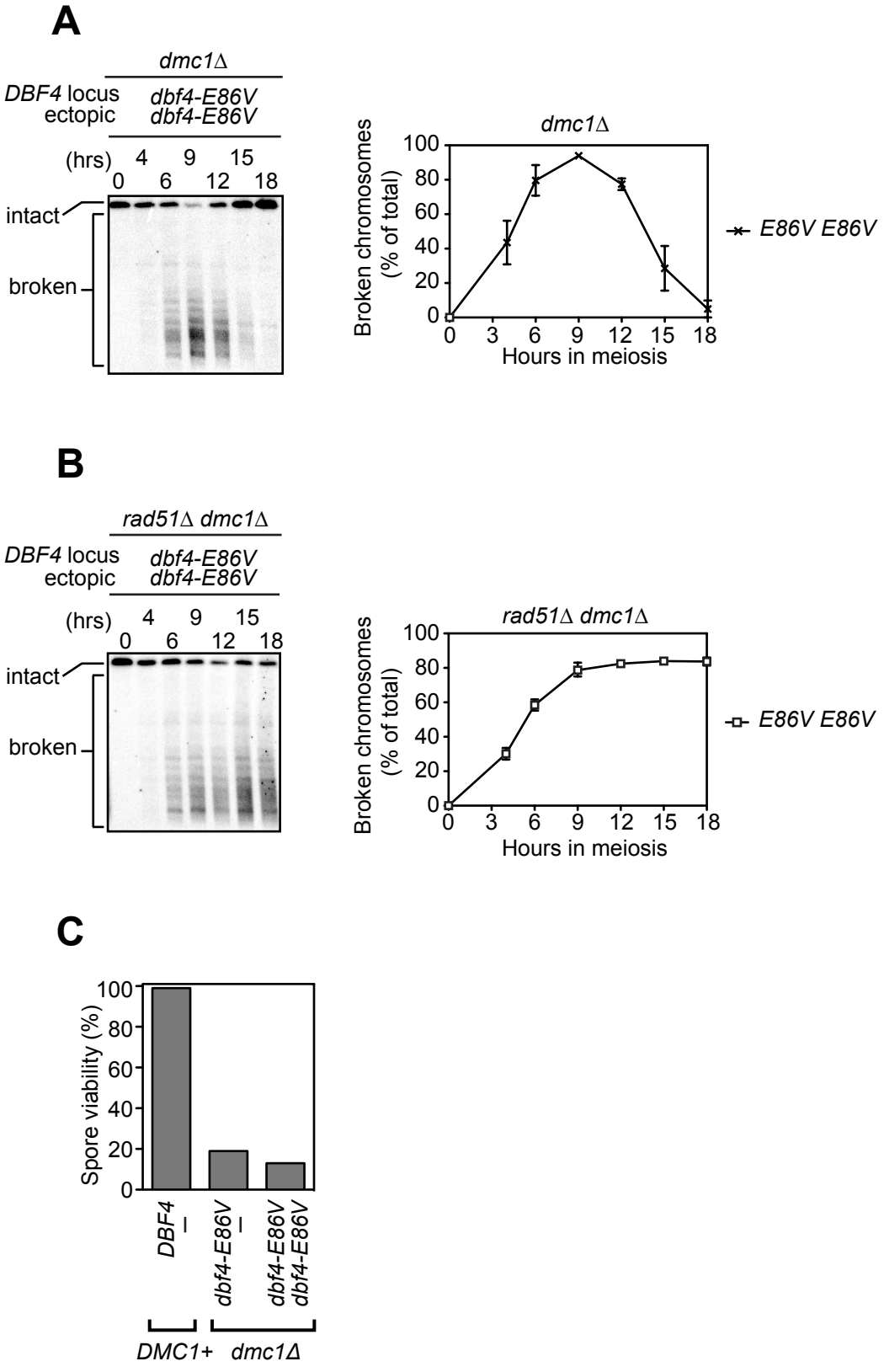
A
dmc1Δ
DBF4 locus
ectopic
dbf4-E86V
dbf4-E86V
(hrs)
0
4
6
9
12
15
18
intact
broken
dmc1Δ
Broken chromosomes
(% of total)
100
80
60
40
20
0
0
3
6
9
12
15
18
Hours in meiosis
E86V E86V
B
rad51Δ dmc1Δ
DBF4 locus
ectopic
dbf4-E86V
dbf4-E86V
(hrs)
0
4
6
9
12
15
18
intact
broken
rad51Δ dmc1Δ
Broken chromosomes
(% of total)
100
80
60
40
20
0
0
3
6
9
12
15
18
Hours in meiosis
E86V E86V
C
Spore viability (%)
100
80
60
40
20
0
DBF4
–
dbf4-E86V
–
dbf4-E86V
dbf4-E86V
DMC1+
dmc1Δ

the viability of *dmc1Δ* spores, the double dosage strain showed an even lower viability than the *dbf4-E86V* strain (**Figure 4.3C**), despite near-complete DSB repair. These data suggest that the reason both *dbf4-E86V* strains in the *dmc1Δ* background exhibit such low levels of viability, irrespective of the extent of DSB repair, is because DSB repair is unproductive with regards to interhomologue crossover formation i.e., these spores likely undergo gross chromosome missegregation due to insufficient interhomologue crossovers.

4.4 Conclusions

In this chapter, I provided evidence that the Dbf4-Cdc5 interaction regulates meiotic HR as opposed to the recombination checkpoint. By utilising both immunofluorescence microscopy and pulsed-field gel electrophoresis followed by Southern blotting, I have provided evidence that when Dbf4 undergoes a high affinity interaction with Cdc5, the mitotic recombination machinery (i.e., Rad51) is relieved of its meiotic inhibition, leading to DSB repair; this occurs before metaphase I since there are no signs of DNA damage by this stage of meiosis. However, despite being able to efficiently repair DSBs, the mitotic machinery is unable to compensate for the loss of the meiotic machinery since the vast majority of spores are inviable, likely because the mitotic machinery is unable to generate productive interhomologue crossovers.

Chapter 5: Dbf4-Cdc5 Interaction Strength is a Key Parameter for Triggering Synaptonemal Complex Disassembly and Rad51-Dependent DSB Repair

There are multiple pathways that act to establish a recombination bias in meiosis. For example, the meiosis-specific Hed1 protein abrogates Rad51's interaction with its accessory factor, Rad54, thereby limiting Rad51's recombinase activity (Busygina et al., 2008). Furthermore, SC proteins Red1, Hop1 and Mek1 have been shown to play crucial roles in ensuring that recombination takes place preferentially between homologous chromosomes as opposed to sister chromatids (Schwacha & Kleckner, 1997; Niu et al., 2005; Niu et al., 2009). Since Cdc5 was previously shown to be the only member of the Ndt80 regulon that is required for SC disassembly during the prophase I to metaphase I transition (Sourirajan & Lichten, 2008), I hypothesised that Cdc5's ability to remove the SC may involve Dbf4. This chapter describes how this possibility was examined.

5.1 Dbf4-Cdc5 interaction strength modulates SC disassembly

In order to determine whether the Dbf4-Cdc5 interaction plays a role in SC disassembly, the system employed by Sourirajan & Lichten (2008) was adopted. In the *ndt80Δ* mutant, cells arrest at the end of pachytene without the robust induction of Cdc5 (Clyne et al., 2003). These cells typically display fully linear SC, as visualised by immunofluorescence cytology using antibodies raised against Zip1 and Red1 (**Figure 5.1A**) (Sourirajan & Lichten, 2008). By placing Cdc5 under the control of the inducible *GAL1* promoter, it is possible to mimic the robust induction of Cdc5 by adding beta-estradiol to cells expressing

Figure 5.1. Dbf4-Cdc5 interaction strength regulates SC disassembly

A Beta-estradiol was added to *ndt80Δ* cells (BR1919) with the indicated genotypes after 20 hours in sporulation medium and meiotic nuclei were examined by immunostaining and categorised as having linear or dotty staining of Zip1 or Red1 (top left panels). The percentage of nuclei with linear Zip1 or Red1 in the indicated strains was scored (top right graph), >80 nuclei were counted per strain. The induction of Cdc5 at the indicated hours after beta-estradiol addition was examined by western blotting (bottom panels).

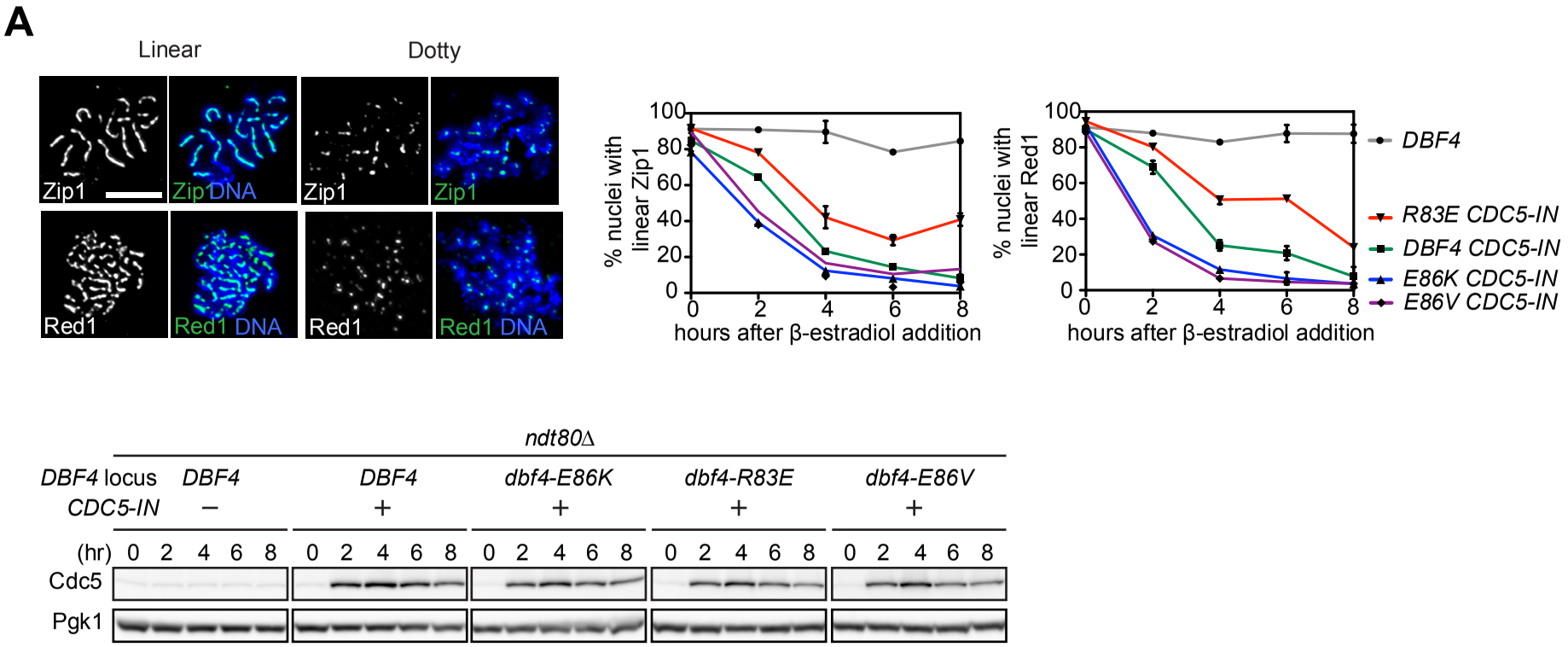
A
Linear
Dotty
Zip1
Zip1 DNA
Zip1
Zip1
Red1
Red1 DNA
Red1
Red1 DNA
% nuclei with linear Zip1
hours after β-estradiol addition
% nuclei with linear Red1
hours after β-estradiol addition
DBF4
R83E CDC5-IN
DBF4 CDC5-IN
E86K CDC5-IN
E86V CDC5-IN
ndt80Δ
DBF4 locus
DBF4
DBF4
dbf4-E86K
dbf4-R83E
dbf4-E86V
CDC5-IN
−
+
+
+
+
(hr) 0 2 4 6 8 0 2 4 6 8 0 2 4 6 8 0 2 4 6 8 0 2 4 6 8
Cdc5
Pgk1

Figure 5.1 (continued). Dbf4-Cdc5 interaction strength regulates SC disassembly

B Beta-estradiol was added to *ndt80Δ* cells (SK1) with the indicated genotypes after 6 hours in sporulation medium and meiotic nuclei were examined by immunostaining and categorised as having linear or dotty staining of Zip1 or Red1 (top left panels). The percentage of nuclei with linear Zip1 or Red1 in the indicated strains was scored (top right graph), >80 nuclei were counted per strain. The induction of Cdc5 at the indicated hours after beta-estradiol addition was examined by western blotting (bottom panels).

B

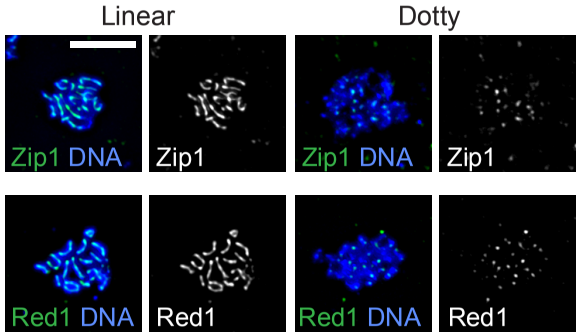
Linear
Dotty
Zip1 DNA
Zip1
Zip1 DNA
Zip1
Red1 DNA
Red1
Red1 DNA
Red1

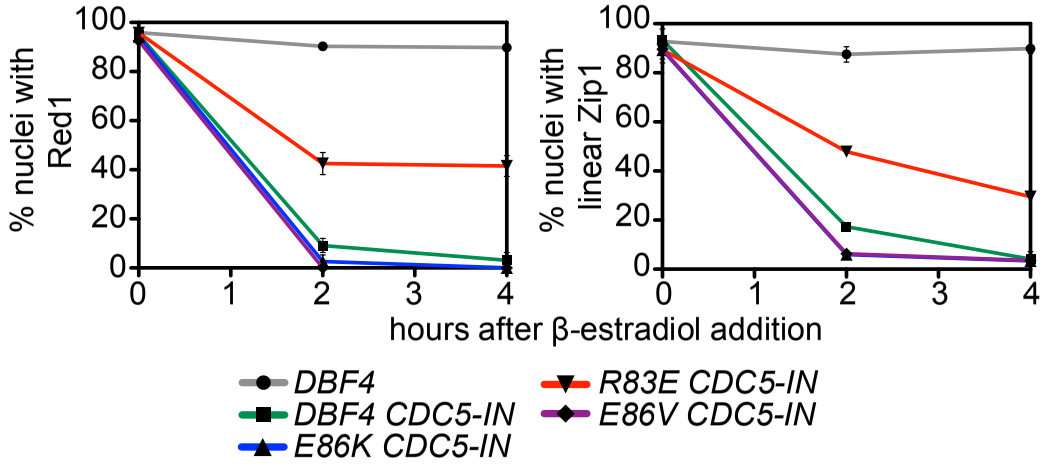
% nuclei with Red1
% nuclei with linear Zip1
100
80
60
40
20
0
0
1
2
3
4
hours after β-estradiol addition
DBF4
DBF4 CDC5-IN
E86K CDC5-IN
R83E CDC5-IN
E86V CDC5-IN

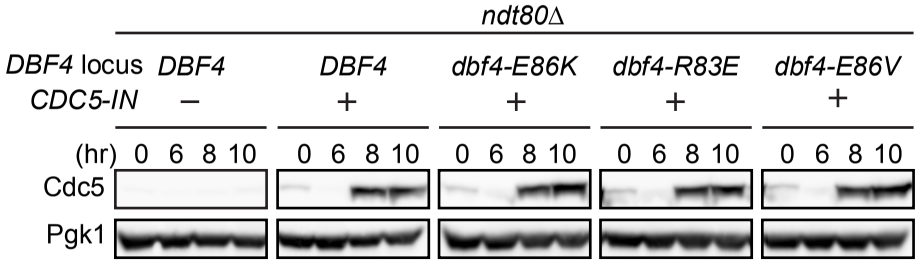
ndt80Δ
DBF4 locus
CDC5-IN
DBF4
–
DBF4
+
dbf4-E86K
+
dbf4-R83E
+
dbf4-E86V
+
(hr) 0 6 8 10
Cdc5
Pgk1

a fusion of the oestrogen receptor and Gal4 transcriptional activator (Benjamin et al., 2003). This inducible allele of *CDC5* will be referred to as *CDC5-IN* hereafter. The artificial synchronisation conferred by deletion of *NDT80* supports the examination of molecular events with higher resolution than would otherwise be possible. Thus, various *DBF4* alleles were combined with *CDC5-IN* in the *ndt80Δ* background. As a negative control, a strain containing WT *DBF4* in the *ndt80Δ* background without *CDC5-IN* was also constructed.

Dbf4-Cdc5 interaction strength was identified as a strong determinant of SC disassembly efficiency, with a weaker or stronger interaction showing less or more efficient SC disassembly, respectively, when compared with WT interaction strength (**Figure 5.1A**). BR1919 cells were induced to enter meiosis. 20 hours into meiosis, pre-induction samples (0 hours) were harvested for immunofluorescence microscopy and western blotting. Beta-estradiol was then added to the cultures and cells were harvested as before at 2 hour intervals. As expected, in the strain lacking *CDC5-IN*, the addition of beta-estradiol had no effect on SC morphology throughout the time course, with ~90% of nuclei displaying linear Zip1 and Red1 at 0 hours and 8 hours (**Figure 5.1A**). In the *DBF4 CDC5-IN* strain, beta-estradiol addition was followed by a decline in the percentage of nuclei that had linear Zip1 and Red1; at the 4 hour time point, ~20% of nuclei had linear SC proteins. In the presence of Dbf4-E86K/V, induction of Cdc5 was accompanied by a rapid decline in the percentage of nuclei with linear Zip1 and Red1; at the 4 hour time point, only ~10% of nuclei had linear SC proteins. In contrast, the effect of Cdc5 induction was most mild in the *dbf4-R83E* background; at the 4 hour time point, ~50% of nuclei still had

linear SC proteins. In each strain, the induction of Cdc5 was confirmed by western blotting (**Figure 5.1A**).

These experiments were repeated in the SK1 background and similar results were obtained (**Figure 5.1B**). However, the efficiency of SC disassembly was increased in the SK1 background (compare **Figures 5.1** and **5.2**), leading to reduced temporal resolution and a less obvious difference in SC disassembly between WT interaction strength (*DBF4*) and enhanced interaction strength (*DBF4-E86K/V*) strains. These data suggest that Cdc5's ability to dismantle the SC is dependent on its interaction strength with Dbf4, with a stronger interaction showing more efficient SC disassembly.

5.2 Dbf4-Cdc5 interaction strength is closely correlated with unshackling of Rad51 activity

The data presented above raised the possibility that the Rad51-dependent repair seen in the *dmc1Δ dbf4-E86V* mutant is due to Cdc5-dependent dismantling of SC proteins. To test this, *CDC5-IN* was combined with various *DBF4* alleles in the *ndt80Δ dmc1Δ* mutant background. In this background, cells arrest at the end of pachytene with unrepaired DSBs but cannot proceed despite the presence of Dbf4-E86K/V due to the absence of Ndt80. These strains were constructed in the SK1 background.

In all strains examined, ~90% of chromosomes were broken at the 6 hour time point (**Figure 5.2A**). In the control strain lacking *CDC5-IN*, this remained unchanged for the duration of the time course. However, in the *DBF4 CDC5-IN* strain, induction of Cdc5 resulted in DSB repair, such that by the 12 hour time point, ~40% of chromosomes were broken. Moreover, Cdc5 induction

Figure 5.2. Dbf4-Cdc5 interaction strength regulates Rad51-dependent DSB repair in *dmc1Δ* cells.

A Beta-estradiol was added to *dmc1Δ ndt80Δ* cells with the indicated genotypes 6 hours into meiosis and chromosomes were examined by pulsed-field gel electrophoresis followed by Southern blotting (panels). The percentage of signal corresponding to broken chromosomes was plotted (graph). Error bars ±SEM, n = 2. **B** Protein extracts from the same cultures shown in **A** were subjected to immunoblotting. **C** A sporulating *rad51Δ dmc1Δ ndt80Δ CDC5-IN* culture was split 6 hours into meiosis and beta-estradiol was added to one subculture and an equal volume of carrier (ethanol) was added to the other subculture. Meiotic chromosomes were examined as in **A**. The percentage of signal corresponding to broken chromosomes was plotted (graph). Error bars ±SEM, n = 2. **D** Protein extracts from the same cultures shown in **C** were subjected to immunoblotting.

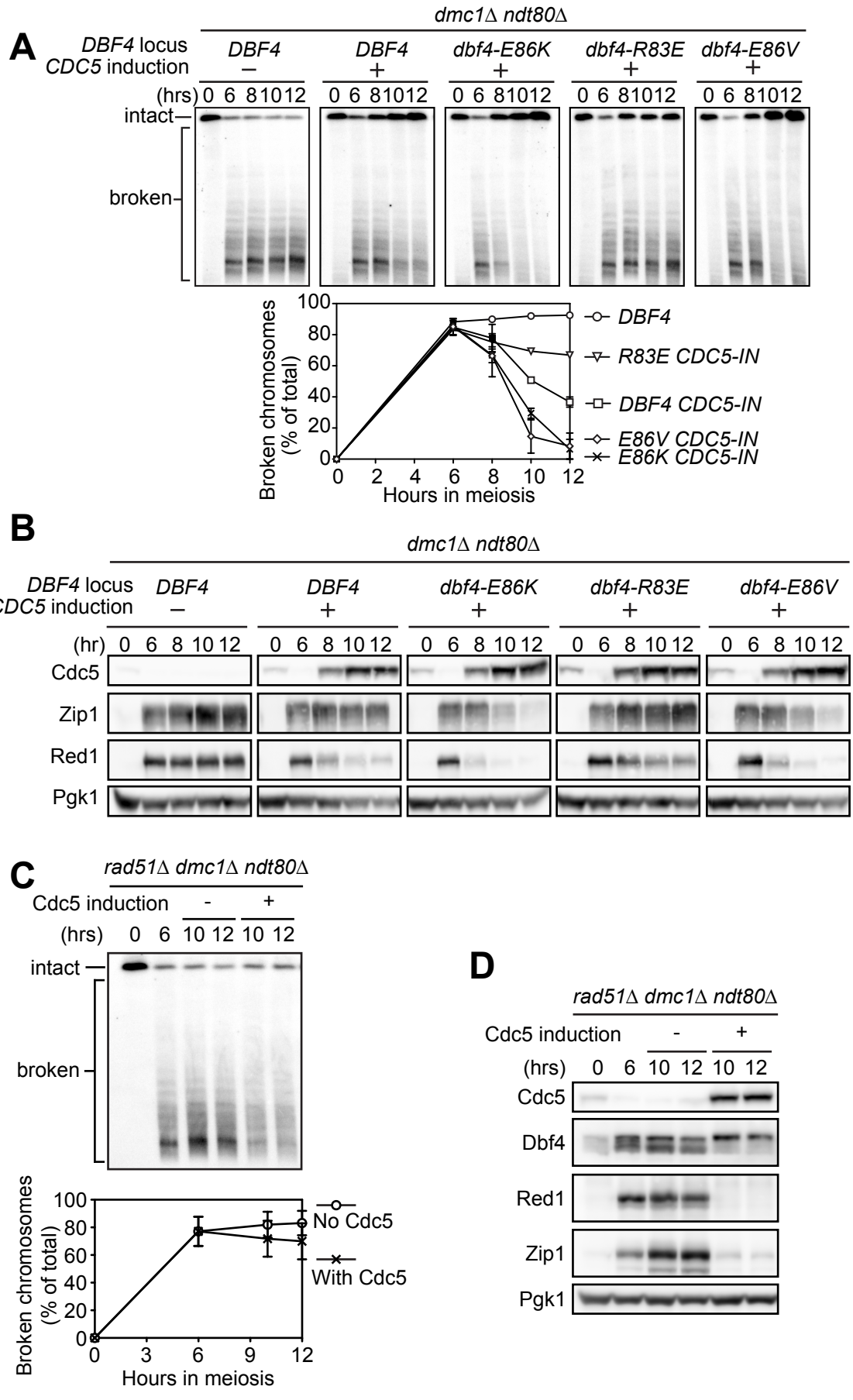
A
dmc1Δ ndt80Δ
DBF4 locus
CDC5 induction
DBF4 –
DBF4 +
dbf4-E86K +
dbf4-R83E +
dbf4-E86V +
(hrs) 0 6 8 10 12
intact
broken
Broken chromosomes (% of total)
Hours in meiosis
DBF4
R83E CDC5-IN
DBF4 CDC5-IN
E86V CDC5-IN
E86K CDC5-IN
B
dmc1Δ ndt80Δ
DBF4 locus
CDC5 induction
(hr)
Cdc5
Zip1
Red1
Pgk1
C
rad51Δ dmc1Δ ndt80Δ
Cdc5 induction
(hrs)
intact
broken
Broken chromosomes (% of total)
Hours in meiosis
No Cdc5
With Cdc5
D
rad51Δ dmc1Δ ndt80Δ
Cdc5 induction
(hrs)
Cdc5
Dbf4
Red1
Zip1
Pgk1

in the *dbf4-E86K/V* strains resulted in more efficient DSB repair, with only ~10% of chromosomes remaining broken at 12 hours. In contrast, Cdc5 induction in the *dbf4-R83E* background resulted in inefficient DSB repair, with cells displaying ~70% broken chromosomes at 12 hours. This trend is consistent with the data presented in **Figure 5.1**. Cdc5 induction was confirmed by western blotting (**Figure 5.2B**). Intriguingly, western blotting against Zip1 and Red1 showed that, rather than simply being removed from chromosomes, Cdc5 induction leads to degradation of SC proteins.

To ensure that the DSB repair seen in the experiments above is mechanistically equivalent to the DSB repair seen in the *dmc1Δ dbf4-E86V* background, *CDC5-IN* was combined with the *rad51Δ dmc1Δ ndt80Δ* mutant. Cells were introduced into meiosis and the culture was split at 6 hours; one subculture was supplemented with beta-estradiol whereas the other received an equal volume of carrier (ethanol). Although a marginal reduction in the percentage of broken chromosomes was observed in the presence of Cdc5 (~10% reduction by 12 hour time point)(**Figure 5.2C**), these data suggest that Cdc5-driven DSB repair within pachytene is dependent on Rad51. In the same time course, protein behaviour was monitored by western blotting. As anticipated, Cdc5 induction lead to the degradation of Zip1 and Red1 (**Figure 5.2D**), but was unable to stimulate DSB repair due to the absence of Rad51; this uncoupling of SC degradation and DSB repair provides clear evidence that Rad51 is crucial for Cdc5-induced DSB repair.

Unsubstantial amounts of recombination in the absence of both Dmc1 and Rad51 has been previously documented (Henry et al., 2006). The small reduction in broken chromosomes in the absence of both recombinases is likely

dependent on Rad52, a recombination mediator that is required for the correct localisation of Rad51 to DSBs and is involved in the single-strand annealing mechanism of HR (Mehta & Haber, 2014).

5.3 Dbf4 and Cdc5 collaborate to regulate SC disassembly in an unperturbed meiosis

The data presented thus far in this chapter indicate that the Dbf4-Cdc5 interaction is important for the timely destruction of the SC proteins Zip1 and Red1. However, in an otherwise WT meiosis, the *dbf4-R83E* strain has no obvious defect; spore viability is 98% compared to 99% in WT (40 tetrads dissected for each strain) and the kinetics of Red1 disappearance are unaffected (**Figure 5.3A**). One possible explanation is that the defect is rather mild and therefore difficult to observe at any single time point in a synchronous time course experiment. Thus, rather than population based analysis, single cell analysis was considered. To this end, the BR1919 background was employed to determine whether the *dbf4-R83E* mutant has a defect in SC disassembly, since this strain background undergoes a relatively asynchronous meiosis and is more receptive to chromosome spreading.

Ndt80 is known to localise to chromosomes soon after it is produced in the form of a cloud (Wang et al., 2011). This Ndt80 cloud can be used as a cytological marker for pachytene exit. By immunostaining both Ndt80 and Zip1, it is possible to visualise the SC during the transition from late prophase I to early metaphase I. In order to visualise Ndt80, a strain in which the *NDT80* ORF is fused to the HA epitope was utilised (Tung et al., 2000). Meiotic nuclei were then assorted into one of three categories based on their immunostaining

Figure 5.3. The Dbf4-Cdc5 interaction regulates SC disassembly in an otherwise wild type meiosis.

A Diploids with the indicated *DBF4* alleles homozygous at the native locus were synchronously introduced into meiosis and protein extracts were examined by immunoblotting. Ponceau stained images of membranes are included as a loading control (total). **B** Indicated strains expressing Ndt80-HA were harvested 16 hours into meiosis and nuclei were surface spread and examined by immunostaining. 200 nuclei were counted per strain and scored based on their staining pattern.

A

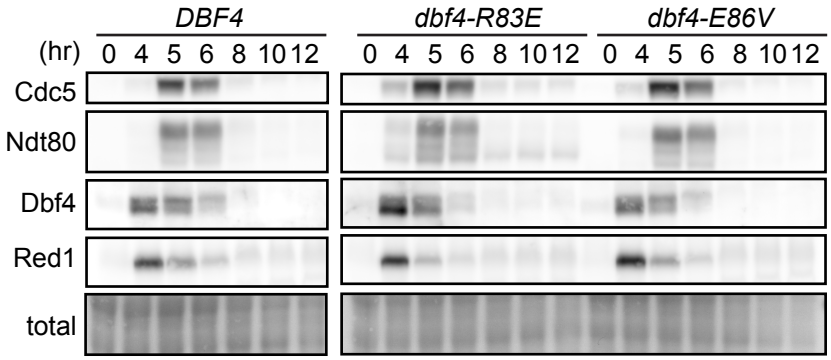
DBF4
dbf4-R83E
dbf4-E86V
(hr) 0 4 5 6 8 10 12
Cdc5
Ndt80
Dbf4
Red1
total

B

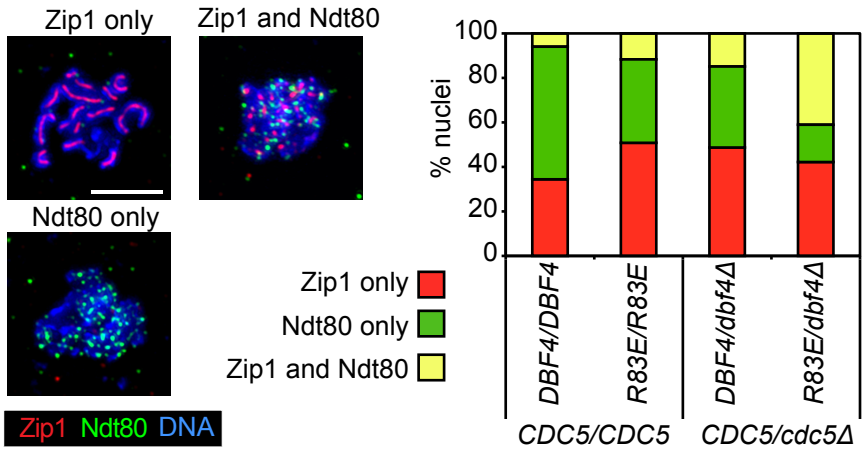
Zip1 only
Zip1 and Ndt80
Ndt80 only
Zip1 Ndt80 DNA
Zip1 only
Ndt80 only
Zip1 and Ndt80
% nuclei
100
80
60
40
20
0
DBF4/DBF4
R83E/R83E
DBF4/dbf4Δ
R83E/dbf4Δ
CDC5/CDC5
CDC5/cdc5Δ

pattern: Zip1 only, Ndt80 only, or both (**Figure 5.3B**, leftmost panels). Nuclei containing both Zip1 and Ndt80 are making the transition from late prophase I to metaphase I and represent cells that are in the process of degrading Zip1.

There was very little difference, if any, between *DBF4* and *dbf4-R83E* diploids (**Figure 5.3B**, leftmost bars on graph). To further deplete cells of Dbf4-Cdc5 complexes, two more strains were made in the *NDT80-HA* background. In both of these diploid strains, one copy of *CDC5* and one copy of *DBF4* is deleted. However, they differ in that one strain has a WT copy of *DBF4* whereas the other strain has *dbf4-R83E* as the sole source of protein. These strains were examined for colocalisation of Ndt80 and Zip1. Although the strain with WT Dbf4 showed only a mild increase in the proportion of nuclei that are double positive for Zip1 and Ndt80 (~10% more than WT), the heterozygous knockout strain with Dbf4-R83E showed an 8-fold increase in the percentage of double positive nuclei compared to WT (**Figure 5.3B**, rightmost bars on graph). These results indicate that, in an undisturbed meiosis, defects in Dbf4-Cdc5 complex formation leads to inefficient SC disassembly.

5.4 Conclusions

In this chapter, I have elucidated how the mitotic recombination machinery is relieved of its meiotic inhibition in the *dmc1Δ dbf4-E86K/V* mutants. An enhanced interaction between Dbf4 and Cdc5 accelerates the speed at which the SC is dismantled, leading to an increase in the rate of Rad51-dependent DSB repair. Conversely, when the Dbf4-Cdc5 interaction is abrogated, there is a substantial delay in SC disassembly and Rad51-dependent DSB repair.

These findings strongly suggest that Dbf4 and Cdc5 interact to trigger SC destruction, which is tightly linked to the liberation of Rad51 activity.

Chapter 6: The Dbf4-Cdc5 Interaction Modulates Cdc5-Dependent Phosphorylation of Dbf4

The primary method of regulating DDK activity was identified as the cyclic production of its regulatory subunit Dbf4, without which Cdc7 is inactive (Cheng et al., 1999). Whereas Cdc5 production is also known to be regulated in a cyclic manner (Hardy & Pautz, 1996), Cdc5 activity was additionally shown to be enhanced through Cdc28-dependent phosphorylation (Mortensen et al., 2005), indicating that phosphorylation is a viable means of regulating Cdc5 kinase activity. When examined by immunoblotting, Dbf4 exists as a doublet in mitotic metaphase, with the identity of the low mobility band being identified as phosphorylated Dbf4 (Ferreira et al., 2000). Dbf4 also exists as a doublet in meiosis (**Figure 3.3B**) (Matos et al., 2008). Interestingly, as cells progressed from prophase I to metaphase I, the electrophoretic mobility of Dbf4 was further reduced, suggesting additional post translational modifications; the appearance of this higher molecular weight species was dependent on the presence of Cdc5 (Matos et al., 2008). Thus, it is likely that Dbf4 undergoes both Cdc5-independent and Cdc5-dependent posttranslational modifications, with the latter occurring during the prophase I to metaphase I transition in meiosis. This chapter describes the characterisation of this posttranslational modification.

6.1 Dbf4 is phosphorylated by Cdc5 within prophase I

Despite concluding that Dbf4 is phosphorylated by Cdc5 in metaphase I-arrested cells, Matos et al. (2008) did not provide any substantial evidence to confirm these claims. Since these cells are arrested in metaphase I, Ndt80 has already been produced and promoted the transcription of ~200 genes that

comprise the Ndt80 regulon, of which Cdc5 is one (Chu & Herskowitz, 1998). Thus, it is formally possible that, although Cdc5 is required for Dbf4 phosphorylation, the actual kinase that phosphorylates Dbf4 is not Cdc5 (e.g., Cdc5 may activate another kinase whose production is also controlled by Ndt80, then this kinase might phosphorylate Dbf4).

I wanted to first test whether a shift to higher molecular weight species can be seen in prophase I-arrested cells. Conveniently, the possibility of another Ndt80-regulated kinase phosphorylating Dbf4 can be excluded by employing the *ndt80Δ* mutant, which also arrests cells at the end of pachytene. The *CDC5-IN* allele was then utilised to achieve inducible production of Cdc5 in the absence of Ndt80. In the absence of Cdc5, Dbf4 persisted as a doublet without any substantial shift to higher or lower molecular weight species (**Figure 6.1A**). However, when Cdc5 was induced at the 6 hour time point, a higher molecular weight species of Dbf4 became apparent at 7.5 hours (indicated by a black arrowhead); this species of Dbf4 migrated even slower than the upper band of the doublet. These results indicate that the production of Cdc5 alone within prophase is sufficient for Dbf4 phosphorylation.

In order to gain further insight into the requirements for Dbf4 phosphorylation, the above experiments were repeated in strains where the Dbf4-Cdc5 interaction is enhanced. Strikingly, in the *dbf4-E86K/V* mutants, the induction of Cdc5 led to a substantially increased fraction of Dbf4 shifting to a higher molecular weight, as can be seen by the intense upper band from 8 hours onwards (**Figure 6.1A**). Furthermore, in the *dbf4-R83E* mutant, the induction of Cdc5 did not lead to the appearance of a band above the upper

Figure 6.1. Cdc5-dependent phosphorylation of Dbf4 requires the Dbf4-Cdc5 interaction and Cdc5 kinase activity.

A Beta-estradiol was added to *ndt80Δ* cells with the indicated genotypes 6 hours into meiosis and protein extracts were examined by immunoblotting. **B** Signal profiles from data in **A**. **C** Beta-estradiol was added to *dmc1Δ ndt80Δ* cells with the indicated genotypes 6 hours into meiosis and protein extracts were examined as in **A**.

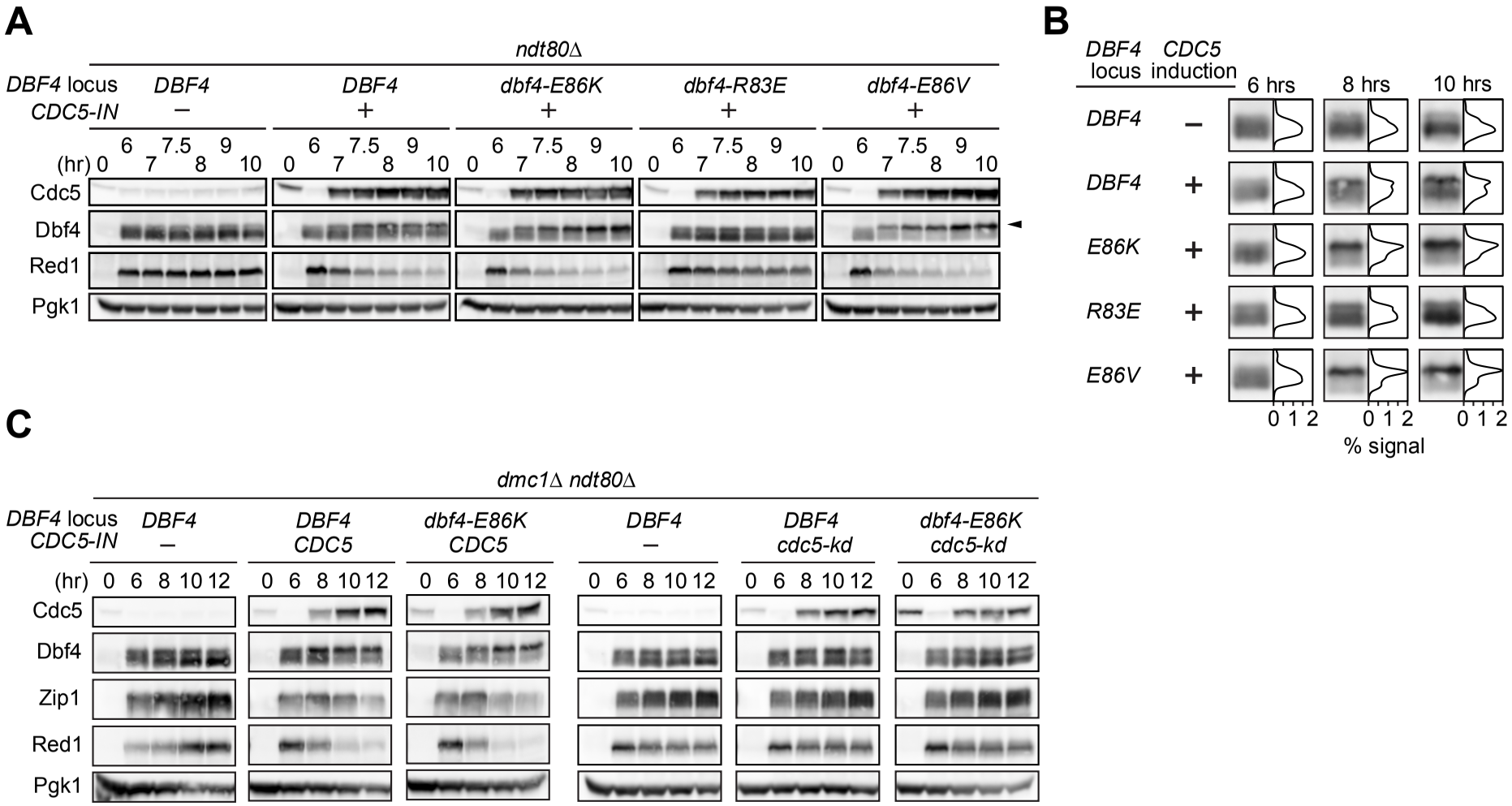
A
ndt80Δ
DBF4 locus
CDC5-IN
DBF4
–
DBF4
+
dbf4-E86K
+
dbf4-R83E
+
dbf4-E86V
+
(hr)
Cdc5
Dbf4
Red1
Pgk1
B
DBF4 locus
CDC5 induction
6 hrs
8 hrs
10 hrs
DBF4 –
DBF4 +
E86K +
R83E +
E86V +
0 1 2
% signal
C
dmc1Δ ndt80Δ
DBF4 locus
CDC5-IN
DBF4
–
DBF4
CDC5
dbf4-E86K
CDC5
DBF4
–
DBF4
cdc5-kd
dbf4-E86K
cdc5-kd
(hr)
Cdc5
Dbf4
Zip1
Red1
Pgk1

band of the doublet. These results indicate that the interaction between Dbf4 and Cdc5 is germane for the prophase I phosphorylation of Dbf4.

To better display this data, I performed profile analysis of the Dbf4 doublet at the designated time points from each of the western blots in **Figure 6.1A.** From the 6 hour to the 10 hour time point, the absence of Cdc5 in the presence of WT Dbf4 led to a marginal shift to a lower molecular weight for Dbf4 (**Figure 6.1B**). However, when Cdc5 is induced at 6 hours, Dbf4 undergoes a subtle shift to the higher molecular weight species. This shift can be seen clearly by comparing the relatively broad peak at 6 hours with the biphasic peak at 10 hours. In addition, the production of Cdc5 in the presence of Dbf4-E86K/V led to the formation of a sharp, narrow peak, corresponding to phosphorylated Dbf4; not only did this peak constitute more Dbf4 molecules (since the signal is more intense), it appeared faster than in WT Dbf4 (the peak is already obvious at 8 hours). Furthermore, the production of Cdc5 in the *dbf4-R83E* background did not lead to the formation of either a biphasic (Dbf4) or sharp (Dbf4-E86K/V) peak, indicating that Dbf4 was not phosphorylated in the absence of the Dbf4-Cdc5 interaction. Moreover, a lower molecular weight species of Dbf4 corresponding to the bottom band of the doublet became more apparent, suggesting that the phosphorylation status of Dbf4 is under continuous regulation. This analysis provides clear-cut evidence that the molecular weight of Dbf4 is modified in an interaction-dependent manner in response to Cdc5 production.

If Cdc5 is the kinase responsible for Dbf4 phosphorylation, then inducing a kinase-dead version of Cdc5 (Cdc5-kd) should not lead to Dbf4 phosphorylation. To test this possibility, a kinase-dead version of Cdc5 (Cdc5-

N209A) (Hardy & Pautz, 1996) under the control of the *GAL1* promoter was integrated at the *URA3* locus; this allele is referred to as *cdc5-kd* hereafter. Importantly, induction of Cdc5-kd did not lead to any apparent mobility shift of Dbf4, even in the *dbf4-E86K* background where the interaction between Dbf4 and Cdc5 is enhanced (**Figure 6.1C**), thus highlighting the requirement for Cdc5's kinase activity in Dbf4 phosphorylation.

Taken together, there are three lines of evidence that Cdc5 is the kinase responsible for phosphorylating Dbf4. Firstly, the induction of Cdc5 alone in the absence of Ndt80 is sufficient for Dbf4 phosphorylation (**Figure 6.1A**). Secondly, the extent of Dbf4 phosphorylation correlates well with Dbf4-Cdc5 interaction strength (**Figure 6.1A, B**). Thirdly, Cdc5's kinase activity is essential for Dbf4 phosphorylation (**Figure 6.1C**).

6.2 The kinase activity of Cdc5 is crucial for activating Rad51-dependent DSB repair

Interestingly, when Cdc5-kd was induced at 6 hours, not only was there no shift in Dbf4's mobility, but there was no drastic decline in the levels of Zip1 and Red1 (**Figure 6.1C**), suggesting that Cdc5 kinase activity is essential for degradation of SC proteins. In order to better correlate the presence of SC proteins with Rad51 inhibition, I monitored whether the induction of Cdc5-kd was able to promote DSB repair in the *dmc1Δ ndt80Δ* mutant, as was seen for the induction of WT Cdc5 (**Figure 5.2A**). Following Cdc5-kd induction at 6 hours, which was confirmed by western blotting (**Figure 6.1C**), DSBs were monitored by pulsed-field gel electrophoresis and Southern blotting in the *DBF4* and *dbf4-E86K* backgrounds. As anticipated, there was no decline in the

percentage of broken chromosomes when Cdc5-kd was not induced (**Figure 6.2**). Moreover, induction of Cdc5-kd did not lead to a reduction in the percentage of broken chromosomes in the presence of either Dbf4 or Dbf4-E86K. These data clearly show that Cdc5's kinase activity is essential for SC degradation and consequent Rad51-dependent DSB repair.

6.3 Phosphorylation of Dbf4 is required for efficient destruction of SC proteins

It is possible that the Cdc5-dependent phosphorylation of Dbf4 is not biologically relevant to SC component degradation. In order to assess the importance of Dbf4 phosphorylation, serine/threonine residues that were identified as being required for the mobility shift of Dbf4 were mutated to nonphosphorylatable alanines. Two alleles were utilised: *dbf4-10A*, which shows a complete loss of Dbf4 phosphorylation, and *dbf4-4A*, which shows a partial reduction in Dbf4 phosphorylation. These residues are highly conserved amongst species within the *Saccharomyces* genus (for more detail on the identification of these alleles, see section **2.4.3**). These alleles were introduced into the *ndt80Δ CDC5-IN* background. Following entry into meiosis, Cdc5 was induced at 6 hours and proteins were analysed by western blotting at hourly time points. If the phosphorylation of Dbf4 is required for efficient destruction of SC proteins, then the *dbf4-10A* strain should show a severe delay in the disappearance of Red1 and Zip1; this delay is shown in **Figure 6.3A**. Furthermore, SC proteins persisted for longer than in wild type in the *dbf4-4A* strain, but this delay was visibly milder than that seen in the *dbf4-10A* strain

Figure 6.2. Cdc5 kinase activity is required for unshackling Rad51.

Beta-estradiol was added to *dmc1Δ ndt80Δ* cells with the indicated genotypes 6 hours into meiosis and chromosomes were examined by pulsed-field gel electrophoresis followed by Southern blotting (panels). The percentage of signal corresponding to broken chromosomes was plotted (graph). Error bars ±SEM, n = 2.

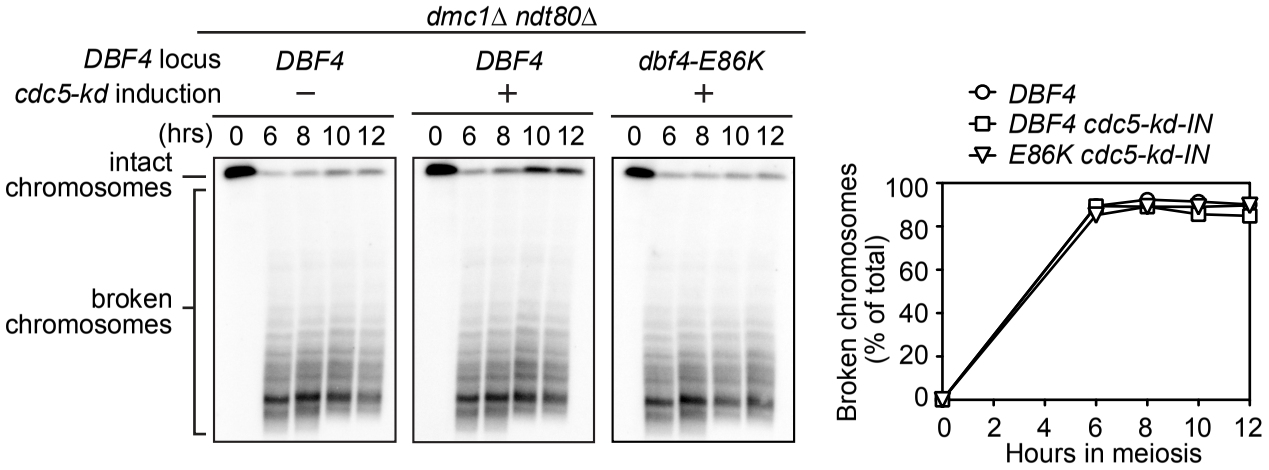
dmc1Δ ndt80Δ
DBF4 locus
cdc5-kd induction
DBF4
DBF4
dbf4-E86K
–
+
+
(hrs) 0 6 8 10 12 0 6 8 10 12 0 6 8 10 12
intact chromosomes
broken chromosomes
DBF4
DBF4 cdc5-kd-IN
E86K cdc5-kd-IN
Broken chromosomes (% of total)
100
80
60
40
20
0
0 2 4 6 8 10 12
Hours in meiosis

Figure 6.3. Phosphorylation of Dbf4 promotes Cdc5-drive SC destruction.

A, B Beta-estradiol was added to *ndt80Δ* cells with the indicated genotypes 6 hours into meiosis and protein extracts were examined by immunoblotting. *dbf4-10A* encodes mutations of the following residues to alanine: 274, 280, 303, 318, 319, 328, 350, 361, 374, 375. *dbf4-4A* encodes mutations of the following residues to alanine: 350, 361, 374, 375.

A

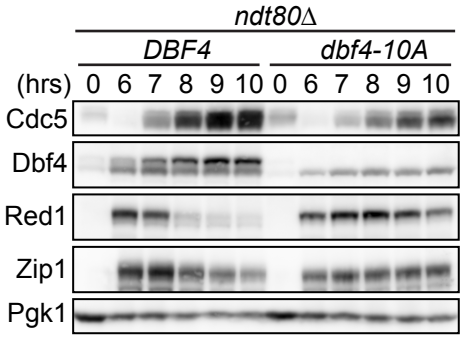
ndt80Δ
DBF4
dbf4-10A
(hrs) 0 6 7 8 9 10 0 6 7 8 9 10
Cdc5
Dbf4
Red1
Zip1
Pgk1

B

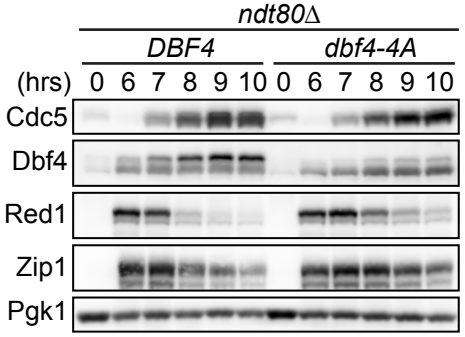
ndt80Δ
DBF4
dbf4-4A
(hrs) 0 6 7 8 9 10 0 6 7 8 9 10
Cdc5
Dbf4
Red1
Zip1
Pgk1

(**Figure 6.3B**). These findings suggest that phosphorylation of Dbf4 is required to facilitate timely destruction of SC proteins Red1 and Zip1.

6.4 Conclusions

In this chapter, I have presented evidence in support of the notion that Dbf4 is phosphorylated by Cdc5. Moreover, I have shown that this phosphorylation is required for efficient destruction of the SC. Previous studies have implicated Cdc5 in directly phosphorylating Dbf4 (Hardy & Pautz, 1996; Matos et al., 2008), but these claims were lacking rigorous testing. Additionally, there was no evidence to suggest what the role of this phosphorylation was. Thus, I set out to determine the requirements for the existence of this molecular species. The modification of Dbf4 not only requires the presence of Cdc5, but it also requires the direction interaction between Dbf4 and Cdc5. In addition, a kinase-dead version of Cdc5 was unable to modify Dbf4. Moreover, Cdc5's kinase activity is essential for destruction of the SC and removal of Rad51 inhibition. Finally, Cdc5 induction in the presence of nonphosphorylatable Dbf4 lead to inefficient SC destruction, highlighting the importance of Dbf4 phosphorylation in ablating Rad51's meiotic inhibition.

Chapter 7: DDK is Required for Positive and Negative Regulation of SC Integrity

Findings presented within this study indicate that DDK plays an important role in facilitating Cdc5-driven SC destruction. It is likely that Cdc5 does not play a role in maintaining SC integrity, since Cdc5 levels are very low throughout early/mid prophase I, when the SC develops and matures (Page & Hawley, 2004). In contrast, DDK is active during early/mid prophase I, where it is required for initiating DSB formation to induce HR (Sasanuma et al., 2008; Wan et al., 2008). Since the Dbf4-Cdc5 interaction is able to mediate dismantling of the SC, it is possible that, in the absence of Cdc5, DDK plays a role in regulating the SC within prophase I. This chapter describes the experiments undertaken to examine the role of DDK in regulating SC maintenance and destruction.

7.1 DDK is essential for maintenance of SC integrity and Rad51 inhibition

In addition to initiating premeiotic DNA replication (Valentin et al., 2006), DDK has been shown to have crucial roles during early prophase I, where it is essential for initiating HR through programmed DSB formation (Sasanuma et al., 2008; Wan et al., 2008), and in metaphase I, where it is required for monoorientation of sister kinetochores (Matos et al., 2008). However, the study of DDK in the intervening period has been hampered due to its role in DSB formation. Since DSB formation is a prerequisite for SC formation (Roeder, 1997), I sought to employ a condition in which I could analyse the mid-to-late prophase I roles of DDK in the presence of fully formed SCs. Thus, I employed the anchor-away technique to conditionally deplete a protein of interest from the nucleus (Haruki et al., 2008). In essence, a nuclear target protein is fused to the

FKBP12-rapamycin-binding (FRB) domain of human mTOR and a cytoplasmic anchor protein is fused to the human FK506-binding protein (FKBP12). Rapamycin can bind to the FKBP12-tagged anchor and form a complex with the FRB-tagged target protein. Importantly, strains are constructed in the *tor1-1 fpr1Δ* background. Both mutations render yeast cells resistant to the toxicity of rapamycin, but the deletion of *FPR1*, which encodes the most abundant rapamycin-binding protein in yeast, also reduces competition between Fpr1 and the FKBP12-anchor construct for rapamycin binding. Since premature ribosomes are actively imported into the nucleus to assemble with rRNAs before being exported to the cytoplasm, Haruki et al. (2008) showed that the ribosomal protein RPL13A is a suitable anchor for depleting nuclear proteins. Thus, by fusing either Cdc7 or Dbf4 to FRB, it should be possible to conditionally inactivate the DDK complex by adding rapamycin to the medium. To confirm this, single colonies were streaked onto rich media either with or without rapamycin. In the absence of rapamycin, FRB-tagged strains grew as well as untagged strains (**Figure 7.1A**). However, in the presence of rapamycin, FRB-tagged strains showed very poor growth characteristic of inviability, which is the expected result since both Dbf4 and Cdc7 are required for the G1-to-S transition (Kitada et al., 1992). It is likely that the poorer growth of *DBF4-FRB* strains compared to *CDC7-FRB* strains is due to the system responding more efficiently to the presence of rapamycin. This result indicates that DDK functionality can be conditionally turned off by adding rapamycin.

To monitor the effect of depleting nuclear DDK on the SC, *ndt80Δ* cells were introduced into SPM for 6 hours and nuclei were examined by immunofluorescence microscopy; at this stage, fully linear Zip1 associated with

Figure 7.1. DDK is required to maintain SC integrity and Rad51 inhibition.
A Single colonies of the indicated strains were streaked on rich media with or without rapamycin. *DBF4-FRB* is more responsive to the drug. **B** *ndt80Δ* cells were synchronously introduced into meiosis and the cultures were split at 6 hours. One subculture was supplemented with rapamycin and the other subculture received carrier (DMSO). Cells from the indicated time points were lysed and chromosomes were surface spread and analysed by immunofluorescence microscopy. Nuclei were categorised as being Red1 positive or negative and having fully established SC as judged by Zip1 staining. 100 nuclei were counted per time point. Error bars ±SEM, n= 2.

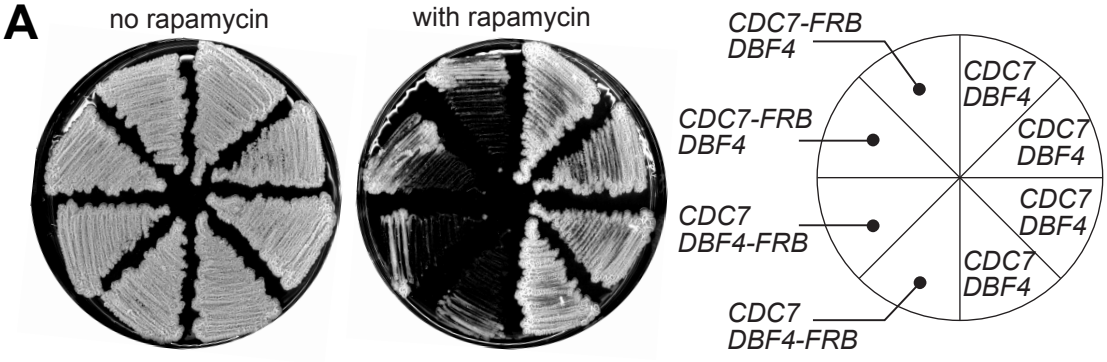
A
no rapamycin
with rapamycin
CDC7-FRB
DBF4
CDC7
DBF4
CDC7-FRB
DBF4
CDC7
DBF4
CDC7
DBF4-FRB
CDC7
DBF4
CDC7
DBF4-FRB

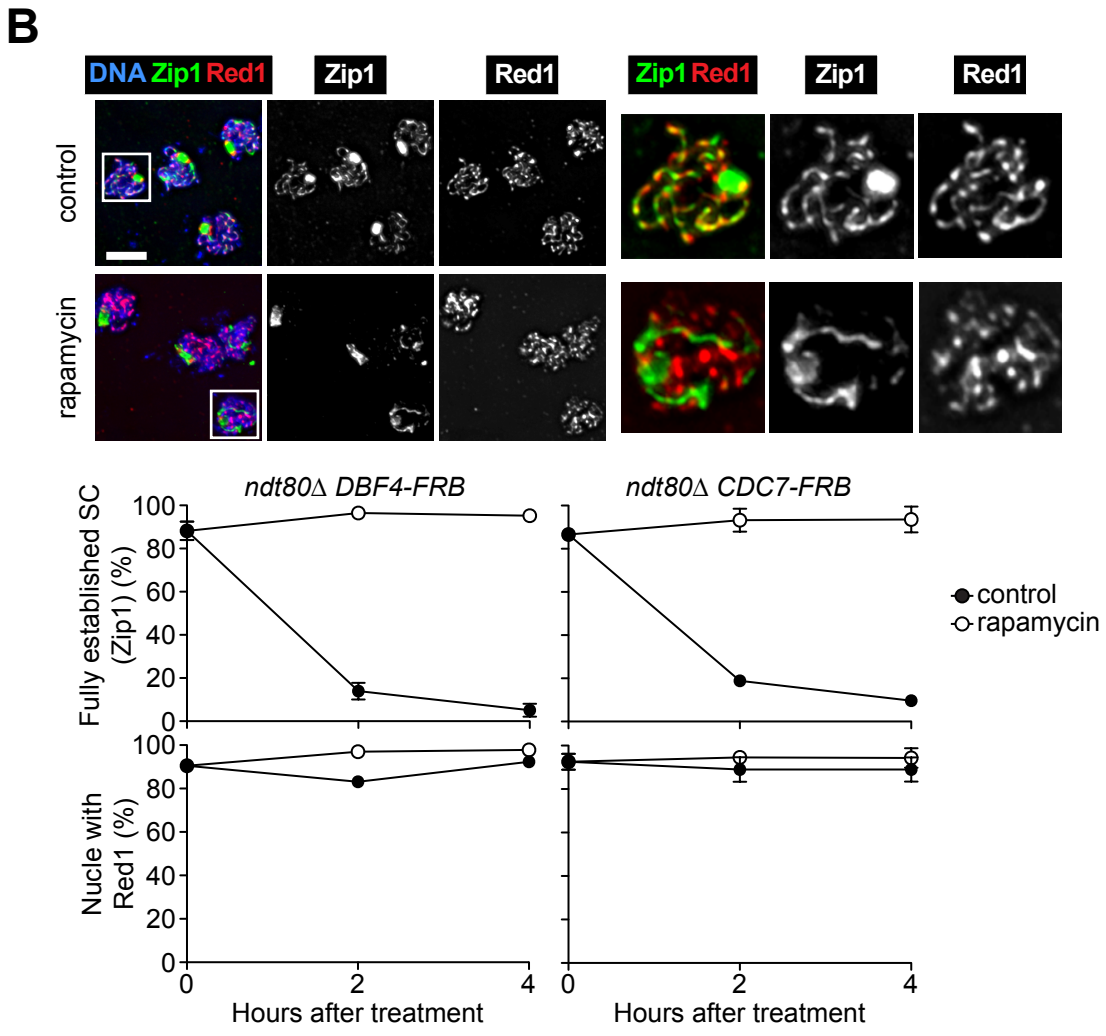
B
DNA Zip1 Red1
Zip1
Red1
Zip1 Red1
Zip1
Red1
control
rapamycin
ndt80Δ DBF4-FRB
ndt80Δ CDC7-FRB
Fully established SC (Zip1) (%)
Nucle with Red1 (%)
100
80
60
40
20
0
0
2
4
Hours after treatment
control
rapamycin

Figure 7.1 (continued). DDK is required to maintain SC integrity and Rad51 inhibition within prophase I.

C *dmc1Δ* cells were synchronously introduced into meiosis and the cultures were split at 9 hours. One subculture was supplemented with rapamycin and the other subculture received carrier (DMSO). Chromosomes from the indicated time points were examined by pulsed-field gel electrophoresis followed by Southern blotting (panels). The percentage of signal corresponding to broken chromosomes was plotted (graphs). Error bars ±SEM, n = 2. **D** *dmc1Δ MER2-FRB* cells were supplemented with rapamycin or carrier (DMSO) upon synchronous induction to meiosis. Cells were harvested at the indicated time points and examined as in **C** (left panel). *dmc1Δ MER2-FRB* cells were synchronously introduced into meiosis and the culture was split at 9 hours and supplemented with either rapamycin or carrier (DMSO). Cells were harvested at the indicated time points and examined as in **C** (right panel). The percentage of signal corresponding to broken chromosomes was plotted (graph). Error bars ±SEM, n = 2.

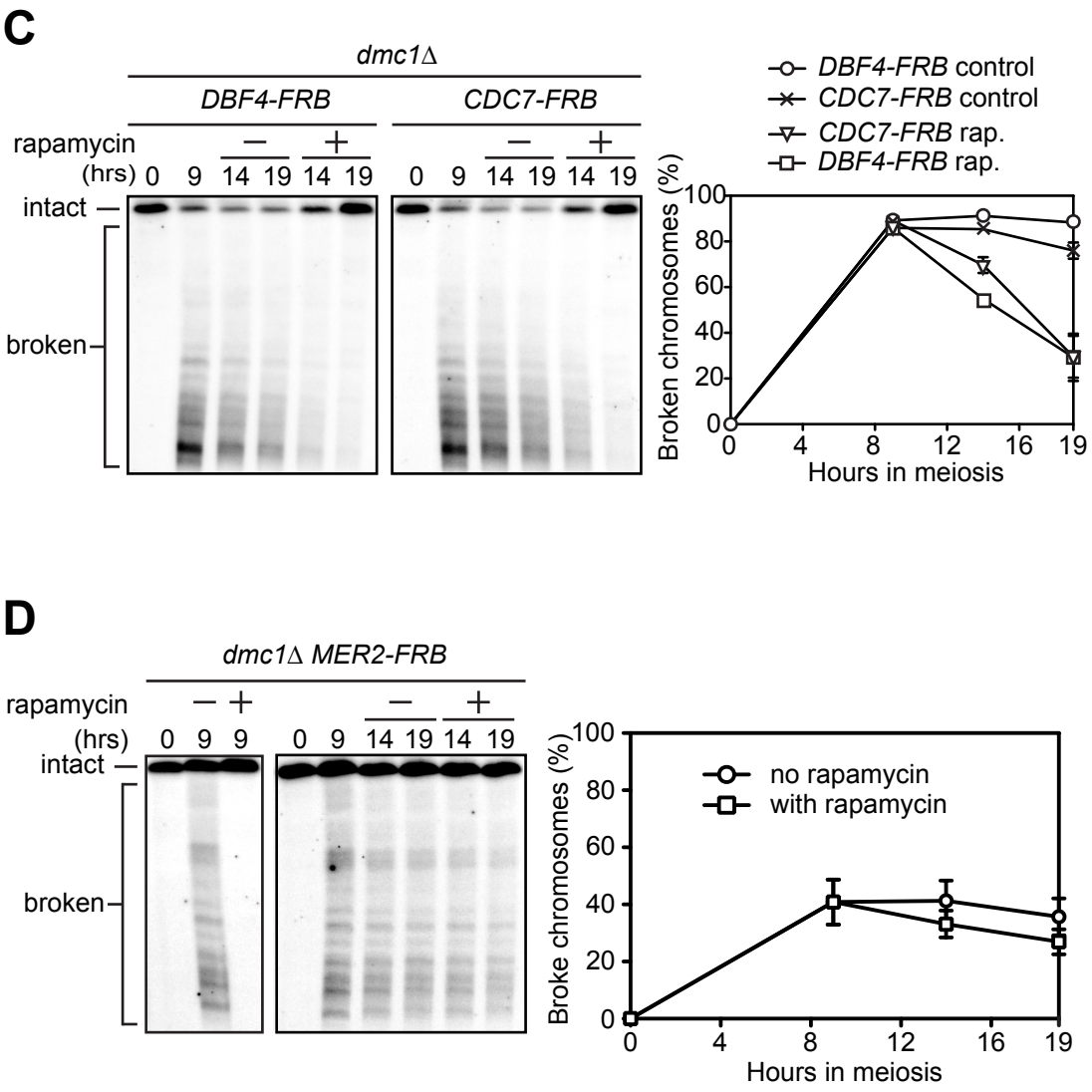
C
dmc1Δ
DBF4-FRB
CDC7-FRB
rapamycin
(hrs)
0 9 14 19 14 19 0 9 14 19 14 19
intact
broken
DBF4-FRB control
CDC7-FRB control
CDC7-FRB rap.
DBF4-FRB rap.
Broken chromosomes (%)
Hours in meiosis
D
dmc1Δ MER2-FRB
rapamycin
(hrs)
0 9 9 0 9 14 19 14 19
intact
broken
no rapamycin
with rapamycin
Broke chromosomes (%)
Hours in meiosis

the meiotic chromosome axis protein Red1 was seen for ~90% of nuclei (**Figure 7.1B**, leftmost graphs). However, the addition of rapamycin led to a drastic change in the Zip1 staining pattern, and a more subtle change in the Red1 staining pattern. 4 hours after the addition of rapamycin, only ~5% of nuclei showed fully linear Zip1 associated with Red1; the vast majority of nuclei displayed an aberrant localisation pattern in which Zip1 was no longer associated with Red1 and Red1 did not form line-like staining patterns (**Figure 7.1B**, inset panels). A similar result was seen with the *CDC7-FRB* strain (**Figure 7.1B**, rightmost graphs). These results indicate that continued DDK activity during prophase I is essential for maintaining SC integrity.

Meiotic HR is subjected to numerous regulations that promote recombination between homologous chromosomes as opposed to sister chromatids, as the latter would not generate the physical linkages between homologues required to faithfully segregate homologous chromosomes at MI (Gerton & Hawley, 2005). Since SC components are key in establishing this meiosis-specific recombination bias (Schwacha & Kleckner, 1997; Niu et al., 2005; Niu et al., 2009), the finding that DDK is required to maintain SC integrity raised the possibility that DDK may also be required to enforce the meiotic recombination bias throughout prophase I. To test this, the *ndt80Δ* mutant background was swapped for the *dmc1Δ* mutant background. In the absence of the meiotic recombinase Dmc1, despite the presence of Rad51, cells arrest in pachytene with unrepaired DSBs (Bishop et al., 1992). Under these conditions, there is essentially no HR (Schwacha & Kleckner, 1997). However, if the absence of DDK activity is able to relieve Rad51 of its meiotic inhibition, then these DSBs should be repaired in the absence of Dmc1. To test this

hypothesis, cells lacking Dmc1 with FRB-tagged Dbf4/Cdc7 were induced into meiosis. At 9 hours, when the amount of broken chromosomes is near its peak (~90%), cultures were split into two and one culture received rapamycin while the other culture received carrier (DMSO). Cells were then harvested at 14 hours and 19 hours. Chromosomes from these harvested cells were subjected to pulsed-field gel electrophoresis and Southern blotting. As anticipated, in the absence of rapamycin, ~80-90% of chromosomes were broken at 19 hours, whereas cultures that received rapamycin had ~30% broken chromosomes at the same time point (**Figure 7.1C**). These data suggest that continued DDK activity is required in prophase I to inhibit Dmc1-independent DSB repair.

Since DDK is required for DSB formation (Sasanuma et al., 2008; Wan et al., 2008), it is possible that the decline in the percentage of broken chromosomes when rapamycin is added is simply due to a reduction in DSB formation. In such a scenario, basal levels of Rad51 activity might be able to repair DSBs in the absence of Dmc1 if given sufficient time, thus accounting for the reappearance of the intact chromosome band (**Figure 7.1C**). Indeed, even in the absence of rapamycin, a small reduction in the percentage of broken chromosomes can be seen. To rule out the possibility that depletion of DDK's DSB forming activity led to such drastic DSB repair, DDK's essential role in DSB formation was considered. Since DDK promotes DSB repair by phosphorylating Mer2 (Sasanuma et al., 2008; Wan et al., 2008), which is another essential component of the DSB machinery (Henderson et al., 2006; Li et al., 2006), I aimed to mimic the effect of DDK depletion on DSB formation by depleting FRB-tagged Mer2. Firstly, to test if Mer2-FRB can be conditionally inactivated by the anchor-away system, a *dmc1Δ MER2-FRB* culture was split

into two before meiotic entry: one culture received rapamycin whereas the other received carrier (DMSO). Chromosomes were then examined 9 hours into meiosis. The culture that received rapamycin showed no signs of DNA breakage, indicating that Mer2 can be conditionally inactivated (**Figure 7.1D**). However, it is immediately evident that FRB-tagged Mer2 does not function as effectively as untagged Mer2; at 9 hours, the culture that did not receive rapamycin only had ~40% broken chromosomes, compared to ~90% in untagged *MER2* strains (**Figure 7.1C, D**). Nonetheless, this strain was introduced into meiosis and the time course was performed identically to the DDK-FRB time courses in **Figure 7.1C**. Shutting off DSB formation could not account for the difference seen between rapamycin treated and untreated cultures of DDK-FRB strains. These findings support the notion that continued DDK activity is required to suppress Rad51 activity throughout prophase I.

7.2 DDK promotes Cdc5-driven destruction of the SC

Although findings from previous chapters have shown that the Dbf4-Cdc5 interaction plays a role in destruction of the SC proteins Red1 and Zip1, it is not clear if DDK is directly or indirectly involved. For instance, taking into account the findings presented in this chapter, it is possible that Cdc5 negates DDK's ability to promote SC maintenance; thus, when Cdc5 and Dbf4 interact with enhanced ability, destruction of SC proteins is accelerated. Conversely, it is also possible that DDK plays a direct role in the destruction of SC proteins. To test this possibility, a meiotic null (*-mn*) allele of *DBF4* was creating by placing the wild type *DBF4* gene under the control of the *CLB2* promoter, which is downregulated only in meiotic cells (Lee & Amon, 2003). The *dbf4-mn* diploid

was induced into meiosis and the kinetics of SC proteins were compared with wild type. In wild type, Cdc5 levels reach a modest peak at ~6 hours, by which time Red1 and Zip1 are already declining (**Figure 7.2A**), indicating that relatively low levels of Cdc5 are required to initiate SC destruction. In comparison, despite substantially more Cdc5 accumulating in *dbf4-mn* cells, Red1 and Zip1 were still clearly detectable at 12 hours, a time by which little/no protein remained in wild type. To rule out the possibility that this finding applied exclusively to conditions involving unreplicated DNA, the *bob1* mutation in *MCM5* was introduced into the *dbf4-mn* strain. This mutation in *MCM5* bypasses DDK's essential role in DNA replication, thus allowing cells without DDK activity to replicate their DNA (Hardy et al., 1997). Nonetheless, the kinetics of SC protein destruction were unaffected (**Figure 7.2A**). These results suggest that DDK, in collaboration with Cdc5, plays an active role in facilitating destruction of SC proteins.

To better illustrate this point, strains were constructed in the *ndt80Δ* mutant background, where differences in protein levels due to asynchrony in the cultures is reduced. By employing *CDC5-IN*, it was possible to initiate destruction of SC proteins by inducing Cdc5 production at 6 hours. Following induction of Cdc5, the *DBF4* strain showed a swift decline in Red1 and Zip1, such that both proteins were hardly detectable at 9 hours (**Figure 7.2B**). In contrast, Red1 and Zip1 showed very little sign of decline when Cdc5 was induced in the *dbf4-mn* strain. Once again, the *dbf4-mn bob1* strain was included to rule out the possibility that this phenotype was due to the absence of DNA replication. These results strongly suggest that DDK plays an active role in promoting Cdc5-driven SC destruction.

Figure 7.2. DDK is required for efficient destruction of the SC.

A The indicated strains were synchronously introduced into meiosis and protein extracts were examined by immunoblotting. **B** *ndt80Δ* cells with the indicated genotypes were synchronously introduced into meiosis and beta-estradiol was added at 6 hours. Protein extracts were examined as in **A**. **C** *ndt80Δ* cells with the indicated genotypes were synchronously introduced into meiosis and cultures were split at 6 hours. One subculture was supplemented with rapamycin and the other subculture received carrier (DMSO). At 8 hours, beta-estradiol was added to both subcultures. Protein extracts were examined as in **A**.

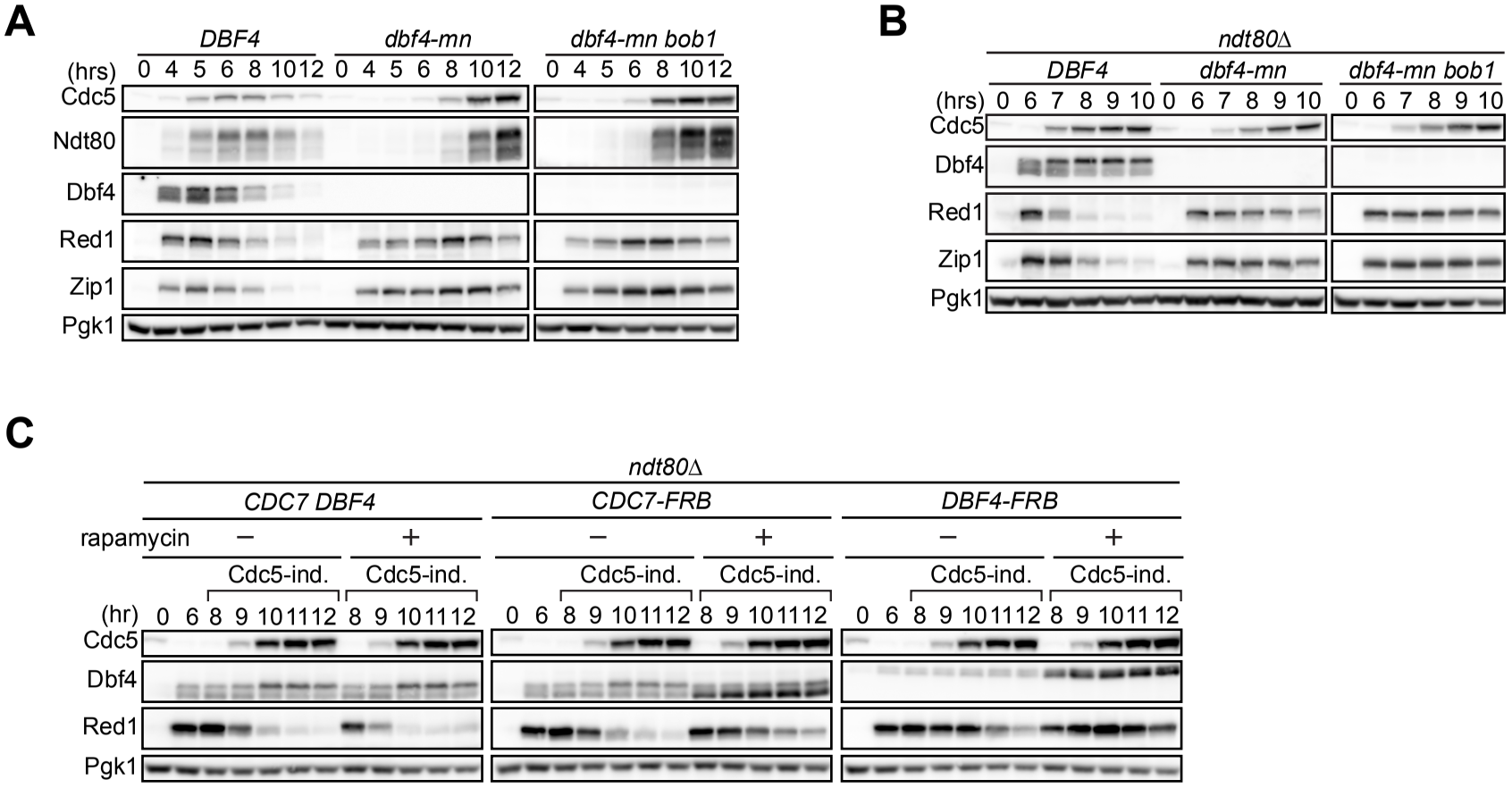
A
DBF4
dbf4-mn
dbf4-mn bob1
(hrs) 0 4 5 6 8 10 12 0 4 5 6 8 10 12 0 4 5 6 8 10 12
Cdc5
Ndt80
Dbf4
Red1
Zip1
Pgk1
B
ndt80Δ
DBF4
dbf4-mn
dbf4-mn bob1
(hrs) 0 6 7 8 9 10 0 6 7 8 9 10 0 6 7 8 9 10
Cdc5
Dbf4
Red1
Zip1
Pgk1
C
ndt80Δ
CDC7 DBF4
CDC7-FRB
DBF4-FRB
rapamycin – + – + – +
Cdc5-ind. Cdc5-ind. Cdc5-ind. Cdc5-ind. Cdc5-ind. Cdc5-ind.
(hr) 0 6 8 9 10 11 12 8 9 10 11 12 0 6 8 9 10 11 12 8 9 10 11 12 0 6 8 9 10 11 12 8 9 10 11 12
Cdc5
Dbf4
Red1
Pgk1

Although the *bob1* mutation bypasses the requirement for DDK in DNA replication, it does not allow DDK-independent DSB formation. Since DSBs are a prerequisite for SC formation (Roeder, 1997), it is formally possible that these findings only apply to conditions in which SC proteins are not properly localised due to the absence of meiotic DSBs (Page & Hawley, 2004). To rule out this possibility, the anchor-away system was employed with the same strains presented in **Figure 7.1B**, along with an untagged control strain. However, instead of monitoring meiotic chromosomes by immunofluorescence microscopy, protein extracts were subjected to western blotting. **Figure 7.1B** shows that ~90% of nuclei had established full SCs by the 6 hour time point, indicating that DSB initiation and consequent SC formation had taken place in the vast majority of cells. Thus, *DBF4-FRB*, *CDC7-FRB* and an untagged control strain in the anchor-away background were induced into meiosis. Cultures were split at 6 hours and either rapamycin or carrier was added, before Cdc5 production was induced at 8 hours in both subcultures. This allowed me to monitor Cdc5-driven SC protein degradation in the presence or absence of DDK activity. Consistent with results presented throughout this study, the induction of Cdc5 in the untagged strain led to rapid destruction of Red1; the addition of rapamycin in this untagged strain did not affect the kinetics of Red1 destruction (**Figure 7.2C**). In contrast, the *CDC7-FRB* subculture supplemented with rapamycin showed a delay in the disappearance of Red1, suggesting that DDK activity is required for efficient destruction of SC components. Moreover, in the *DBF4-FRB* strain, which responds more efficiently to rapamycin (**Figure 7.1A**), there was a more pronounced delay in the disappearance of Red1, indicating that DDK is required for the timely destruction of SC proteins.

7.3 Conclusions

Having shown in previous chapters that Dbf4 interacts with Cdc5 to regulate disassembly of the SC and destruction of SC proteins, I wanted to identify 1) whether DDK is able to regulate the SC independently of Cdc5 and 2) the requirement for DDK in Cdc5-driven SC destruction. Here, I have shown that continued DDK activity is required throughout prophase I to maintain correct SC structure. In the absence of DDK activity, SC integrity is compromised and Dmc1-independent DSB repair is activated. Furthermore, I showed that DDK plays an active role in facilitating Cdc5-driven SC destruction; in the absence of DDK activity, Cdc5 was less able to promote destruction of the SC protein Red1. Taken together, the data presented in this chapter highlight the dual roles of DDK in regulating the SC. Throughout prophase I, DDK is required to maintain SC integrity and suppress Rad51 activity. However, once cells commit to meiosis and Cdc5 is upregulated, DDK collaborates with Cdc5 to promptly destroy SC proteins and relieve Rad51 of its meiotic inhibition, leading to the repair of any persisting DSBs before the onset of anaphase I.

Chapter 8: Checkpoint Kinases Mec1 and Tel1 and the Polo-like Kinase Cdc5 Regulate Meiotic DSB Formation

Although much is known about the requirements for the initiation of meiotic DSB formation (de Massy, 2013), relatively little is known about how the dynamic process of meiotic DSB formation is regulated. When the total number of meiotic DSBs formed are compromised, such as when hypomorphic alleles of *SPO11* are employed, it has been shown that the numbers of crossovers are maintained at the expense of noncrossovers, a process known as CO homeostasis (Martini et al., 2006). Thus, the numbers of DSBs formed during meiotic prophase I are important because too few breaks could potentially result in homologue pairs without at least a single CO, and too many breaks could overload the recombination machinery, resulting in unrepaired DSBs. In either case, the reproductive value of the resultant gametes is likely to be drastically reduced. It is therefore likely that fine-tuning mechanisms exist to ensure that the number of DSBs formed is kept within an acceptable range. Indeed, it has been shown that ATM, the mammalian homologue of Tel1, is required to downregulate meiotic DSB formation in mice (Lange et al., 2011).

The Tel1 pathway of the DNA damage checkpoint is thought to respond to unresected DSB ends whereas the Mec1 (budding yeast ATR) pathway is thought to detect mainly exposed ssDNA at resected DSB ends (Lydall et al., 1996; Usui et al., 2001). Mutant backgrounds such as *sae2Δ* and *rad51Δ dmc1Δ* accumulate unrepaired DSBs with unresected and hyperresected ends, respectively (Shinohara et al., 1997; Neale & Keeney, 2006). Thus, by employing *sae2Δ* and *rad51Δ dmc1Δ* mutant backgrounds, it is possible to

exclusively activate either the Tel1-dependent or the Mec1-dependent checkpoint pathway, respectively.

During this chapter, I will present my findings on the regulation of meiotic DSB formation by the checkpoint kinases Tel1 and Mec1, and the budding yeast polo-like kinase, Cdc5.

8.1 The Tel1 pathway of the DNA damage checkpoint positively regulates meiotic DSB formation

Meiotic chromosomes from the *sae2Δ* single mutant and the *sae2Δ tel1Δ* double mutant were compared through a combination of pulsed-field gel electrophoresis and Southern blotting with probes that anneal to the ends of specific chromosomes (**Figure 8.1A**). The absence of Tel1 caused a ~35% reduction in DSB levels across the larger chromosomes (IV, VII, II, XI), while smaller chromosomes (III, VI) were unaffected (**Figure 8.1B**). This is more obvious when comparing lane profiles (**Figure 8.1C**) and estimates of the number of breaks suffered per chromosome (**Figure 8.1B, D**). A more extreme form of this chromosome size-dependent effect has previously been reported in the absence of the *PCH2* gene (Farmer et al., 2012), thus cells lacking Pch2 were also included in this analysis as a comparison.

Meiotic DSB formation is supposedly a prophase I-specific event, with DSB formation continuing until the end of pachytene (de Massy, 2013); these chromosome breaks trigger activation of the recombination checkpoint, which delays/arrests the cell cycle until DSBs are repaired and the damage signal is extinguished (Hochwagen & Amon, 2006). However, since the recombination checkpoint is partially reliant on the same components as the DNA damage

Figure 8.1. The Tel1 branch of the DNA damage checkpoint upregulates meiotic DSB formation.

A The indicated strains were synchronously introduced into meiosis and chromosomes were analysed by pulsed-field gel electrophoresis followed by Southern blotting with chromosome-specific probes. **B** An estimate of the number of DSBs across different chromosome was calculated (Toyoizumi and Tsubouchi, 2012). Error bars ±SEM, n = 2. These experiments were performed by Sarah Farmer and Hideo Tsubouchi.

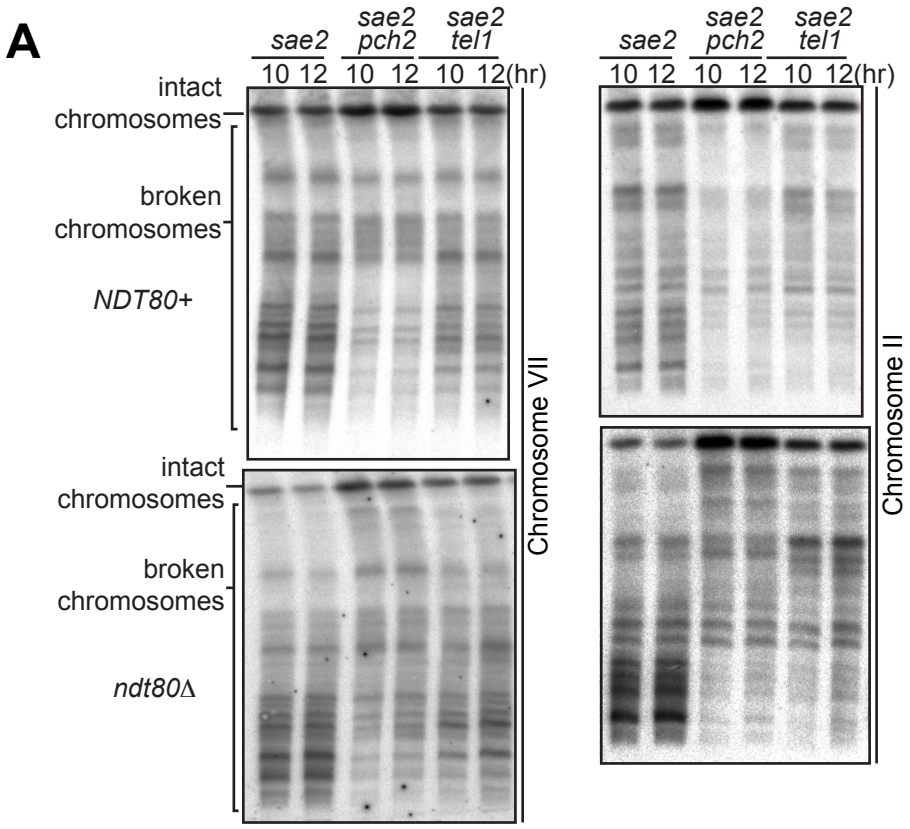
A
sae2
sae2 pch2
sae2 tel1
10 12 10 12 10 12(hr)
intact chromosomes
broken chromosomes
NDT80+
intact chromosomes
broken chromosomes
ndt80Δ
Chromosome VII
Chromosome II

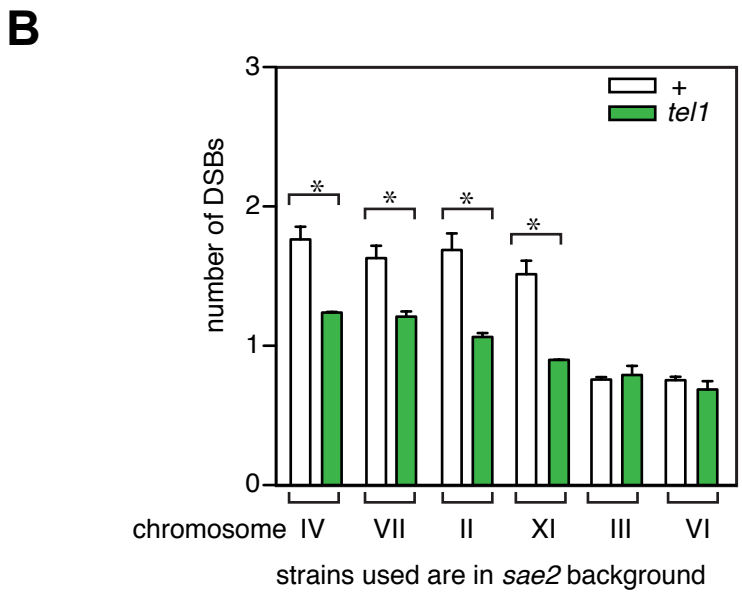
B
number of DSBs
+
tel1
chromosome IV VII II XI III VI
strains used are in sae2 background

Figure 8.1 (continued). The Tel1 branch of the DNA damage checkpoint upregulates meiotic DSB formation.

C Signal lane profiles were constructed for blots shown in **A**. Shown are averages of the 10 and 12 hour time points. **D** An estimate of the number of DSBs per chromosome was calculated for the indicated strains (Toyoizumi and Tsubouchi, 2012). Error bars ±SEM, n = 2. These analyses were performed by Sarah Farmer and Hideo Tsubouchi.

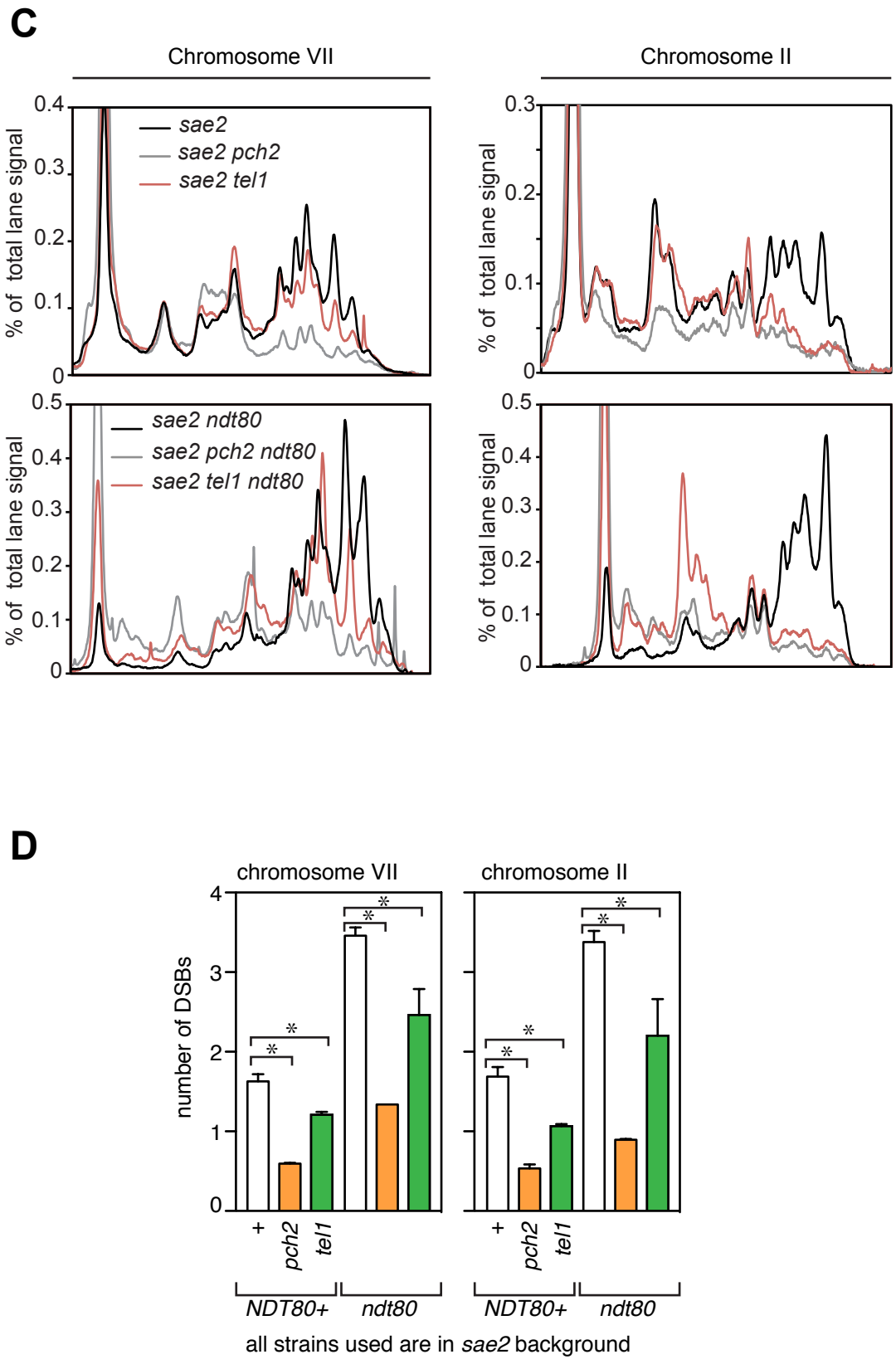
C
Chromosome VII
Chromosome II
% of total lane signal
sae2
sae2 pch2
sae2 tel1
sae2 ndt80
sae2 pch2 ndt80
sae2 tel1 ndt80
D
chromosome VII
chromosome II
number of DSBs
+
pch2
tel1
NDT80+
ndt80
all strains used are in sae2 background

checkpoint (Lydall et al., 1996), the absence of Tel1 can lead to a defect in the checkpoint mechanism, leading to cells with persisting DSBs progressing beyond prophase I; these cells may stop forming DSBs following exit from prophase I. Thus, it is possible that cells lacking Tel1 show fewer DSBs due to untimely progression from prophase I. To test this possibility, we introduced the *ndt80Δ* mutation into this analysis. Ndt80 is a meiosis-specific transcription factor whose production and activity is under the control of the recombination checkpoint; without Ndt80, cells show a permanent arrest at the end of pachytene (i.e., when DSBs are still forming) and cannot complete the meiotic programme (Xu et al., 1995). As anticipated, prophase I-arrested cells showed higher overall levels of DSBs (**Figure 8.1**), indicating that the Ndt80-dependent transition from prophase I to metaphase I is a key event in downregulating DSB formation. As in the wild type *NDT80* background, the absence of Tel1 led to a reduction in DSBs seen in larger chromosomes (**Figure 8.1**), suggesting that the Tel1-dependent mechanism responsible for downregulating meiotic DSBs has its execution point within prophase I. These findings suggest that the Tel1 pathway of the DNA damage checkpoint plays a crucial role in downregulating the number of meiotic DSBs formed within prophase I. In addition, these data identify the Ndt80-dependent transition from prophase I to metaphase I as a key event in the inhibition of meiotic DSB formation.

8.2 The Mec1 pathway of the DNA damage checkpoint differentially regulates meiotic DSB formation

To best study conditions in which the Mec1 pathway of the DNA damage checkpoint is activated, the *rad51Δ dmc1Δ* double mutant was employed. Under

these conditions, not only do DSBs accumulate due to the absence of recombinational repair, DSB ends are extensively resected, leading to the accumulation of 3'-tailed ssDNA (Lydall et al., 1996). Rad17 is required for activation of Mec1, but unlike Mec1, Rad17 is not essential for supporting viability (Harrison & Haber, 2006). Nonetheless, introducing the *rad17Δ* mutation into *rad51Δ* cells lead to a synergistic decrease in viability (data not shown). Such unhealthy cells show poor induction into meiosis, which can hinder population-based analysis. Thus, rather than employ the *rad17Δ* mutation, the promoter of *RAD17* was replaced with the *CLB2* promoter, which is upregulated in vegetative cells but not in meiotic cells (Lee & Amon, 2003). This allele is referred to as *rad17-mn* (meiotic null).

To confirm that the *rad17-mn* allele confers a checkpoint defect exclusively in meiotic cells, the viability of *rad17-mn*, *rad17Δ*, and wild type cells was compared by challenging respective strains with the DNA damaging agent methyl methanesulfonate (MMS). As expected, *rad17Δ* cells were highly sensitive to MMS, whereas the growth of *rad17-mn* cells was comparable to wild type (**Figure 8.2A**), suggesting that *rad17-mn* cells have a functional DNA damage checkpoint during vegetative growth. Furthermore, the viability of spores from respective diploid strains was examined. Consistent with the previous result, the viability of *rad17-mn* spores was ~50% compared to ~98% in wild type strains (**Figure 8.2B**). Although not as low as *rad17Δ* spore viability (~30%), this large reduction in spore viability supports the notion that the *rad17-mn* allele confers a meiosis-specific defect in the DNA damage checkpoint. Consistently, HA-tagged Rad17 could not be detected in *rad17-mn* prophase I cells (**Figure 8.2C**). Finally, a robust induction of Cdc5, which is a landmark

Figure 8.2. The Mec1 branch of the DNA damage checkpoint downregulates meiotic DSB formation.

A Cell cultures from the indicated strains were grown to saturation and serially diluted before spotting onto rich media with and without 0.01% MMS. The results from two duplicate cultures are shown. **B** Strains were sporulated on a plate for 24 hours and 40 tetrads were dissected per strain to determine spore viability. **C, D** The indicated strains were synchronously introduced into meiosis and protein extracts were examined by immunoblotting. Images of membranes stained with Ponceau are included as a loading control. veg., vegetative sample.

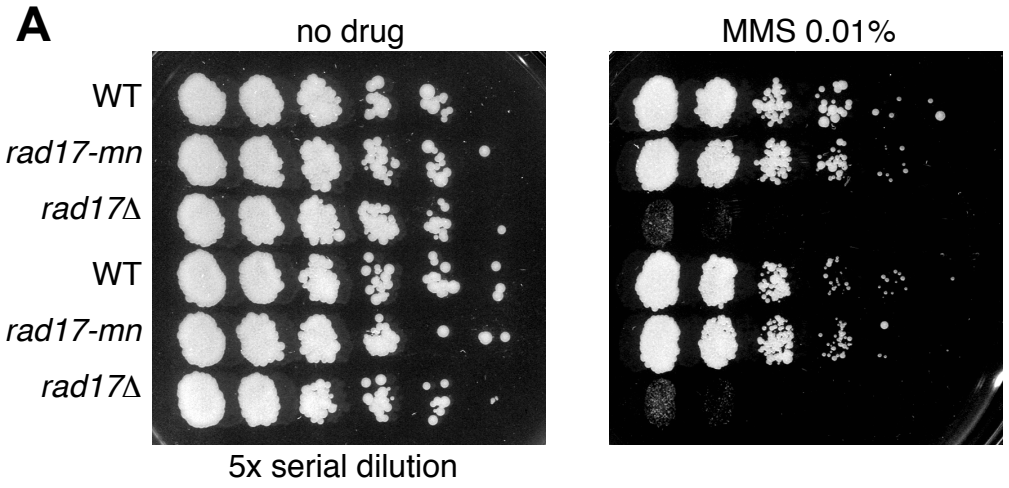
A
no drug
MMS 0.01%
WT
rad17-mn
rad17Δ
WT
rad17-mn
rad17Δ
5x serial dilution

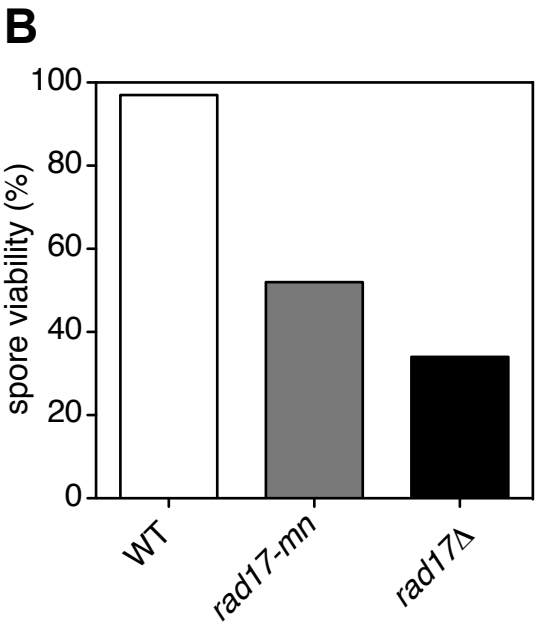
B
spore viability (%)
100
80
60
40
20
0
WT
rad17-mn
rad17Δ

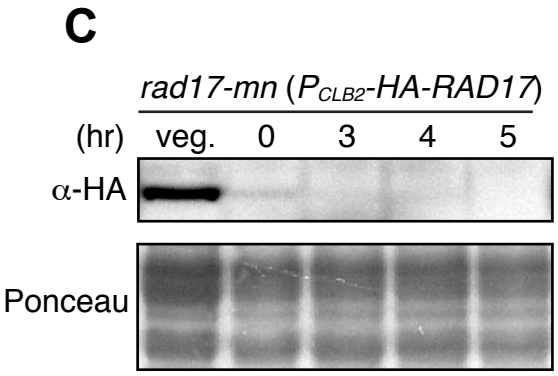
C
rad17-mn (PCLB2-HA-RAD17)
(hr)
veg.
0
3
4
5
α-HA
Ponceau

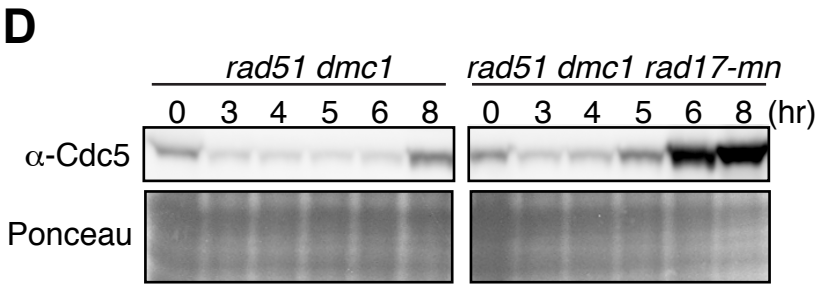
D
rad51 dmc1
rad51 dmc1 rad17-mn
0 3 4 5 6 8
0 3 4 5 6 8 (hr)
α-Cdc5
Ponceau

Figure 8.2 (continued). The Mec1 branch of the DNA damage checkpoint downregulates meiotic DSB formation.

E The indicated strains were synchronously introduced into meiosis and chromosomes were analysed by pulsed-field gel electrophoresis followed by Southern blotting with chromosome-specific probes.

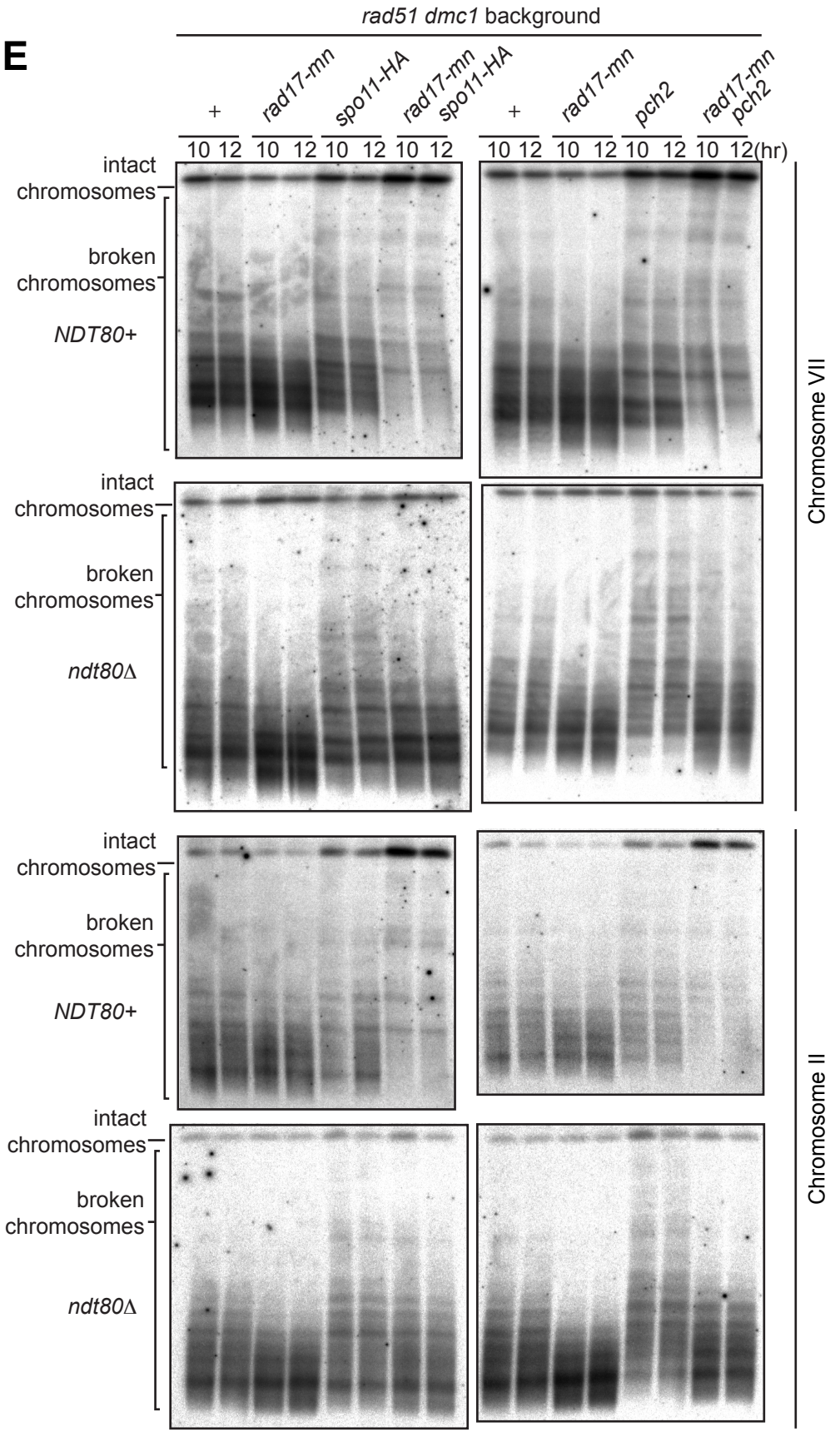
E
rad51 dmc1 background
+
rad17-mn
spo11-HA
rad17-mn spo11-HA
+
rad17-mn
pch2
rad17-mn pch2
10 12 10 12 10 12 10 12 10 12 10 12 10 12 10 12 (hr)
intact chromosomes
broken chromosomes
NDT80+
intact chromosomes
broken chromosomes
ndt80Δ
Chromosome VII
intact chromosomes
broken chromosomes
NDT80+
intact chromosomes
broken chromosomes
ndt80Δ
Chromosome II

Figure 8.2 (continued). The Mec1 branch of the DNA damage checkpoint downregulates meiotic DSB formation.

F Signal lane profiles were constructed for blots shown in **E**. Shown are averages of the 10 and 12 hour time points.

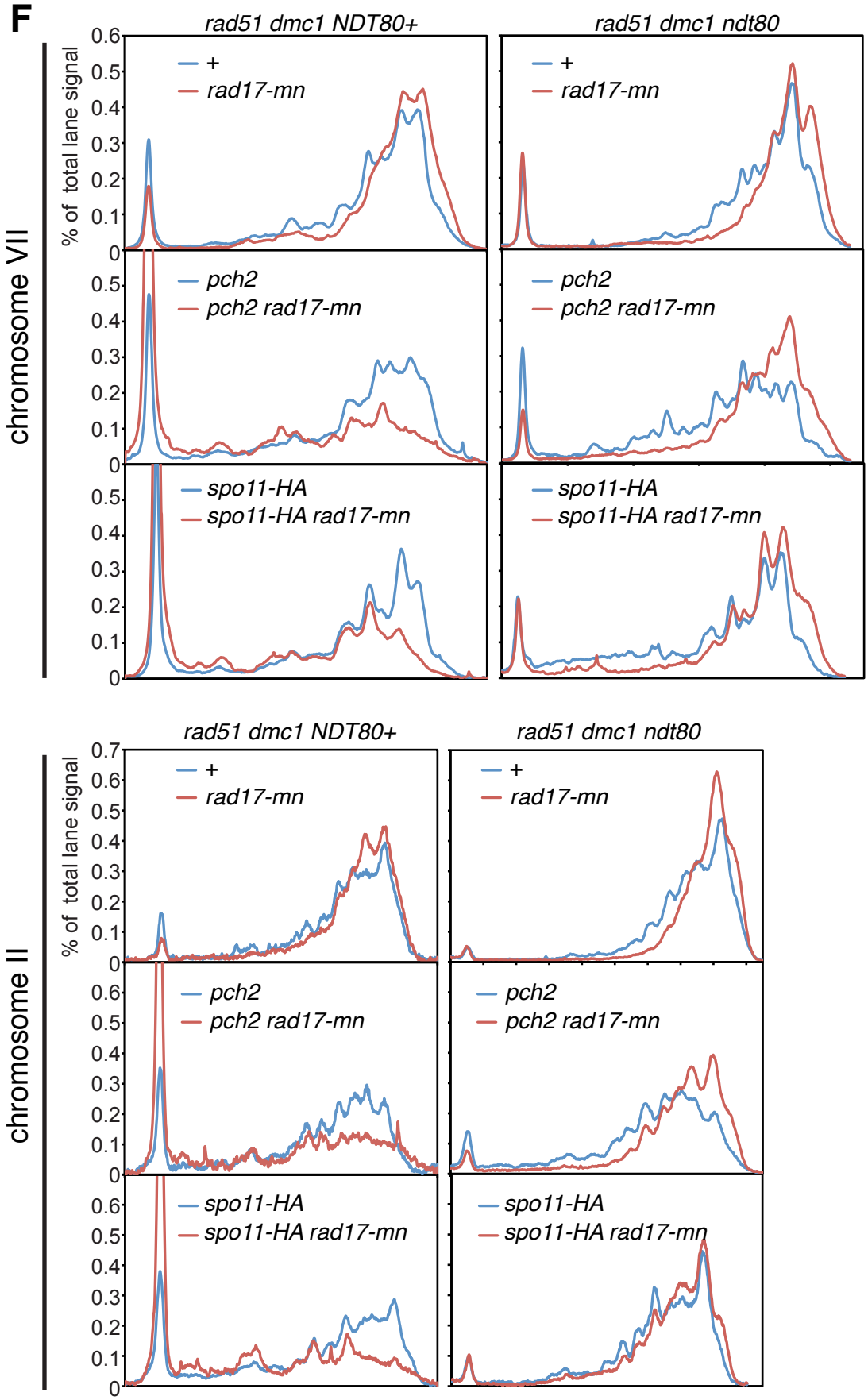
F
chromosome VII
chromosome II
% of total lane signal
rad51 dmc1 NDT80+
rad51 dmc1 ndt80
+
rad17-mn
pch2
pch2 rad17-mn
spo11-HA
spo11-HA rad17-mn

Figure 8.2 (continued). The Mec1 branch of the DNA damage checkpoint downregulates meiotic DSB formation.

G An estimate of the number of DSBs per chromosome was calculated for the indicated strains (Toyoizumi and Tsubouchi, 2012). Error bars ±SEM, n = 2.

G

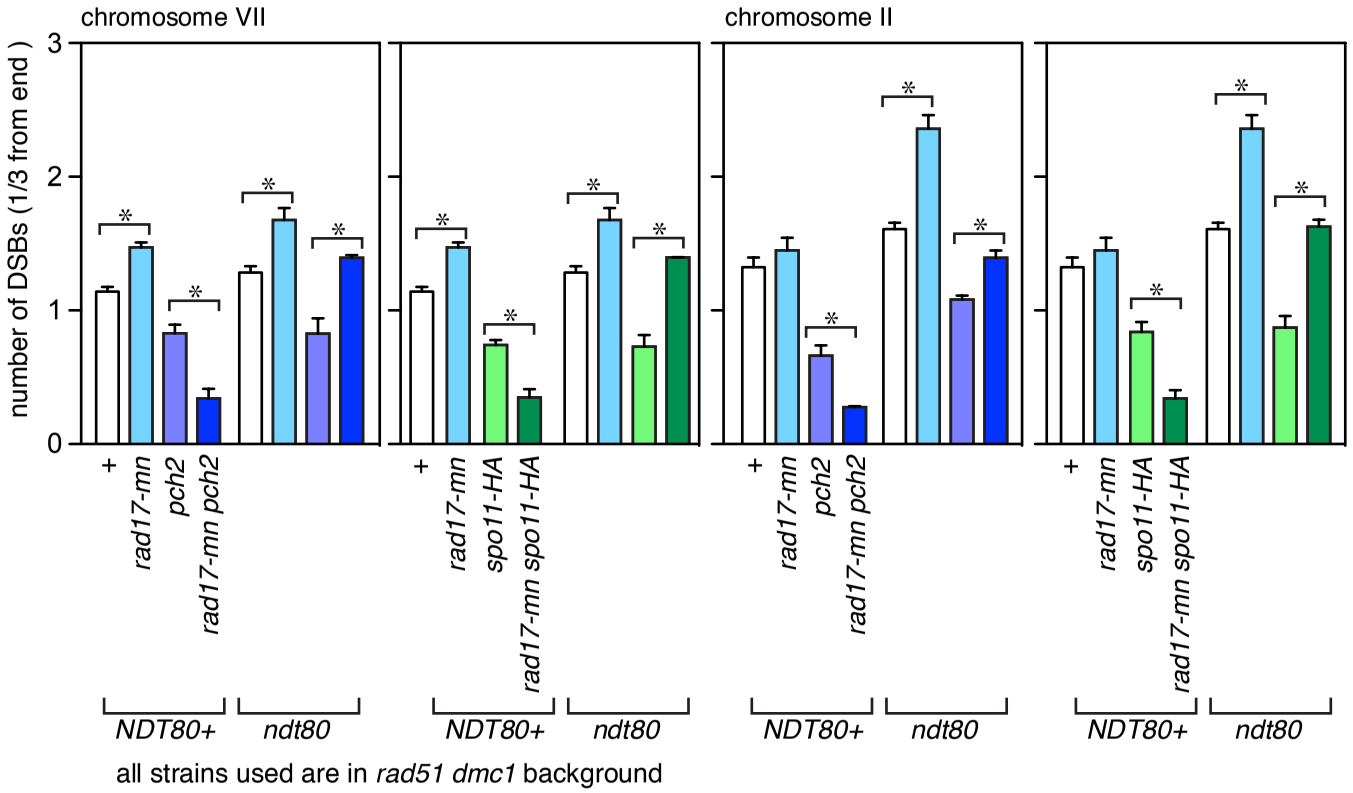
chromosome VII
chromosome II
number of DSBs (1/3 from end)
0
1
2
3
+
rad17-mn
pch2
rad17-mn pch2
spo11-HA
rad17-mn spo11-HA
NDT80+
ndt80
all strains used are in rad51 dmc1 background

event for prophase I exit, is seen in *rad51Δ dmc1Δ rad17-mn* cells, confirming the idea that meiotic cells without Rad17 lack a functional recombination checkpoint and are unable to enforce prophase I arrest (**Figure 8.2D**).

Meiotic chromosomes II and VII from *rad51Δ dmc1Δ* cells were compared with those from *rad51Δ dmc1Δ rad17-mn* cells through a combination of pulsed-field gel electrophoresis and Southern blotting. The number of DSBs was increased in the absence of Rad17 (**Figure 8.2E**). This is better seen when comparing the lane profiles (**Figure 8.2F**). However, the analysis to estimate the number of breaks per chromosome relies on the fraction of intact chromosomes, which is further reduced in the *rad51Δ dmc1Δ* double mutant. Thus, only a part of the chromosome signal was analysed (from the end of a chromosome to one-third of the total lane signal, which corresponds to most, but not all, of the signal in the *rad51Δ dmc1Δ* background). This analysis revealed that the number of DSBs increased in the absence of Rad17, although the difference seen for chromosome II was not statistically significant (**Figure 8.2G**). These results suggest that, unlike the Tel1 pathway, the Mec1 pathway of the DNA damage checkpoint actively downregulates meiotic DSB formation.

The viabilities of *pch2Δ* and *rad17Δ* cells was previously shown to be ~94% and ~34%, respectively (Wu & Burgess, 2006). Interestingly, the double mutant showed ~1% viability, indicating the existence of a genetic interaction. In addition, it was previously shown that the *pch2Δ* mutation leads to a reduction in DSB numbers (Farmer et al., 2012). To examine whether crippling the Mec1 pathway under conditions where DSB formation is already compromised further reduces the number of DSBs, meiotic chromosomes from *pch2Δ*, *rad17-mn*, and *pch2Δ rad17-mn* strains were subjected to pulsed-field gel electrophoresis

and Southern blotting. Also included in the analysis was a strain in which *SPO11* is HA-tagged; this hypomorphic allele confers a reduction in DSB numbers (Martini et al., 2006). Consistent with previously published results, *pch2Δ* (Farmer et al., 2012) and *spo11-HA* (Martini et al., 2006) strains showed a reduction in DSBs (**Figure 8.2**). Intriguingly, combining *rad17-mn* with either *pch2Δ* or *spo11-HA* in the presence of Ndt80 led to a further decrease in the number of DSBs. To test the possibility that this decrease was due to cell cycle progression associated with a defective DNA damage checkpoint, these experiments were repeated in the *ndt80Δ* mutant background. Strikingly, the effect of *rad17-mn* was now reversed; when combined with either *pch2Δ* or *spo11-HA*, *rad17-mn* conferred a statistically significant increase in the number of DSBs. These data suggest that the decrease in DSBs seen when *rad17-mn* was combined with either *pch2Δ* or *spo11-HA* is due to unscheduled cell cycle progression. Furthermore, the finding that *rad17-mn* stimulates DSB formation within prophase I indicates that the Mec1 pathway of the DNA damage checkpoint plays a crucial role in downregulating meiotic DSB formation. In addition, these results are consistent with the notion that the Ndt80-dependent transition from prophase I to metaphase I is a key factor in downregulating meiotic DSB formation.

8.3 Cdc5 can downregulate meiotic DSBs independently of DDK and Red1

Having presented evidence that an Ndt80-dependent mechanism is responsible for downregulating meiotic DSB formation, I wanted to further investigate this phenomenon. Serendipitously, preliminary findings suggested that Cdc5 might play a role in downregulating DSB formation (**Figure 5.2C**), and since Cdc5 is

under the control of Ndt80, I decided to examine whether Cdc5 can downregulate meiotic DSB formation.

It is necessary to employ conditions in which DSBs cannot be repaired, so the *rad51Δ dmc1Δ* background was employed. Furthermore, to focus solely on the effects exerted by Cdc5, it is necessary to remove any interfering effect from other members of the Ndt80 regulon. Thus, the *rad51Δ dmc1Δ* mutant was combined with the *ndt80Δ* mutation. Additionally, *CDC5-IN* was included to allow for the inducible production of Cdc5. 3.5 hours into meiosis, cultures were split and supplemented with either beta-estradiol or carrier (ethanol), and the two subcultures were allowed to sporulate further. Meiotic DSBs were monitored by pulsed-field gel electrophoresis followed by Southern blotting. When the *DBF4* culture was split at 3.5 hours, ~30% of chromosomes were broken (**Figure 8.3A**). In the absence of Cdc5, meiotic DSBs accumulated and ~80% of chromosomes were broken at the 9.5 hour time point. Strikingly, the induction of Cdc5 had a robust negative impact on DSB formation; by the 9.5 hour time point, ~35% of chromosomes were broken, a ~5% increase from the 3.5 hour time point. These data indicate that Cdc5 acts to prohibit meiotic DSB formation. The induction of Cdc5 was confirmed by Western blotting (**Figure 8.3B**). In addition, the induction of Cdc5 in early prophase mimicked the induction of Cdc5 at late prophase in that SC proteins Zip1 and Red1 were degraded and Dbf4 was phosphorylated, suggesting that Cdc5 induction during early prophase is phenotypically comparable to Cdc5 induction at the end of pachytene.

Since this study has presented substantial evidence that Dbf4 and Cdc5 interact to regulate multiple facets of meiotic prophase I, and previous work has

Figure 8.3. Cdc5 can prohibit DSB formation independently of both DDK and Red1.

Strains were synchronously introduced into meiosis. At 3.5 hours, cultures were split into two and one subculture received beta-estradiol and the other subculture received carrier (ethanol). **A** Meiotic chromosomes were examined at the indicated time points by pulsed-field gel electrophoresis followed by Southern blotting (panels). The percentage of signal corresponding to broken chromosomes was plotted (graphs). Error bars ±SEM, n = 3. **B** Protein extracts at the indicated time points were examined by immunoblotting.

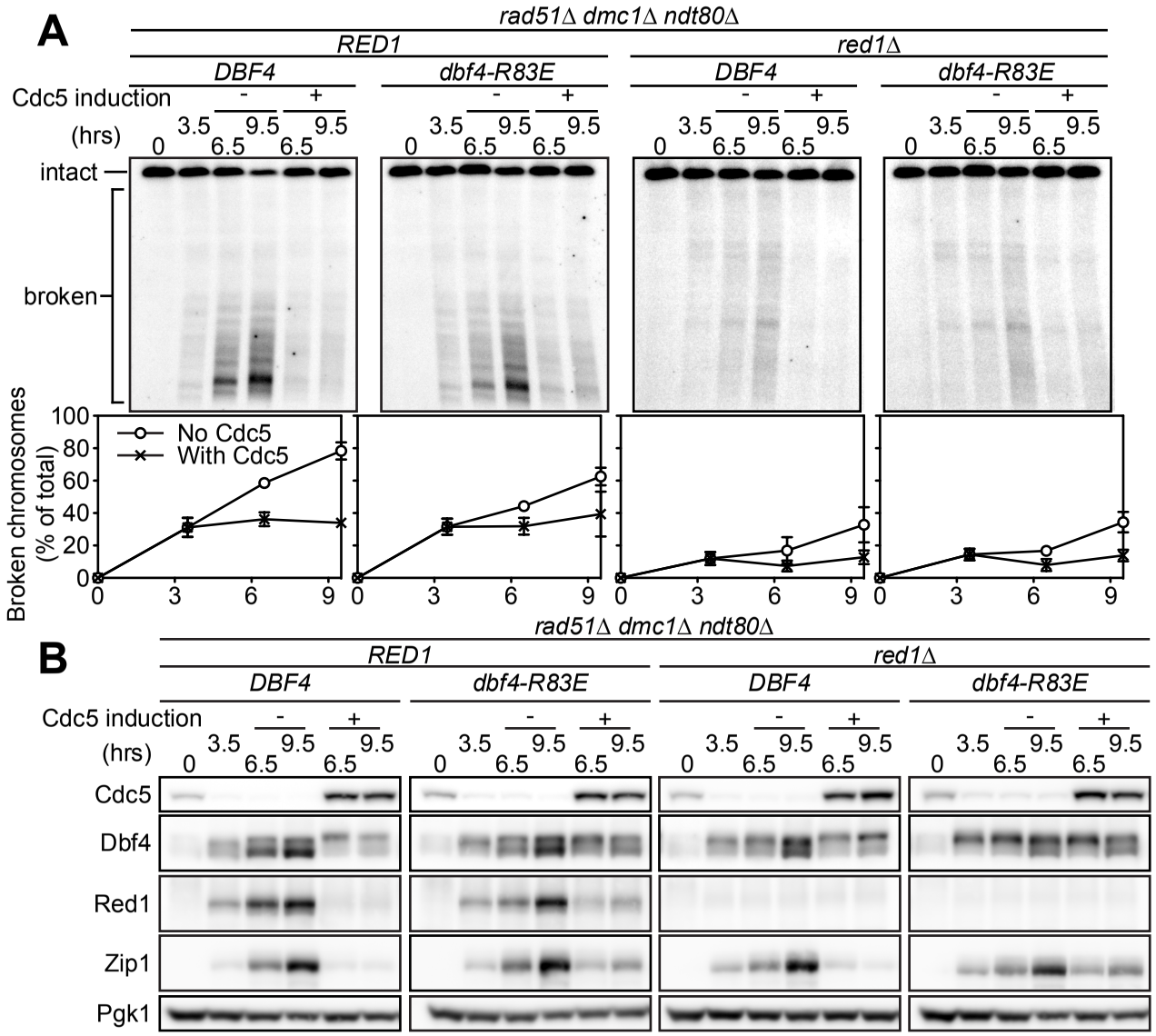
A
rad51Δ dmc1Δ ndt80Δ
RED1
red1Δ
DBF4
dbf4-R83E
DBF4
dbf4-R83E
Cdc5 induction
-
+
(hrs)
0
3.5
6.5
9.5
6.5
intact
broken
Broken chromosomes (% of total)
No Cdc5
With Cdc5
100
80
60
40
20
0
0
3
6
9
B
rad51Δ dmc1Δ ndt80Δ
RED1
red1Δ
DBF4
dbf4-R83E
DBF4
dbf4-R83E
Cdc5 induction
(hrs)
Cdc5
Dbf4
Red1
Zip1
Pgk1

shown that DDK is required for meiotic DSB formation (Sasanuma et al., 2008; Wan et al., 2008), I considered the possibility that Cdc5 might downregulate DSBs through inactivation of DDK. Matos et al. (2008) showed that Cdc5 immunoprecipitates with Cdc7, but that this interaction requires the presence of Cdc5's polo-box domain and Dbf4, strongly suggesting that Cdc5 interacts indirectly with Cdc7 through Dbf4. Thus, if Cdc5 is able to downregulate DSB formation through DDK, then abrogating its interaction with Dbf4 should lessen its ability to downregulate DSB formation. To this end, the *dbf4-R83E* mutation was introduced into the *rad51Δ dmc1Δ ndt80Δ CDC5-IN* strain, and meiotic DSBs were monitored. At 3.5 hours, when the culture was split, ~30% of chromosomes were broken (**Figure 8.3A**). As anticipated, DSBs accumulated in the absence of Cdc5 and broken chromosomes comprised ~65% of the total signal at the 9.5 hour time point. In stark contrast, Cdc5 induction prevented DSB formation such that ~40% of chromosomes were broken at the 9.5 hour time point, which constitutes a ~10% increase from the 3.5 hour time point. Cdc5 induction was confirmed by western blotting **(Figure 8.3B**). These data suggest that Cdc5's ability to downregulate meiotic DSB formation is largely independent of DDK.

The SC protein Red1 is required for the full induction of meiotic DSBs, with reports indicating that in the absence of Red1, the amount of DSBs is ~25% of that seen in WT (Schwacha & Kleckner, 1997; Xu et al., 1997). Since Cdc5 induction leads to the degradation of Red1 (this study) (Okaz et al., 2012), it is possible that Cdc5 indirectly downregulates DSB formation by initiating the destruction of Red1. However, if this was the case, one would have expected to see a milder effect exerted by Cdc5 in the *dbf4-R83E* strain, in which Red1 is

more resistant to degradation (**Figure 8.3B**). To directly examine the possibility that Cdc5 indirectly downregulates meiotic DSB formation through Red1 degradation, the *red1Δ* mutation was introduced into the *rad51Δ dmc1Δ ndt80Δ CDC5-IN* strain. At the 3.5 hour time point, when the culture was split, ~10% of total signal corresponded to broken chromosomes (**Figure 8.3A**). In the absence of Cdc5, ~30% of chromosomes were broken at the 9.5 hour time point. However, in the subculture where Cdc5 was induced, ~10% of chromosomes were broken at the 9.5 hour time point, indicating that Cdc5 was able to exert its inhibitory influence on DSB formation even in the absence of Red1. The induction of Cdc5 was confirmed by western blotting (**Figure 8.3B**).

To confirm that Cdc5's ability to downregulate DSB formation is indeed independent of both Red1 and DDK, the *dbf4-R83E* mutation was introduced into the *rad51Δ dmc1Δ ndt80Δ red1Δ CDC5-IN* strain. For example, it is formally possible that Cdc5 can exert its effect equally through both Red1 and DDK, and in the absence of one, Cdc5 can still downregulate DSB formation by utilising the other pathway. ~15% of chromosomes were broken at the 3.5 hour time point (**Figure 8.3A**). As anticipated, in the subculture without Cdc5, ~35% of chromosomes were broken at the 9.5 hour time point. Even in the absence of Red1 and the Dbf4-Cdc5 interaction, Cdc5 was able to prevent DSB formation, such that only ~15% of chromosomes were broken in the subculture containing Cdc5. Cdc5 induction was confirmed by western blotting (**Figure 8.3B**). This result clearly illustrates that Cdc5 is able to downregulate meiotic DSB formation independently of its interaction with DDK and its ability to induce Red1 degradation.

8.4 Conclusions

Despite the depth of knowledge regarding the initiation of meiotic DSB formation, relatively little is known about how this process, once initiated, is regulated. In this chapter, I have presented evidence that the DNA damage checkpoint plays important roles in both negatively and positively regulating meiotic DSB formation. Furthermore, I have presented evidence suggesting that Cdc5 alone can prevent meiotic DSB formation. The ability of Cdc5 to downregulate meiotic DSB formation is independent of its role in promoting Red1 degradation. Moreover, the Dbf4-Cdc5 interaction is dispensable for the inhibition of meiotic DSB formation, suggesting that Cdc5 does not downregulate meiotic DSB formation by deactivating DDK. Taken together, these findings raise the possibility that Cdc5 targets a component of the DSB formation machinery other than DDK to prevent DSB formation after pachytene.

Chapter 9: Discussion

The results presented in this thesis uncover novel roles for DDK and Cdc5 in mediating the change in HR modes during meiosis. Here, I will briefly summarise the results presented in the preceding chapters then discuss the relevance of these findings to the literature.

9.1 Summary of results

I showed that overproduction of Dbf4 or enhancing/enforcing the interaction between Dbf4 and Cdc5 allowed pachytene-arrested cells with defects in meiosis-specific HR machinery to complete meiosis (**Figure 3**). Importantly, meiotic DSBs were repaired by Rad51 in the cells that completed meiosis, indicating that the Dbf4-Cdc5 interaction regulates the meiotic inhibition of Rad51 (**Figure 4**). Cdc5 was known to play a role in disassembly of the SC (Sourirajan & Lichten, 2008), but I showed that this function of Cdc5 was dependent on its interaction with Dbf4, since enhancing or ablating the Dbf4-Cdc5 interaction resulted in increased or decreased SC disassembly efficiency, respectively (**Figures 5.1, 5.3**). Crucially, the efficiency of SC disassembly showed a strong correlation with the efficiency of Rad51-dependent DSB repair, suggesting that removal of the SC structure at the end of prophase I relieves Rad51 of its meiotic inhibition and permits Dmc1-independent DSB repair (**Figure 5.2**).

Additionally, my data strongly suggest that Cdc5 directly phosphorylates Dbf4. The extent of Dbf4 phosphorylation correlated well with the efficiency of Cdc5-driven SC destruction, suggesting that phosphorylation of Dbf4 is required for timely destruction of the SC (**Figures 6.1, 6.3**). Moreover, in the absence of

DDK activity, the ability of Cdc5 to induce SC destruction was compromised, indicating that DDK itself plays an important role in facilitating SC destruction (**Figure 7.2**). Interestingly, during prophase I when Cdc5 is absent, DDK was shown to be required for maintaining SC integrity and Rad51 inhibition (**Figure 7.1**), indicating that DDK has opposing roles in regulating the SC. I further showed that the checkpoint kinases Mec1 and Tel1 act during prophase I to downregulate and upregulate meiotic DSB formation, respectively (**Figures 8.1, 8.2**). Pertinent to the regulation of DSB formation, the ectopic production of Cdc5 in early prophase I was shown to be sufficient to prohibit DSB formation, suggesting that Cdc5 alone can prevent any further DSB formation as cells exit pachytene (**Figure 8.3**). Taken together, these results indicate that DDK and Cdc5 play a crucial role in coordinating SC morphogenesis, and hence inhibition of Rad51, with the meiotic cell cycle. Furthermore, the recombination checkpoint is responsible for fine-tuning of meiotic DSB formation before pachytene, and the upregulation of Cdc5 as cells exit pachytene acts to prohibit any further DSB formation. These findings are summarised in **Figure 9**.

9.2 Different modes of HR in meiosis

Meiotic HR is often noted for its differences to mitotic HR. The process of mitotic HR is strongly biased to involve sister chromatids and result in noncrossover products (Moynahan & Jasin. 2010). In contrast, meiotic HR is regulated to ensure that the homologous chromosome as opposed to the sister chromatid is utilised for DSB repair, and that the outcome of such repair is biased towards forming crossovers (Humphryes & Hochwagen, 2014). These differences can be explained when considering the functions of the two modes of HR. Mitotic

Figure 9. DDK and Cdc5 are key regulators of the synaptonemal complex.
From left to right. Schematic summarising the findings presented in this thesis. Graphical display at the top of the schematic is a relative representation of kinase activity throughout meiosis I (this is not drawn to scale). Chromosome behaviour is described and portrayed in the middle of the schematic with the corresponding stage in meiosis stated at the bottom. Descriptions in bold are contributions made by this study. **1)** During leptotene, DDK activity is high and promotes DSB formation by phosphorylating Mer2. DSB formation is fine-tuned through the combined activities of Mec1 and Tel1, which are activated in response to DSB formation. Conversely, Cdc5 activity remains low until the end of pachytene, when Cdc5 is upregulated by Ndt80. **2)** DDK activity remains high in zygotene and pachytene, where it is required to maintain the integrity of the SC, which reinforces the inhibition towards the mitotic recombination machinery and supports the preference for interhomologue HR. **3)** Cdc5 activity increases as cells exit pachytene, resulting in the DDK-independent prohibition of DSB formation. Concurrently, Dbf4 is phosphorylated by Cdc5, resulting in DDK promoting Cdc5-driven SC destruction, which relieves the mitotic recombination machinery of its meiotic inhibition. Consequently, any persisting DSBs are efficiently repaired without any pressure to form interhomologue crossovers and no acentric chromosome fragments persist into metaphase I. Since DSBs are repaired, the pachytene checkpoint is turned off and Mec1 and Tel1 are inactivated. **4)** Persisting DDK activity is required to ensure the monoorientation of sister chromatids in metaphase I. **5)** Following activation of the APC/C, Dbf4 is rapidly targeted for destruction and DDK activity is depleted in preparation for the G1 phase of the upcoming mitotic cell cycle. Cdc5 facilitates resolution of chiasmata and destruction of arm cohesin, liberating homologous chromosomes from their physical connection. Consequently, homologous chromosomes as opposed to sister chromatids are pulled to opposite poles of the cell in anaphase I. Eventually, Cdc5 is also targeted by the APC/C and its activity declines into meiosis II, where it is not known to have any function.

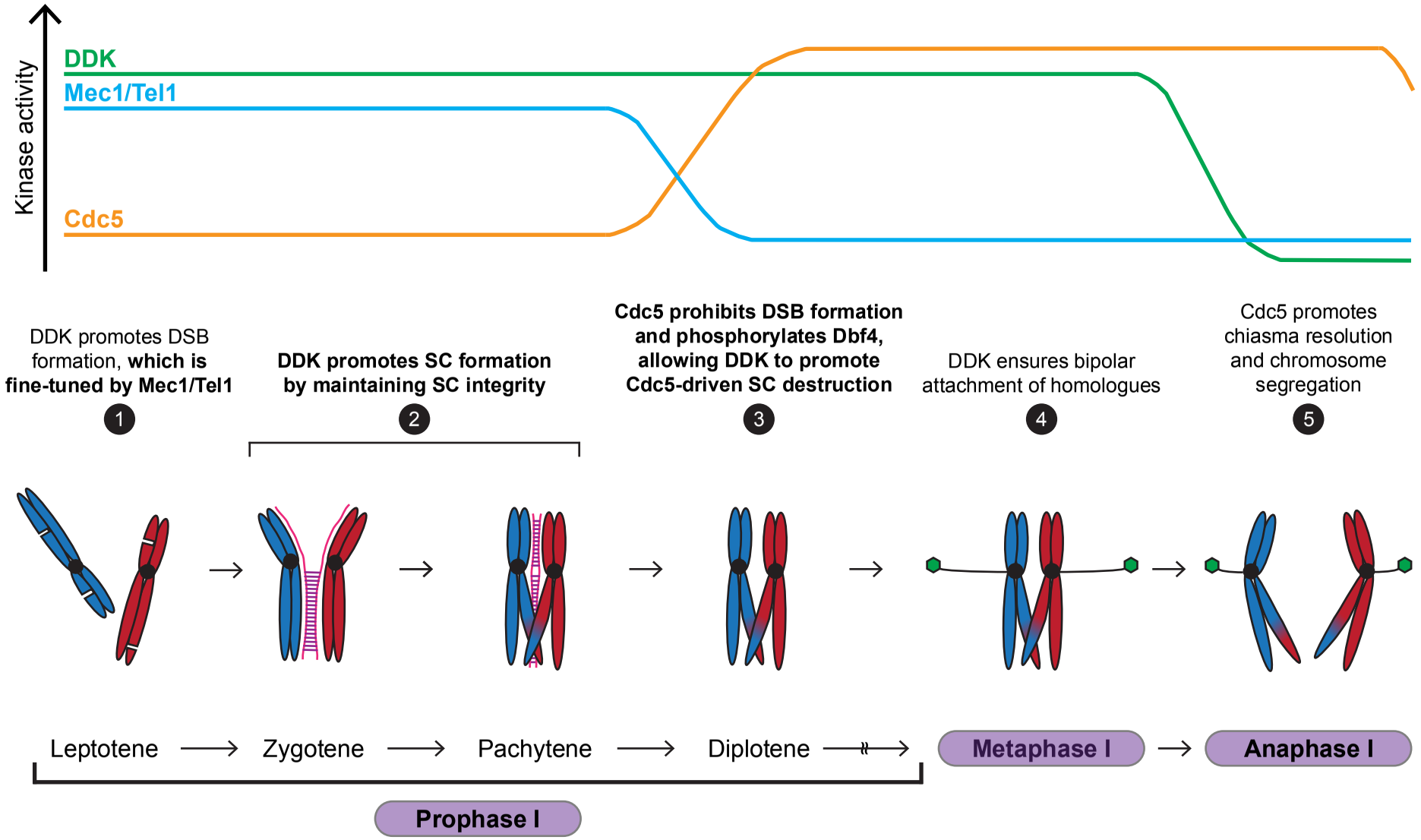
Kinase activity
DDK
Mec1/Tel1
Cdc5
DDK promotes DSB formation, which is fine-tuned by Mec1/Tel1
1
DDK promotes SC formation by maintaining SC integrity
2
Cdc5 prohibits DSB formation and phosphorylates Dbf4, allowing DDK to promote Cdc5-driven SC destruction
3
DDK ensures bipolar attachment of homologues
4
Cdc5 promotes chiasma resolution and chromosome segregation
5
Leptotene
Zygotene
Pachytene
Diplotene
Metaphase I
Anaphase I
Prophase I

HR is generally tasked with repairing DSBs that arise as a result of spontaneous damage or DNA replication, thus it is beneficial for the broken DNA to be restored to its exact previous state (Lambert & Carr, 2013). In contrast, meiotic HR in budding yeast is responsible for repairing the ~150 self-inflicted DSBs that are induced by the topoisomerase-like enzyme Spo11 to ensure physical linkages between homologues (Keeney et al., 1997).

An important consideration of meiotic HR is that the number of DSBs induced is far greater than the number of resultant crossovers, thus increasing the likelihood that every chromosome receives at least one crossover, which is known as the obligate crossover (Lynn et al., 2007; Globus & Keeney, 2012). Since the average number of crossovers per budding yeast chromosome is ~6 (Mancera et al., 2008), a large number of DSBs are repaired either as intersister crossovers/noncrossovers, which are undetectable, or interhomologue noncrossovers. In any case, all of the outcomes that are not interhomologue crossovers make no direct contribution to the formation of physical linkages between homologues. Irrespective of this fact, every single meiotic DSB must be repaired before the separation of chromosomes, as the existence of any acentric chromosomal fragments will result in the formation of gametes lacking potentially essential genetic material (Gerton & Hawley, 2005). An inherent consequence of this is that the specialised mode of meiotic HR must also be able to perform mitotic HR-like DSB repair, a notion that is supported by an abundance of data (Schwacha & Kleckner, 1997; Hunter & Kleckner, 2001; Goldfarb & Lichten, 2010). Owing to the spatial convenience of utilising a donor sequence located on the sister chromatid, intersister recombination is generally more efficient than interhomologue recombination (Kadyk & Hartwell, 1992).

Thus, mitotic HR is a more suitable method to swiftly repair DSBs with no pressure to form interhomologue joint molecules; there is a narrow window of time during the meiotic cell cycle when this is the case.

By the end of pachytene (i.e., before the robust induction of Ndt80), the SC is fully matured and interhomologue double Holliday junctions have been formed, thus there is no longer any pressure to form more interhomologue double Holliday junctions (Schwacha & Kleckner, 1994; Xu et al., 1995; Allers & Lichten, 2001). Indeed, following the induction of Ndt80, joint molecules are resolved and further DSB formation is discouraged (this thesis: (Argunhan et al., 2013)) (Xu et al., 1995; Sourirajan & Lichten, 2008), suggesting that this is the crucial point in the meiotic cell cycle when the meiotic mode of HR becomes dispensable. Moreover, due to the complexity of DSB formation, it is unlikely that the termination of DSB formation is an immediate process; this is highly pertinent because the persistence of even a single DSB during chromosome segregation can be disastrous for the viability of the resultant gametes (Gerton & Hawley, 2005). Taking these considerations into account, it seems reasonable that, following the induction of Ndt80, meiotic cells can switch from the meiotic mode of HR to the mitotic mode of HR, which is dependent on Rad51 but not Dmc1.

To understand the mechanism that promotes switching of the HR mode in meiosis, it was necessary to identify the factor(s) under the control of Ndt80 that is responsible for this switching. I have provided evidence that this factor is Cdc5, since the induction of Cdc5 alone in *ndt80Δ dmc1Δ* cells permits Rad51-dependent DSB repair (**Figures 5.2A, C**). This repair is dependent on the kinase activity of Cdc5, since the induction of catalytically inactive Cdc5, which

was unable to evoke SC destruction, did not lead to Rad51-dependent DSB repair (**Figures 6.1C, 6.2**). Moreover, the ability of Cdc5 to mediate the switching of HR modes is dependent on its interaction with DDK, since the efficiency of SC destruction and Rad51-dependent DSB repair showed a strong correlation with Cdc5-DDK interaction strength (**Figures 5.2A, B**), which determines the extent of Dbf4 phosphorylation (**Figure 6.1**). When combined with the findings that cells with reduced Dbf4 phosphorylation or DDK activity show impaired SC destruction (**Figures 6.3, 7.2**), I propose that the activities of DDK and Cdc5 cooperatively promote the switching of HR modes from meiotic to mitotic by initiating SC destruction as cells exit the pachytene stage of prophase I.

Although the DSB repair discussed above was shown to be Rad51-dependent and Dmc1-independent, this itself does not exclude the possibility that the repair is proficient for generating more interhomologue joint molecules. Consistent with this notion, under conditions where Rad51 is overproduced or the inhibition to Rad51-mediated HR is ablated through deletion of *HED1*, spore viability of *dmc1Δ* cells is rescued due to the production of interhomologue crossovers (Tsubouchi & Roeder, 2003; Tsubouchi & Roeder, 2006). However, there is evidence to suggest that this is not the case here. In the *dmc1Δ dbf4-E86V* mutant, Dbf4 and Cdc5 showed an enhanced interaction and cells were able to complete meiosis due to Rad51-dependent repair of DSBs (**Figures 3.3, 4.2**). This Rad51-dependent DSB repair only mildly improved spore viability when compared to conditions where there is no DSB repair i.e., the *dmc1Δ* mutant (~1% viability) (**Figure 4.3C**) (Tsubouchi & Roeder, 2006). Moreover, when an additional copy of *dbf4-E86V* was homozygously integrated at the

URA3 locus, *dmc1Δ dbf4-E86V* cells showed near complete DSB repair (**Figures 4.3A, B**). Nonetheless, spore viability was no higher than that seen in the strain without additional copies of *dbf4-E86V*, which showed substantially less DSB repair (**Figure 4.3C**). These findings argue that the main cause of spore inviability in cells that complete meiosis as a consequence of Rad51-dependent DSB repair is chromosome nondisjunction, suggesting that, under these conditions, DSB repair by Rad51 is unproductive for interhomologue crossover formation and thus resembles mitotic HR.

Evidence exists to suggest that a change in the mode of HR during meiosis might be evolutionarily conserved. The nematode *Caenorhabditis elegans* does not have a Dmc1 homologue (Youds & Boulton, 2011). In the absence of RAD-50, homologue of budding yeast Rad50 (Youds & Boulton, 2011), no chiasmata were observed between homologous chromosomes, suggesting that RAD-50 is essential for interhomologue recombination (Hayashi et al., 2007). This suggestion was supported by the finding that RAD-50 is required for the loading of RAD-51 onto DNA during early/mid-pachytene (Hayashi et al., 2007). The recombination complexes that assemble on ssDNA during this period were shown to have the capacity to form chiasmata (Hayashi et al., 2007). Importantly, Hayashi et al. (2007) reported RAD-50-independent loading of RAD-51 late in pachytene, progression to which is controlled by a MAP kinase signalling programme in mid-pachytene. Moreover, Hayashi et al. (2007) showed that the RAD-50-independent recombination complexes that assemble on ssDNA during late pachytene are incompetent for chiasmata formation, suggesting that they are involved in intersister DSB repair. Such repair likely requires BRC-1, the BRCA1 homologue in *C. elegans*, which has

been shown to be required only for intersister HR during meiosis (Adamo et al., 2008). Taken together, these findings point towards the existence of a switch in the mode of HR in *C. elegans*.

There are several parallels between these findings in *C. elegans* and the data presented in this thesis using *S. cerevisiae*. First, a switch to a mitotic mode of HR is preceded by a checkpoint that is able to arrest the cell cycle. In *C. elegans*, this is the MAP kinase developmental switch, activation of which coincides with the progression of recombination intermediates (Hayashi et al., 2007). In *S. cerevisiae*, this is the recombination checkpoint, which only permits progression through the cell cycle once most/all DSBs are repaired (Roeder & Bailis, 2000). Second, the repair of DSBs that are induced in late pachytene does not result in chiasmata formation in *C. elegans* (Hayashi et al., 2007). Likewise, the Rad51-dependent repair of DSBs in *S. cerevisiae* does not rescue the spore inviability of *dmc1Δ* cells despite near complete DSB repair (**Figure 4.3**), suggesting that chromosomes undergo missegregation due to an absence of chiasmata. Third, the repair of DSBs by recombination complexes that form late in pachytene likely depends on BRC-1, which is dispensable for chiasmata formation but nonetheless essential for viability of the progeny (Adamo et al., 2008). This possibility, though yet to be demonstrated, would suggest that *C. elegans* utilises mitotic HR machinery to impose the mitotic mode of HR in meiosis. Similarly, the DSB repair seen in *S. cerevisiae* is independent of the meiotic recombinase Dmc1 but dependent on Rad51 (**Figures 4.2, 4.3**), the only recombinase operating in mitotic cells (Krogh & Symington, 2004). Fourth, the meiotic mode of HR in *C. elegans* is characterised by a dependence on RAD-50 for loading of RAD-51 onto DNA, which itself requires the presence of

SC lateral element proteins (Hayashi et al., 2007). The mitotic mode of HR uncovered in this thesis can only operate in the absence of the lateral element protein Red1 (**Figure 5.2A, B, 6.1C**), consistent with the notion that the SC's lateral elements are crucial in enforcing the meiotic mode of HR (Page & Hawley, 2004).

9.3 Novel roles for DDK in SC regulation

In mitotic cells, DDK has an essential role in initiating DNA replication (Sclafani, 2000). In meiotic cells, DDK has well established roles in in early prophase I, where it is required for DSB formation, and in metaphase I, where it is required for sister chromatid monoorientation (Marston, 2009). This thesis has provided strong evidence that DDK also plays a key role in the intervening events. More specifically, DDK is identified as a key regulator of the SC.

Up until the end of pachytene, DDK is required for maintaining SC integrity and imposing the meiotic mode of HR. In the *ndt80Δ* mutant, where there is only basal levels of Cdc5, DDK inactivation by nuclear depletion of Dbf4/Cdc7 through the anchor-away technique led to a loss of SC integrity, as the central element protein Zip1 no longer localised with the chromosome axes protein Red1 (**Figure 7.1B**). These findings indicate that DDK is required for the correct localisation of either/both Zip1/Red1. It is known that, while correct Zip1 localisation requires Red1, Red1 can localise correctly to chromosome axes in the absence of Zip1 (Smith & Roeder, 1997). Upon closer inspection (**Figure 7.1B**, inset panels), the localisation of both Red1 and Zip1 after DDK inactivation seems altered, suggesting that the mislocalisation of Zip1 could be a consequence of defective Red1 localisation. Thus, it is likely that constitutive

DDK activity throughout early/mid prophase I is required for correct chromosome axes structure.

Proteins involved in establishing meiosis-specific chromosome structure, such as Red1, have well established roles in enforcing the interhomologue recombination bias seen in meiosis (Schwacha & Kleckner, 1997; Kim et al., 2010). Thus, if the localisation of these proteins is in fact altered in the absence of DDK activity, as suggested by **Figure 7.1B**, then it is possible that the interhomologue recombination bias will be lost and DSBs will be repaired independently of the meiotic HR machinery. This is indeed the case (**Figure 7.1C**), indicating that DDK activity is required to enforce the meiotic mode of HR and providing further support for the finding that DDK is required to maintain SC integrity.

It has previously been shown that Cdc5 is the only member of the Ndt80 regulon required to drive SC disassembly (Chu & Herskowitz, 1998; Sourirajan & Lichten, 2008). However, when Cdc5 was artificially induced in *ndt80Δ* cells that lack DDK activity, SC destruction was consistently delayed (**Figure 7.2B, C**). Moreover, when this experiment was repeated in *NDT80* cells, which produce Cdc5 naturally, SC destruction was once again delayed (**Figure 7.2A**). These data indicate that DDK, whose production is Ndt80-independent, is also required for efficient disassembly of the SC.

The implication of these findings becomes clear when considering the temporally distinct requirements for DDK in meiosis. After initiating DSB formation in early prophase I (Sasanuma et al., 2008; Wan et al., 2008), it was previously not known whether DDK had any other functions in the highly extended prophase I. However, DDK was known to participate in the

monoorientation of sister chromatids during metaphase I (Matos et al., 2008). In hindsight, due to DDK being regulated by the cyclic production of Dbf4 (Cheng et al., 1999; Ferreira et al., 2000), it seems plausible that DDK would be required for molecular events that take place in mid/late prophase I, since it is required (and therefore active) at the times that flank this stage in meiosis I i.e., early prophase I and metaphase I. The data presented in this thesis indicates that DDK is required during early/mid prophase I to maintain SC integrity and enforce the meiotic mode of HR. Furthermore, as Ndt80 and Cdc5 are produced in mid/late prophase I and cells commit to meiosis I, DDK contributes to Cdc5-driven SC destruction. Thus, I propose that DDK is a central regulator of meiosis I since it regulates numerous biological phenomena that are exclusively associated with meiosis I: the programmed induction of DSBs, which initiates meiotic HR (Sasanuma et al., 2008; Wan et al., 2008); the SC, which is a meiosis-specific macromolecule that enforces the meiotic mode of HR (this thesis); and the monoorientation of sister chromatids, which allows separation of homologous chromosomes during the first meiotic division (Matos et al., 2008).

9.4 Interplay between DDK and the budding yeast polo kinase Cdc5

The first major result presented in this thesis was that an interaction between Dbf4 and Cdc5 regulates cell cycle progression in meiosis (**Figure 3**). The results presented in the subsequent chapters highlighted the important role this interaction plays in promoting destruction of the SC and consequently facilitating the switch from the meiotic mode of HR to the mitotic mode. In the absence of Cdc5, DDK is required for SC integrity within prophase I (discussed

above in section **9.2**). However, as cells make the commitment to execute meiosis I, Cdc5 is produced and interacts with DDK through Dbf4, leading to efficient SC destruction, which in turn promotes the switch from meiotic HR to mitotic HR.

How does DDK make the transition from positively regulating the SC to negatively regulating the SC? Since Cdc5 only negatively regulates the SC, it is likely that the interaction between Cdc5 and Dbf4 leads to DDK negatively regulating the SC. In support of this, SC destruction was inefficient in the *dbf4-R83E* mutant background, which encodes a version of Dbf4 that does not interact with Cdc5 (**Figures 3.2C, D, 5.1A, B, 5.2B, 5.3B**). Moreover, I provided evidence to strongly suggest that Cdc5 phosphorylates Dbf4 as cells make the transition from prophase I to metaphase I (**Figure 6.1**), raising the possibility that this phosphorylation event is responsible for converting DDK from a positive to a negative regulator of the SC. Consistent with this notion, when the phosphorylation of Dbf4 was compromised by substituting certain Ser/Thr residues into nonphosphorylatable Ala residues, SC disassembly was less efficient (**Figure 6.3**), indicating that phosphorylation of Dbf4 at the prophase I/metaphase I transition contributes to negative regulation of the SC.

An alternative possibility is that DDK does not negatively regulate the SC. In this scenario, the positive role DDK plays in SC maintenance is simply negated by the activity of Cdc5, which inhibits the ability of DDK to support SC integrity. Thus, when the interaction between Dbf4 and Cdc5 is lost, DDK is better able to maintain SC integrity, which opposes the role of Cdc5 in SC destruction and leads to inefficient SC destruction. This possibility postulates that the phosphorylation of Dbf4 by Cdc5 leads to inactivation of DDK. I favour

the former scenario in which DDK negatively regulates the SC at the prophase I/metaphase I transition. If DDK's only role in SC regulation is to maintain SC integrity, and Cdc5 interacts with Dbf4 to negate this role of DDK, then the production of Cdc5 in the absence of DDK activity should have a neutral effect on SC destruction. Strikingly, Cdc5-driven SC destruction is inefficient in the absence of DDK activity (**Figure 7.2**), suggesting that DDK plays an active role in negatively regulating the SC upon Cdc5 production.

It is important to note that Dbf4 also undergoes Cdc5-independent phosphorylation. Throughout prophase I, SDS-PAGE separated Dbf4 exists as a doublet, even though Cdc5 levels are barely detectable by western blotting. Moreover, as cells make the transition from prophase I to metaphase I, even in the absence of Cdc5, Dbf4 shifts to a lower mobility form, although this shift is more substantial in the presence of Cdc5 (Matos et al., 2008). These findings strongly suggesting that Dbf4 undergoes Cdc5-independent phosphorylation, although the identity of the kinase responsible remains to be determined.

The cell cycle stage of Cdc5 production is pertinent to this discussion. By the end of pachytene, homologous chromosomes have synapsed and formed chiasmata, which will facilitate their correct segregation (discussed above in section **9.2**). Hence, interhomologue HR, which occurs in the context of the SC, becomes dispensable, paving the way for SC destruction. There is a strong correlation between Dbf4 phosphorylation at the end of prophase I and the efficiency of SC destruction (**Figure 6.3**). Thus, the Cdc5-dependent phosphorylation of Dbf4 might act as a signal that communicates with Cdc7, DDK's catalytic component, to convey that pachytene is finished and the SC is no longer required. Consequently, Cdc5 and DDK can combine their activities

to target SC components Red1 and Zip1 for rapid destruction, although there is currently no evidence in the literature to suggest that DDK or Cdc5 phosphorylates Red1 or Zip1. Finally, due to the absence of the SC, the meiotic mode of HR is ablated and the mitotic mode of HR is unshackled, leading to efficient repair of any persisting meiotic DSBs through use of the sister chromatid.

In addition to its role in SC destruction, Cdc5 has been shown to regulate the Mus81-Mms4-dependent resolution of double Holliday junctions in meiosis by phosphorylation of Mms4, leading to upregulation of Mus81-Mms4 activity (Matos et al., 2011). Interestingly, this occurs at the same time as Cdc5 promotes SC destruction (Sourirajan & Lichten, 2008), raising the possibility that DDK could also be involved in regulating the resolution of recombination intermediates. Such regulation could be direct, by phosphorylation of Mms4 (or Mus81), or indirect, by phosphorylation of Cdc5.

There is ample genetic evidence to suggest that Dbf4 and Cdc5 interact during the vegetative cell cycle to fulfil an as yet unidentified function. The *dbf4-1* mutant is temperature sensitive and has a similar terminal phenotype as the *dbf4Δ* mutant i.e., cell cycle arrest with unreplicated DNA (Kitada et al., 1993). However, overproduction of Cdc5 can suppress this arrest phenotype (Kitada et al., 1993), suggesting that the interaction between Dbf4 and Cdc5 can somehow compensate or bypass the need for DDK in DNA replication. It is known that mutations in genes required for initiation of DNA replication often leads to a chromosome maintenance defect that can be suppressed by introducing more origins of replication onto a centromere-bearing plasmid (Hartwell & Smith, 1985). Kitada et al. (1993) showed the same to be true for

the *cdc5-1* mutant, suggesting that Cdc5 might have a role in DNA replication. Further investigation is needed to substantiate these claims. Additionally, there is biochemical evidence suggesting that the Dbf4-Cdc5 interaction also takes place in mitotic cells and that Cdc5 is capable of phosphorylating Dbf4 (Hardy & Pautz, 1996).

Cdc5 is required for exit from mitosis (Saunders, 2002), thus the terminal phenotype of the *cdc5-1* mutant at the restrictive temperature is arrest in late telophase (Hartwell et al., 1973). This arrest phenotype is presumably due to insufficient Cdc5 activity to promote mitotic exit. Examination of *cdc5-1* cells expressing *dbf4-NΔ109*, a truncated version of Dbf4 that does not interact with Cdc5, revealed that the absence of interaction with Dbf4 can suppress the arrest of *cdc5-1* cells (Miller et al., 2009). This finding suggests that, during mitosis, Dbf4 inhibits Cdc5 through a direct interaction. Consistently, *cdc5-1* temperature sensitivity was shown to be exacerbated through introduction of the *dbf4-E86K* allele, which encodes a version of Dbf4 that shows an enhanced interaction with Cdc5 (Chen & Weinreich, 2010). Speculatively, it is plausible that cells can only exit mitosis when sufficient Dbf4 has been destroyed following APC activation (Ferreira et al., 2000) and Cdc5, which is known to regulate mitotic exit (Saunders 2002), is unshackled from its Dbf4-dependent inhibition.

Taken together, there are strong indications that the Dbf4-Cdc5 interaction has biological significance in mitotic cells. Crucially, the impact that DDK has on Cdc5 and vice versa could be highly relevant to human health, given that 1) both DDK and polo kinases are highly conserved among eukaryotes and have homologues in humans (Masai & Arai, 2000; Barr et al.,

2004) and 2) the human homologue of Cdc5, Plk1, is known to be upregulated in cancers and is currently under investigation for cancer therapeutics (de Cárcer et al., 2011). Thus, it is plausible that the DDK-Polo interaction could be exploited as a tool to downregulate Plk1 in human cells. It would first be necessary to determine whether human DDK interacts with human PLK1.

9.5 Regulation of meiotic DSB formation by the recombination checkpoint and Cdc5

Although much is known about the factors required for the initiation of meiotic DSB formation, relatively little is know about how, once initiated, this dynamic process is regulated (de Massy, 2013). The regulation of DSB formation is of interest because, if DSBs are formed in inadequate numbers, the likelihood of a chromosome not receiving a crossover increases. In contrast, if DSBs form in superfluous numbers, the integrity of the genome is at risk since it is possible that the HR machinery will be overloaded and unable to repair every DSB. In either case, misregulation of DSB formation increases the likelihood of aneuploidy. Thus, logic dictates that mechanisms should exist to regulate DSB formation both positively and negatively, to ensure that the total number of DSBs in a given cell is kept within an acceptable range. Here, I identified two distinct mechanisms that execute this regulatory function: the recombination checkpoint (Argunhan et al., 2013) and the budding yeast polo kinase Cdc5.

The recombination checkpoint responds to the presence of DSBs by delaying or halting cell cycle progression to provide more time for the DNA damage to be repaired (Roeder & Bailis, 2000). Thus, the recombination checkpoint is very capable of detecting and responding to DSBs. The highly

conserved checkpoint kinases Mec1 and Tel1, respective homologues of ATR and ATM in yeast, are key components of the mitotic DNA damage checkpoint and the meiotic recombination checkpoint (Carballo & Cha, 2007). Moreover, Mec1 and Tel1 are thought to regulate/enforce numerous biological processes including homologue synapsis, the interhomologue recombination bias, and crossover distribution (Carballo & Cha, 2007). However, in order to effectively study differences in DSB formation, it is necessary to eliminate the possibility that any difference in DSB levels is due to the disappearance of DSBs by DNA repair. Thus, mutant backgrounds that block DNA repair were utilised to study the effects of Mec1 and Tel1 on DSB formation.

By taking advantage of the preference for Tel1 to respond to unresected DSB ends (Usui et al., 2001), which was achieved by employing strains that lack Sae2 and consequently accumulate unresected DSB ends (Neale & Keeney, 2006), I showed that the Tel1 pathway of the recombination checkpoint upregulates meiotic DSB formation specifically in larger chromosomes (**Figure 8.1**). A similar, more substantial chromosome size-specific phenotype was previously reported by Farmer et al. (2012). When the *PCH2* gene was deleted, DSB formation was specifically reduced in larger chromosomes in the *sae2Δ* background with only a mild reduction in the *rad51Δ dmc1Δ* background (Farmer et al., 2012), which accumulates hyperresected DSBs and hence primarily activates the Mec1 pathway of the recombination checkpoint (Lydall et al., 1996; Shinohara et al., 1997). This similarity in phenotype raises the possibility that Tel1 and Pch2 act together during meiosis to upregulate DSB formation. Although a direct interaction between Tel1 and Pch2 has not been reported, there is evidence to suggest that Tel1 and Pch2 could come into close

proximity through an interaction with Xrs2 (Ho & Burgess, 2011). Alternatively, any potential cooperative role of Tel1 and Pch2 could be independent of a direct interaction. There is currently no evidence to explain why this effect is restricted to the larger chromosomes.

In mice lacking the Tel1 homologue ATM, the amount of Spo11-oligonucleotide complexes detected was increased, indicating that ATM downregulates meiotic DSB formation in mice (Lange et al., 2011). Additionally, ATM-deficient flies show an increase in the levels of phosphorylated H2AV, which is a marker for unrepaired DSBs, suggesting that ATM downregulates meiotic DSB formation in flies as well as mice (Joyce et al., 2011). Thus, the finding that Tel1 upregulates meiotic DSB formation in budding yeast is somewhat unexpected. A potential explanation could be provided by reconsidering the use of the *sae2Δ* mutant background throughout the analyses, since the difference in DSB formation between *sae2Δ* and *sae2Δ tel1Δ* could be restricted only to the *sae2Δ* background. Alternatively, differences between the model systems could reflect evolutionary differences in the usage of Mec1/ATR and Tel1/ATM.

By employing the *rad51Δ dmc1Δ* mutant background, I exploited the preference for Mec1 to respond to resected DSB ends (Lydall et al., 1996) and presented evidence that the Mec1 pathway of the recombination checkpoint downregulates meiotic DSB formation (**Figure 8.2**). For the purpose of depleting Mec1 activity, *RAD17*, which is a component of the Mec1 branch of the DNA damage checkpoint (Hochwagen & Amon, 2006), was downregulated in a meiosis-specific manner to yield a meiotic null (*-mn*) allele (**Figures 8.2A-D**). The *rad17-mn* allele was combined with *ndt80Δ* to eliminate the possibility

that cell cycle progression associated with defects in the DNA damage checkpoint is indirectly responsible for any reduction in DSBs. In the absence of Rad17, DSB formation was increased compared to WT (**Figures 8.2E-G**), indicating that the Mec1 branch of the recombination checkpoint is required to downregulate meiotic DSB formation. Similar findings were reported by Gray et al., (2013).

An ancillary yet nonetheless informative interpretation of these experiments is the role played by Ndt80-dependent cell cycle progression in downregulating meiotic DSB formation. First, introduction of the *ndt80Δ* mutation lead to an overall increase in DSB formation in both the *sae2Δ* and *rad51Δ dmc1Δ* backgrounds (**Figures 8.1, 8.2**). Second, when DSB formation was compromised (e.g., through inclusion of *pch2Δ* or *spo11-HA*), the defect in DSB formation was further exacerbated by the absence of Rad17 only in the presence of *NDT80*. When the *ndt80Δ* background was employed, the introduction of *rad17-mn* to *pch2Δ* or *spo11-HA* led to an increase in DSB formation, indicating that the synergistic effect seen in the *NDT80* background is an indirect consequence of cell cycle progression. These results are summarised in **Figure 8.2G**. Taken together, these findings indicate that, while the Tel1 branch of the DNA damage checkpoint specifically upregulates meiotic DSB formation on larger chromosomes, the Mec1 branch of the DNA damage checkpoint downregulates meiotic DSB formation, indicating that the DNA damage checkpoint can fine-tune meiotic DSB formation. Additionally, genome integrity is protected by the Ndt80-dependent cell cycle progression that acts to downregulate meiotic DSB formation after the pachytene stage of prophase I.

How might the checkpoint kinases exert their effects on meiotic DSB formation? Rec114, an integral component of the DSB forming machinery, is phosphorylated by Mec1 and/or Tel1 in a DSB-dependent manner (Carballo et al., 2013). By employing Ser/Thr to Ala or Ser/Thr to Asp mutations that abolish or mimic phosphorylation, respectively, Carballo et al. (2013) presented evidence to suggest that phosphorylation of Rec114 downregulates meiotic DSB formation. Although these findings provide a direct link between the DNA damage checkpoint kinases Mec1/Tel1 and the DSB forming machinery, the relevant experiments were performed in an *NDT80* background, the drawbacks of which have been highlighted above. Additionally, the authors provided no clear cut evidence that the phosphorylation status of Rec114 can upregulate meiotic DSB formation, raising the possibility that other DSB formation proteins could be targeted by the DNA damage checkpoint to upregulate meiotic DSB formation.

The importance of Ndt80-dependent cell cycle progression in downregulating meiotic DSB formation was discussed above. However, since Ndt80 regulates the transcription of ~200 genes (Chu & Herskowitz, 1998), it was not known how Ndt80 managed to downregulate meiotic DSB formation. During the experiments conducted throughout this thesis, I made the serendipitous discovery that production of Cdc5, which is regulated by Ndt80, downregulates meiotic DSB formation (**Figure 8.3**). In fact, ectopic production of Cdc5 in early prophase I strongly prohibited DSB formation in *ndt80Δ* cells, suggesting that the production of Cdc5 alone is sufficient to prevent further DSB formation following exit from pachytene. The results presented within this thesis have provided strong evidence that 1) Cdc5 and DDK collaborate in meiosis

through an interaction that is dependent on Dbf4 and 2) Cdc5 induction is swiftly followed by destruction of Red1. Since DSB formation is reduced or abolished in the absence of Red1 or DDK (Schwacha & Kleckner, 1997; Sasanuma et al., 2008; Wan et al., 2008), respectively, the possibility that Cdc5 prohibits DSB formation through an interaction with Dbf4 and/or indirectly by inducing Red1 destruction was examined. Interestingly, these experiments clearly demonstrated that Cdc5 downregulates DSB formation independently of its role in inducing Red1 destruction or its interaction with Dbf4. These findings raise the possibility that Cdc5 targets another member of the DSB formation machinery to prohibit DSB formation.

Whereas cells lacking Ndt80 and Cdc5 are unable to shut off meiotic DSB formation (Xu et al., 1995; Allers & Lichten, 2001), cells only lacking Cdc5 manage to shut off DSB formation like WT (Clyne et al., 2003). This is surprising given the fact that production of Cdc5 alone in *ndt80Δ* cells is enough to prohibit further DSB formation (**Figure 8.3**). It is therefore likely that there are multiple parallel pathways responsible for prohibiting further DSB formation following Ndt80 production at the exit from pachytene.

9.6 Concluding remarks

This thesis has uncovered how the cooperation between two highly conserved cell cycle kinases, DDK and Cdc5, links the destruction of the meiosis-specific SC structure to the meiotic cell cycle. In doing so, DDK and Cdc5 facilitate the switch from a meiotic mode of HR to a mitotic mode of HR. In addition, evidence has been presented to implicate the recombination checkpoint and Cdc5 in differentially regulating meiotic DSB formation. Hence, the results presented

here should ignite further research into a broad range of subjects including but not limited to meiotic and mitotic HR, assembly and disassembly of the SC, role of the Dbf4-Cdc5 interaction in mitotic cells, and the regulation of meiotic DSB formation.

Bibliography

Acosta I., Ontoso D. & San-Segundo P.A. (2011). The budding yeast polo-like kinase Cdc5 regulates the Ndt80 branch of the meiotic recombination checkpoint pathway. *Molecular Biology of the Cell*, 22(18), pp. 3478-90.

Adamo A., Montemauri P., Silva N., Ward J.D., Boulton S.J. & La Volpe A. (2008). BRC-1 acts in the inter-sister pathway of meiotic double-strand break repair. *EMBO Reports*, 9(3), pp. 287-92.

Agarwal S. & Roeder G.S. (2000). Zip3 provides a link between recombination enzymes and synaptonemal complex proteins. *Cell*, 102(2), pp. 245-55.

Aguilera A. & Gómez-González B. (2008). Genome instability: a mechanistic view of its causes and consequences. *Nature Reviews. Genetics*, 9(3), pp. 204-17.

Alexandru G., Uhlmann F., Mechtler K., Poupart M.A. & Nasmyth K. (2001). Phosphorylation of the cohesin subunit Scc1 by Polo/Cdc5 kinase regulates sister chromatid separation in yeast. *Cell*, 105(4), pp. 459-72.

Allers T. & Lichten M. (2001). Differential timing and control of noncrossover and crossover recombination during meiosis. *Cell*, 106(1), pp. 47-57.

Arbel A., Zenvirth D. & Simchen G. (1999). Sister chromatid-based DNA repair is mediated by RAD54, not by DMC1 or TID1. *The EMBO Journal*, 18(9), pp. 2648-58.

Argunhan B., Farmer S., Leung W.K., Terentyev Y., Humphryes N., Tsubouchi T., Toyoizumi H. & Tsubouchi H. (2013). Direct and indirect control of the initiation of meiotic recombination by DNA damage checkpoint mechanisms in budding yeast. *PLOS ONE*, 8(6), p. e65875.

Arora C., Kee K., Maleki S. & Keeney S. (2004). Antiviral protein Ski8 is a direct partner of Spo11 in meiotic DNA break formation, independent of its cytoplasmic role in RNA metabolism. *Molecular Cell*, 13(4), pp. 549-59.

Attner M.A., Miller M.P., Ee L.S., Elkin S.K. & Amon A. (2013) Polo kinase Cdc5 is a central regulator of meiosis I. *Proceedings of the National Academy of Sciences of the United States of America*, 110(35), pp. 14278-83.

Bailis J.M. & Roeder G.S. (1998). Synaptonemal complex morphogenesis and sister-chromatid cohesion require Mek1-dependent phosphorylation of a meiotic chromosomal protein. *Genes & Development*, 12(22), pp. 3551-63.

Barr F.A., Silljé H.H. & Nigg E.A. (2004). Polo-like kinases and the orchestration of cell division. *Nature Reviews Molecular Cell Biology*, 5(6), pp. 429-40.

Benjamin K.R., Zhang C., Shokat K.M. & Herskowitz I. (2003). Control of landmark events in meiosis by the CDK Cdc28 and the meiosis-specific kinase Ime2. *Genes & Development*, 17(12), pp. 1524-39.

Bernstein K.A. & Rothstein R. (2009). At loose ends: resecting a double-strand break. *Cell*, 137(5), pp. 807-10.

Bishop D.K. (1994). RecA homologs Dmc1 and Rad51 interact to form multiple nuclear complexes prior to meiotic chromosome synapsis. *Cell*, 79(6), pp. 1081-92.

Bishop D.K., Park D., Xu L. & Kleckner N. (1992). DMC1: a meiosis-specific yeast homolog of E. coli recA required for recombination, synaptonemal complex formation, and cell cycle progression. *Cell*, 69(3), pp. 439-56.

Borde V., Goldman A.S. & Lichten M. (2000). Direct coupling between meiotic DNA replication and recombination initiation. *Science*, 290(5492), pp. 806-9.

Brill S.J. & Stillman B. (1991). Replication factor-A from Saccharomyces cerevisiae is encoded by three essential genes coordinately expressed at S phase. *Genes & Development*, 5(9), pp. 1589-600.

Buck V., White A. & Rosamond J. (1991). CDC7 protein kinase activity is required for mitosis and meiosis in Saccharomyces cerevisiae. *Molecular & General Genetics : MGG*, 227(3), pp. 452-7.

Busygina V., Saro D., Williams G., Leung W.K., Say A.F., Sehorn M.G., Sung P. & Tsubouchi, H. (2012). Novel attributes of Hed1 affect dynamics and activity of the Rad51 presynaptic filament during meiotic recombination. *The Journal of Biological Chemistry*, 287(2), pp. 1566-75.

Busygina V., Sehorn M.G., Shi I.Y., Tsubouchi H., Roeder G.S. & Sung P. (2008). Hed1 regulates Rad51-mediated recombination via a novel mechanism. *Genes & Development*, 22(6), pp. 786-95.

Cannavo E. & Cejka P. (2014). Sae2 promotes dsDNA endonuclease activity within Mre11-Rad50-Xrs2 to resect DNA breaks. *Nature*, 514(7520), pp. 122-5.

Carballo J.A. & Cha R.S. (2007). Meiotic roles of Mec1, a budding yeast homolog of mammalian ATR/ATM. *Chromosome Research*, 15(5), pp. 539-50.

Carballo J.A., Johnson A.L., Sedgwick S.G. & Cha R.S. (2008) Phosphorylation of the axial element protein Hop1 by Mec1/Tel1 ensures meiotic interhomolog recombination. *Cell*, 132(5), pp. 758-70.

Carballo J.A., Panizza S., Serrentino M.E., Johnson A.L., Geymonat M., Borde V., Klein F. & Cha R.S. (2013). Budding yeast ATM/ATR control meiotic double-strand break (DSB) levels by down-regulating Rec114, an essential component of the DSB-machinery. *PLOS GENETICS*, 9(6), p. e1003545.

de Cárcer G., Escobar B., Higuero A.M., García L., Ansón A., Pérez G., Mollejo M., Manning G., Meléndez B., Abad-Rodríguez J. & Malumbres M. (2011). Plk5, a polo box domain-only protein with specific roles in neuron differentiation and glioblastoma suppression. *Molecular and Cellular Biology*, 31(6), pp. 1225-39.

Charles J.F., Jaspersen S.L., Tinker-Kulberg R.L., Hwang L., Szidon A. & Morgan D.O. (1998). The Polo-related kinase Cdc5 activates and is destroyed by the mitotic cyclin destruction machinery in S. cerevisiae. *Current Biology*, 8(9), pp. 497-507.

Chen Y.C. & Weinreich M. (2010). Dbf4 regulates the Cdc5 Polo-like kinase through a distinct non-canonical binding interaction. *The Journal of Biological Chemistry*, 285(53), pp. 41244-54.

Cheng L., Collyer T. & Hardy C.F. (1999). Cell cycle regulation of DNA replication initiator factor Dbf4p. *Molecular and Cellular Biology*, 19(6), pp. 4270-8.

Chu S. & Herskowitz I. (1998). Gametogenesis in yeast is regulated by a transcriptional cascade dependent on Ndt80. *Molecular Cell*, 1(5), pp. 685-96.

Chua P.R. & Roeder G.S. (1998). Zip2, a meiosis-specific protein required for the initiation of chromosome synapsis. *Cell*, 93(3), pp. 349-59.

Cloud V., Chan Y.L., Grubb J., Budke B. & Bishop D.K. (2012). Rad51 is an accessory factor for Dmc1-mediated joint molecule formation during meiosis. *Science*, 337(6099), pp. 1222-5.

Clyne R.K., Katis V.L., Jessop L., Benjamin K.R., Herskowitz I., Lichten M. & Nasmyth K. (2003). Polo-like kinase Cdc5 promotes chiasmata formation and cosegregation of sister centromeres at meiosis I. *Nature Cell Biology*, 5(5), pp. 480-5.

Dowell S.J., Romanowski P. & Diffley J.F. (1994). Interaction of Dbf4, the Cdc7 protein kinase regulatory subunit, with yeast replication origins in vivo. *Science*, 265(5176), pp. 1243-6.

Dresser M.E., Ewing D.J., Conrad M.N., Dominguez A.M., Barstead R., Jiang H. & Kodadek T. (1997). DMC1 functions in a Saccharomyces cerevisiae meiotic pathway that is largely independent of the RAD51 pathway. *Genetics*, 147(2), pp. 533-44.

Farmer S., Leung W.K. & Tsubouchi H. (2011). Characterization of meiotic recombination initiation sites using pulsed-field gel electrophoresis. *Methods in Molecular Biology*, 745: 33-45

Farmer S., Hong E.J., Leung W.K., Argunhan B., Terentyev Y., Humphryes N., Toyoizumi H. & Tsubouchi H. (2012). Budding yeast pch2, a widely conserved meiotic protein, is involved in the initiation of meiotic recombination. *PLOS ONE*, 7(6), p. e39724.

Ferrari S.R., Grubb J. & Bishop D.K. (2009). The Mei5-Sae3 protein complex mediates Dmc1 activity in Saccharomyces cerevisiae. *The Journal of Biological Chemistry*, 284(18), pp. 11766-70.

Ferreira M.F., Santocanale C., Drury L.S. & Diffley J.F. (2000). Dbf4p, an essential S phase-promoting factor, is targeted for degradation by the anaphase-promoting complex. *Molecular and Cellular Biology*, 20(1), pp. 242-8.

Francis L.I., Randell J.C., Takara T.J., Uchima L. & Bell S.P. (2009). Incorporation into the prereplicative complex activates the Mcm2-7 helicase for Cdc7-Dbf4 phosphorylation. *Genes & Development*, 23(5), pp. 643-54.

Garcia V., Phelps S.E., Gray S. & Neale M.J. (2011). Bidirectional resection of DNA double-strand breaks by Mre11 and Exo1. *Nature*, 479(7372), pp. 241-4.

Gerton J.L. & Hawley R.S. (2005). Homologous chromosome interactions in meiosis: diversity amidst conservation. *Nature Reviews. Genetics*, 6(6), pp. 477-87.

Gietz R.D. & Woods R.A. (2002). Transformation of yeast by lithium acetate/single-stranded carrier DNA/polyethylene glycol method. *Methods in Enzymology*, 350: 87-96.

Globus S.T. & Keeney S. (2012). The joy of six: how to control your crossovers. *Cell*, 149(1), pp. 11-2.

Goldfarb T. & Lichten M. (2010). Frequent and efficient use of the sister chromatid for DNA double-strand break repair during budding yeast meiosis. *PLOS BIOLOGY*, 8(10), p. e1000520.

Gray S., Allison R.M., Garcia V., Goldman A.S. & Neale M.J. (2013). Positive regulation of meiotic DNA double-strand break formation by activation of the DNA damage checkpoint kinase Mec1(ATR). *Open Biology*, 3(7), p. 130019.

Gregan J., Spirek M. & Rumpf C. (2008) Solving the shugoshin puzzle. *Trends in Genetics*, 24(5), pp. 205-7.

Hardy C.F. & Pautz A. (1996). A novel role for Cdc5p in DNA replication. *Molecular and Cellular Biology*, 16(12), pp. 6775-82.

Hardy C.F., Dryga O., Seematter S., Pahl P.M. & Sclafani R.A. (1997). mcm5/cdc46-bob1 bypasses the requirement for the S phase activator Cdc7p. *Proceedings of the National Academy of Sciences of the United States of America*, 94(7), pp. 3151-5.

Harrison J.C. & Haber J.E. (2006) Surviving the breakup: the DNA damage checkpoint. *Annual Review of Genetics*, 40, pp. 209-35.

Hartwell L.H. & Smith D. (1985). Altered fidelity of mitotic chromosome transmission in cell cycle mutants of S. cerevisiae. *Genetics*, 110(3), pp. 381-95.

Hartwell L.H., Mortimer R.K., Culotti J. & Culotti M. (1973). Genetic Control of the Cell Division Cycle in Yeast: V. Genetic Analysis of cdc Mutants. *Genetics*, 74(2), pp. 267-86.

Haruki H., Nishikawa J. & Laemmli U.K. (2008). The anchor-away technique: rapid, conditional establishment of yeast mutant phenotypes. *Molecular Cell*, 31(6), pp. 925-32.

Hayase A., Takagi M., Miyazaki T., Oshiumi H., Shinohara M. & Shinohara A. (2004). A protein complex containing Mei5 and Sae3 promotes the assembly of the meiosis-specific RecA homolog Dmc1. *Cell*, 119(7), pp. 927-40.

Hayashi M., Chin G.M. & Villeneuve A.M. (2007). C. elegans germ cells switch between distinct modes of double-strand break repair during meiotic prophase progression. *PLOS GENETICS*, 3(11), p. e191.

Henderson K.A., Kee K., Maleki S., Santini P.A. & Keeney S. (2006). Cyclin-dependent kinase directly regulates initiation of meiotic recombination. *Cell*, 125(7), pp. 1321-32.

Henry J.M., Camahort R., Rice D.A., Florens L., Swanson S.K., Washburn M.P. & Gerton J.L. (2006). Mnd1/Hop2 facilitates Dmc1-dependent interhomolog crossover formation in meiosis of budding yeast. *Molecular and Cellular Biology*, 26(8), pp. 2913-23.

Ho H.C. & Burgess S.M. (2011). Pch2 acts through Xrs2 and Tel1/ATM to modulate interhomolog bias and checkpoint function during meiosis. *PLOS GENETICS*, 7(11), p. e1002351.

Hochwagen A. & Amon A. (2006). Checking your breaks: surveillance mechanisms of meiotic recombination. *Current Biology*, 16(6), pp. R217-28.

Hoeijmakers J.H. (2001). Genome maintenance mechanisms for preventing cancer. *Nature*, 411(6835), pp. 366-74.

Hollingsworth N.M. & Byers B. (1989) HOP1: a yeast meiotic pairing gene. *Genetics*, 121(3), pp. 445-62.

Hollingsworth N.M., Goetsch L. & Byers B. (1990). The HOP1 gene encodes a meiosis-specific component of yeast chromosomes. *Cell*, 61(1), pp. 73-84.

Hollingsworth N.M., Ponte L. & Halsey C. (1995). MSH5, a novel MutS homolog, facilitates meiotic reciprocal recombination between homologs in Saccharomyces cerevisiae but not mismatch repair. *Genes & Development*, 9(14), pp. 1728-39.

Hong S., Sung Y., Yu M., Lee M., Kleckner N. & Kim K.P. (2013). The logic and mechanism of homologous recombination partner choice. *Molecular Cell*, 51(4), pp. 440-53.

Humphryes N. & Hochwagen A. (2014). A non-sister act: recombination template choice during meiosis. *Experimental cell research*, http://dx.doi.org/10.1016/j.yexcr.2014.08.024

Hunter N. & Kleckner N. (2001). The single-end invasion: an asymmetric intermediate at the double-strand break to double-holliday junction transition of meiotic recombination. *Cell*, 106(1), pp. 59-70.

Jackson A.L., Pahl P.M., Harrison K., Rosamond J. & Sclafani R.A. (1993). Cell cycle regulation of the yeast Cdc7 protein kinase by association with the Dbf4 protein. *Molecular and Cellular Biology*, 13(5), pp. 2899-908.

Jiao K., Salem L. & Malone R. (2003). Support for a meiotic recombination initiation complex: interactions among Rec102p, Rec104p, and Spo11p. *Molecular and Cellular Biology*, 23(16), pp. 5928-38.

Joyce E.F., Pedersen M., Tiong S., White-Brown S.K., Paul A., Campbell S.D. & McKim K.S. (2011). Drosophila ATM and ATR have distinct activities in the regulation of meiotic DNA damage and repair. *The Journal of Cell Biology*, 195(3), pp. 359-67.

Kadyk L.C. & Hartwell L.H. (1992). Sister chromatids are preferred over homologs as substrates for recombinational repair in Saccharomyces cerevisiae. *Genetics*, 132(2), pp. 387-402.

Katis V.L., Lipp J.J., Imre R., Bogdanova A., Okaz E., Habermann B., Mechtler K., Nasmyth K. & Zachariae W. (2010). Rec8 phosphorylation by casein kinase 1 and Cdc7-Dbf4 kinase regulates cohesin cleavage by separase during meiosis. *Developmental Cell*, 18(3), pp. 397-409.

Kee K. & Keeney S. (2002). Functional interactions between SPO11 and REC102 during initiation of meiotic recombination in Saccharomyces cerevisiae. *Genetics*, 160(1), pp. 111-22.

Kee K., Protacio R.U., Arora C. & Keeney S. (2004). Spatial organization and dynamics of the association of Rec102 and Rec104 with meiotic chromosomes. *The EMBO Journal*, 23(8), pp. 1815-24.

Keeney S., Giroux C.N. & Kleckner N. (1997). Meiosis-specific DNA double-strand breaks are catalyzed by Spo11, a member of a widely conserved protein family. *Cell*, 88(3), pp. 375-84.

Kim K.P., Weiner B.M., Zhang L., Jordan A., Dekker J. & Kleckner N. (2010). Sister cohesion and structural axis components mediate homolog bias of meiotic recombination. *Cell*, 143(6), pp. 924-37.

Kitada K., Johnson A.L., Johnston L.H. & Sugino A. (1993). A multicopy suppressor gene of the Saccharomyces cerevisiae G1 cell cycle mutant gene dbf4 encodes a protein kinase and is identified as CDC5. *Molecular and Cellular Biology*, 13(7), pp. 4445-57.

Kitada K., Johnston L.H., Sugino T. & Sugino A. (1992). Temperature-sensitive cdc7 mutations of Saccharomyces cerevisiae are suppressed by the DBF4 gene, which is required for the G1/S cell cycle transition. *Genetics*, 131(1), pp. 21-9.

Klapholz S., Waddell C.S. & Esposito R.E. (1985). The role of the SPO11 gene in meiotic recombination in yeast. *Genetics*, 110(2), pp. 187-216.

Krogh B.O. & Symington L.S. (2004). Recombination proteins in yeast. *Annual Review of Genetics*, 38, pp. 233-71.

Lambert S. & Carr A.M. (2013). Replication stress and genome rearrangements: lessons from yeast models. *Current Opinion in Genetics & Development*, 23(2), pp. 132-9.

Lange J., Pan J., Cole F., Thelen M.P., Jasin M. & Keeney S. (2011). ATM controls meiotic double-strand-break formation. *Nature*, 479(7372), pp. 237-40.

Lao J.P. & Hunter N. (2010) Trying to avoid your sister. *PLOS BIOLOGY*, 8(10), p. e1000519.

Lee B.H. & Amon A. (2003). Role of Polo-like kinase CDC5 in programming meiosis I chromosome segregation. *Science*, 300(5618), pp. 482-6.

Lee K.S., Park J.E., Asano S. & Park C.J. (2005). Yeast polo-like kinases: functionally conserved multitask mitotic regulators,. *Oncogene*, 24(2), pp. 217-29.

Leu J.Y. & Roeder G.S. (1999). The pachytene checkpoint in S. cerevisiae depends on Swe1-mediated phosphorylation of the cyclin-dependent kinase Cdc28. *Molecular Cell*, 4(5), pp. 805-14.

Leu J.Y., Chua P.R. & Roeder G.S. (1998). The meiosis-specific Hop2 protein of S. cerevisiae ensures synapsis between homologous chromosomes. *Cell*, 94(3), pp. 375-86.

Lew D.J. & Kornbluth S. (1996). Regulatory roles of cyclin dependent kinase phosphorylation in cell cycle control. *Current Opinion in Cell Biology*, 8(6), pp. 795-804.

Li J., Hooker G.W. & Roeder G.S. (2006). Saccharomyces cerevisiae Mer2, Mei4 and Rec114 form a complex required for meiotic double-strand break formation. *Genetics*, 173(4), pp. 1969-81.

Lo H.C., Kunz R.C., Chen X., Marullo A., Gygi S.P. & Hollingsworth N.M. (2012). Cdc7-Dbf4 is a gene-specific regulator of meiotic transcription in yeast. *Molecular and Cellular Biology*, 32(2), pp. 541-57.

Lo H.C., Wan L., Rosebrock A., Futcher B. & Hollingsworth N.M. (2008). Cdc7-Dbf4 regulates NDT80 transcription as well as reductional segregation during budding yeast meiosis. *Molecular Biology of the Cell*, 19(11), pp. 4956-67.

Lydall D., Nikolsky Y., BIshop D. & Weinert T. (1996). A meiotic recombination checkpoint controlled by mitotic checkpoint genes. *Nature*, 383, pp. 840-3.

Lynn A., Soucek R. & Börner G.V. (2007). ZMM proteins during meiosis: crossover artists at work. *Chromosome research*, 15(5), pp. 591-605.

Mancera E., Bourgon R., Brozzi A., Huber W. & Steinmetz L.M. (2008). High-resolution mapping of meiotic crossovers and non-crossovers in yeast. *Nature*, 454(7203), pp. 479-85.

Marston A.L. (2009). Meiosis: DDK is not just for replication. *Current Biology*, 19(2), pp. R74-6.

Martini E., Diaz R.L., Hunter N. & Keeney S. (2006). Crossover homeostasis in yeast meiosis. *Cell*, 126(2), pp. 285-95.

Masai H. & Arai K. (2000). Dbf4 motifs: conserved motifs in activation subunits for Cdc7 kinases essential for S-phase. *Biochemical and Biophysical Research Communications*, 275(1), pp. 228-32.

Masson J.Y. & West S.C. (2001). The Rad51 and Dmc1 recombinases: a non-identical twin relationship. *Trends in Biochemical Sciences*, 26(2), pp. 131-6.

de Massy B. (2013). Initiation of meiotic recombination: how and where? Conservation and specificities among eukaryotes. *Annual Review of Genetics*, 47, pp. 563-99.

Matos J., Blanco M.G., Maslen S., Skehel J.M. & West S.C. (2011). Regulatory control of the resolution of DNA recombination intermediates during meiosis and mitosis. *Cell*, 147(1), pp. 158-72.

Matos J., Lipp J.J., Bogdanova A., Guillot S., Okaz E., Junqueira M., Shevchenko A. & Zachariae W. (2008). Dbf4-dependent CDC7 kinase links DNA replication to the segregation of homologous chromosomes in meiosis I *Cell*, 135(4), pp. 662-78.

Mazina O.M., Mazin A.V., Nakagawa T., Kolodner R.D. & Kowalczykowski S.C. (2004). Saccharomyces cerevisiae Mer3 helicase stimulates 3'-5' heteroduplex extension by Rad51; implications for crossover control in meiotic recombination. *Cell*, 117(1), pp. 47-56.

Mehta A. & Haber J.E. (2014). Sources of DNA double-strand breaks and models of recombinational DNA repair. *Cold Spring Harbor Perspectives in Biology*, 6(9), p. a016428.

Miller C.T., Gabrielse C., Chen Y.C. & Weinreich M. (2009). Cdc7p-Dbf4p regulates mitotic exit by inhibiting Polo kinase. *PLOS GENETICS*, 5(5), p. e1000498.

Mitra N. & Roeder G.S. (2007). A novel nonnull ZIP1 allele triggers meiotic arrest with synapsed chromosomes in Saccharomyces cerevisiae. *Genetics*, 176(2), pp. 773-87.

Mortensen E.M., Haas W., Gygi M., Gygi S.P. & Kellogg D.R. (2005). Cdc28-dependent regulation of the Cdc5/Polo kinase. *Current Biology*, 15(22), pp. 2033-7.

Moynahan M.E. & Jasin M. (2010). Mitotic homologous recombination maintains genomic stability and suppresses tumorigenesis. *Nature Reviews Molecular Cell Biology*, 11(3), pp. 196-207.

Murakami H. & Keeney S. (2008). Regulating the formation of DNA double-strand breaks in meiosis. *Genes & Development*, 22(3), pp. 286-92.

Murakami H. & Keeney S. (2014). Temporospatial Coordination of Meiotic DNA Replication and Recombination via DDK Recruitment to Replisomes. *Cell*, 158(4), pp. 861-73.

Nakagawa T. & Ogawa H. (1999). The Saccharomyces cerevisiae MER3 gene, encoding a novel helicase-like protein, is required for crossover control in meiosis. *The EMBO Journal*, 18(20), pp. 5714-23.

Neale M.J. & Keeney S. (2006). Clarifying the mechanics of DNA strand exchange in meiotic recombination. *Nature*, 442(7099), pp. 153-8.

Neale M.J., Pan J. & Keeney S. (2005). Endonucleolytic processing of covalent protein-linked DNA double-strand breaks. *Nature*, 436(7053), pp. 1053-7.

Niu H., Wan L., Baumgartner B., Schaefer D., Loidl J. & Hollingsworth N.M. (2005). Partner choice during meiosis is regulated by Hop1-promoted dimerization of Mek1. *Molecular Biology of the Cell*, 16(12), pp. 5804-18.

Niu H., Wan L., Busygina V., Kwon Y., Allen J.A., Li X., Kunz R.C., Kubota K., Wang B., Sung P., Shokat K.M., Gygi S.P. & Hollingsworth N.M. (2009). Regulation of meiotic recombination via Mek1-mediated Rad54 phosphorylation. *Molecular Cell*, 36(3), pp. 393-404.

Ohtoshi A., Miyake T., Arai K. & Masai H. (1997). Analyses of Saccharomyces cerevisiae Cdc7 kinase point mutants: dominant-negative inhibition of DNA replication on overexpression of kinase-negative Cdc7 proteins. *Molecular & General Genetics : MGG*, 254(5), pp. 562-70.

Okaz E., Argüello-Miranda O., Bogdanova A., Vinod P.K., Lipp J.J., Markova Z., Zagoriy I., Novak B. & Zachariae W. (2012). Meiotic prophase requires proteolysis of M phase regulators mediated by the meiosis-specific APC/CAma1. *Cell*, 151(3), pp. 603-18.

Page S.L. & Hawley R.S. (2004). The genetics and molecular biology of the synaptonemal complex. *Annual Review of Cell and Developmental Biology*, 20, pp. 525-58.

Petronczki M., Siomos M.F. & Nasmyth K. (2003). Un ménage à quatre: the molecular biology of chromosome segregation in meiosis. *Cell*, 112(4), pp. 423-40.

Rockmill B. & Roeder G.S. (1991). A meiosis-specific protein kinase homolog required for chromosome synapsis and recombination. *Genes & Development*, 5(12B), pp. 2392-404.

Rockmill B., Sym M., Scherthan H. & Roeder G.S. (1995). Roles for two RecA homologs in promoting meiotic chromosome synapsis. *Genes & Development*, 9(21), pp. 2684-95.

Roeder G.S. (1997). Meiotic chromosomes: it takes two to tango. *Genes & Development*, 11(20), pp. 2600-21.

Roeder G.S. & Bailis J.M. (2000). The pachytene checkpoint. *Trends in Genetics*, 16(9), pp. 395-403.

Ross-Macdonald P. & Roeder G.S. (1994). Mutation of a meiosis-specific MutS homolog decreases crossing over but not mismatch correction. *Cell*, 79(6):1069-80.

Rossi A.M. & Taylor C.W. (2011). Analysis of protein-ligand interactions by fluorescence polarization. *Nature Protocols*, 6(3), pp. 365-87.

San-Segundo P.A. & Roeder G.S. (1999). Pch2 links chromatin silencing to meiotic checkpoint control. *Cell*, 97(3), pp. 313-24.

Sasanuma H., Hirota K., Fukuda T., Kakusho N., Kugou K., Kawasaki Y., Shibata T., Masai H. & Ohta K. (2008). Cdc7-dependent phosphorylation of Mer2 facilitates initiation of yeast meiotic recombination. *Genes & Development*, 22(3), pp. 398-410.

Saunders W.S. (2002). The FEAR factor. *Molecular Cell*, 9(2), pp. 207-9.

Schwacha A. & Kleckner N. (1994). Identification of joint molecules that form frequently between homologs but rarely between sister chromatids during yeast meiosis. *Cell*, 76(1), pp. 51-63.

Schwacha A. & Kleckner N. (1995). Identification of double Holliday junctions as intermediates in meiotic recombination. *Cell*, 83(5), pp. 783-91.

Schwacha A. & Kleckner N. (1997). Interhomolog bias during meiotic recombination: meiotic functions promote a highly differentiated interhomolog-only pathway. *Cell*, 90(6), pp. 1123-35.

Sclafani R.A. (2000). Cdc7p-Dbf4p becomes famous in the cell cycle. *Journal of Cell Science*, 113 (Pt 12), pp. 2111-7.

Sheridan S. & Bishop D.K. (2006). Red-Hed regulation: recombinase Rad51, though capable of playing the leading role, may be relegated to supporting Dmc1 in budding yeast meiosis. *Genes & Development*, 20(13), pp. 1685-91.

Sheu Y.J. & Stillman B. (2006). Cdc7-Dbf4 phosphorylates MCM proteins via a docking site-mediated mechanism to promote S phase progression. *Molecular Cell*, 24(1), pp. 101-13.

Sheu Y.J. & Stillman B. (2010). The Dbf4-Cdc7 kinase promotes S phase by alleviating an inhibitory activity in Mcm4. *Nature*, 463(7277), pp. 113-7.

Shinohara A., Gasior S., Ogawa T., Kleckner N. & Bishop D.K. (1997). Saccharomyces cerevisiae recA homologues RAD51 and DMC1 have both distinct and overlapping roles in meiotic recombination. *Genes to Cells*, 2(10), pp. 615-29.

Shinohara A., Ogawa H. & Ogawa T. (1992). Rad51 protein involved in repair and recombination in S. cerevisiae is a RecA-like protein. *Cell*, 69(3), pp. 457-70.

Shirayama M., Zachariae W., Ciosk R. & Nasmyth K. (1998). The Polo-like kinase Cdc5p and the WD-repeat protein Cdc20p/fizzy are regulators and substrates of the anaphase promoting complex in Saccharomyces cerevisiae. *The EMBO Journal*, 17(5), pp. 1336-49.

Smith A.V. & Roeder G.S. (1997). The yeast Red1 protein localizes to the cores of meiotic chromosomes. *The Journal of Cell Biology*, 136(5), pp. 957-67.

Snead J.L., Sullivan M., Lowery D.M., Cohen M.S., Zhang C., Randle D.H., Taunton J., Yaffe M.B., Morgan D.O. & Shokat K.M. (2007). A coupled chemical-genetic and bioinformatic approach to Polo-like kinase pathway exploration. *Chemistry & Biology*, 14(11), pp. 1261-72.

Sourirajan A. & Lichten M. (2008). Polo-like kinase Cdc5 drives exit from pachytene during budding yeast meiosis. *Genes & Development*, 22(19), pp. 2627-32.

Sun H., Treco D. & Szostak J.W. (1991). Extensive 3'-overhanging, single-stranded DNA associated with the meiosis-specific double-strand breaks at the ARG4 recombination initiation site. *Cell*, 64(6), pp. 1155-61.

Sung P. (1997). Yeast Rad55 and Rad57 proteins form a heterodimer that functions with replication protein A to promote DNA strand exchange by Rad51 recombinase. *Genes & Development*, 11(9), pp. 1111-21.

Sym M. & Roeder G.S. (1995). Zip1-induced changes in synaptonemal complex structure and polycomplex assembly. *The Journal of Cell Biology*, 128(4), pp. 455-66.

Sym M., Engebrecht J.A. & Roeder G.S. (1993). ZIP1 is a synaptonemal complex protein required for meiotic chromosome synapsis. *Cell*, 72(3), pp. 365-78.

Szostak J.W., Orr-Weaver T.L., Rothstein R.J. & Stahl F.W. (1983). The double-strand-break repair model for recombination. *Cell*, 33(1), pp. 25-35.

Toyoizumi H. & Tsubouchi H. (2012). Estimating the number of double-strand breaks formed during meiosis from partial observation. *Journal of Computational Biology*, 19(12), pp. 1277-83.

Tsubouchi H. & Ogawa H. (1998). A novel mre11 mutation impairs processing of double-strand breaks of DNA during both mitosis and meiosis. *Molecular and Cellular Biology*, 18(1), pp. 260-8.

Tsubouchi H. & Ogawa H. (2000). Exo1 roles for repair of DNA double-strand breaks and meiotic crossing over in Saccharomyces cerevisiae. *Molecular Biology of the Cell*, 11(7), pp. 2221-33.

Tsubouchi H. & Roeder G.S. (2002). The Mnd1 protein forms a complex with hop2 to promote homologous chromosome pairing and meiotic double-strand break repair. *Molecular and Cellular Biology*, 22(9), pp. 3078-88.

Tsubouchi H. & Roeder G.S. (2003). The importance of genetic recombination for fidelity of chromosome pairing in meiosis. *Developmental Cell*, 5(6), pp. 915-25.

Tsubouchi H. & Roeder G.S. (2004). The budding yeast mei5 and sae3 proteins act together with dmc1 during meiotic recombination. *Genetics*, 168(3), pp. 1219-30.

Tsubouchi H. & Roeder G.S. (2006). Budding yeast Hed1 down-regulates the mitotic recombination machinery when meiotic recombination is impaired. *Genes & Development*, 20(13), pp. 1766-75.

Tsubouchi T., Zhao H. & Roeder G.S. (2006). The meiosis-specific zip4 protein regulates crossover distribution by promoting synaptonemal complex formation together with zip2. *Developmental Cell*, 10(6), pp. 809-19.

Tsuchiya D., Yang Y. & Lacefield S. (2014). Positive Feedback of NDT80 Expression Ensures Irreversible Meiotic Commitment in Budding Yeast. *PLOS GENETICS*, 10(6), p. e1004398.

Tung K.S., Hong E.J. & Roeder G.S. (2000). The pachytene checkpoint prevents accumulation and phosphorylation of the meiosis-specific transcription factor Ndt80. *Proceedings of the National Academy of Sciences of the United States of America*, 97(22), pp. 12187-92.

Uhlmann F., Lottspeich F. & Nasmyth K. (1999). Sister-chromatid separation at anaphase onset is promoted by cleavage of the cohesin subunit Scc1. *Nature*, 400(6739), pp. 37-42.

Usui T., Ogawa H. & Petrini J.H. (2001). A DNA damage response pathway controlled by Tel1 and the Mre11 complex. *Molecular Cell*, 7(6), pp. 1255-66.

Usui T., Ohta T., Oshiumi H., Tomizawa J., Ogawa H. & Ogawa T. (1998). Complex formation and functional versatility of Mre11 of budding yeast in recombination. *Cell*, 95(5), pp. 705-16.

Valentin G., Schwob E. & Della Seta F. (2006). Dual role of the Cdc7-regulatory protein Dbf4 during yeast meiosis. *The Journal of Biological Chemistry*, 281(5), pp. 2828-34.

Wan L., de los Santos T., Zhang C., Shokat K. & Hollingsworth N.M. (2004). Mek1 kinase activity functions downstream of RED1 in the regulation of meiotic double strand break repair in budding yeast. *Molecular Biology of the Cell*, 15(1), pp. 11-23.

Wan L., Niu H., Futcher B., Zhang C., Shokat K.M., Boulton S.J. & Hollingsworth N.M. (2008). Cdc28-Clb5 (CDK-S) and Cdc7-Dbf4 (DDK) collaborate to initiate meiotic recombination in yeast. *Genes & Development*, 22(3), pp. 386-97.

Wan L., Zhang C., Shokat K.M. & Hollingsworth N.M. (2006). Chemical inactivation of cdc7 kinase in budding yeast results in a reversible arrest that allows efficient cell synchronization prior to meiotic recombination. *Genetics*, 174(4), pp. 1767-74.

Wang Y., Chang C.Y., Wu J.F. & Tung K.S. (2011). Nuclear localization of the meiosis-specific transcription factor Ndt80 is regulated by the pachytene checkpoint. *Molecular Biology of the Cell*, 22(11), pp. 1878-86.

Weinreich M. & Stillman B. (1999). Cdc7p-Dbf4p kinase binds to chromatin during S phase and is regulated by both the APC and the RAD53 checkpoint pathway. *The EMBO Journal*, 18(19), pp. 5334-46.

Woltering D., Baumgartner B., Bagchi S., Larkin B., Loidl J., de los Santos T. & Hollingsworth N.M. (2000). Meiotic segregation, synapsis, and recombination checkpoint functions require physical interaction between the chromosomal proteins Red1p and Hop1p. *Molecular and Cellular Biology*, 20(18), pp. 6646-58.

Wu H.Y. & Burgess S.M. (2006). Two distinct surveillance mechanisms monitor meiotic chromosome metabolism in budding yeast. *Current Biology*, 16(24), pp. 2473-9.

Wu H.Y., Ho H.C. & Burgess S.M. (2010). Mek1 kinase governs outcomes of meiotic recombination and the checkpoint response. *Current Biology*, 20(19), pp. 1707-16.

Xu L., Ajimura M., Padmore R., Klein C. & Kleckner N. (1995). NDT80, a meiosis-specific gene required for exit from pachytene in Saccharomyces cerevisiae. *Molecular and Cellular Biology*, 15(12), pp. 6572-81.

Xu L., Weiner B.M. & Kleckner N. (1997). Meiotic cells monitor the status of the interhomolog recombination complex. *Genes & Development*, 11(1), pp. 106-18.

Youds J.L. & Boulton S.J. (2011). The choice in meiosis - defining the factors that influence crossover or non-crossover formation. *Journal of Cell Science*, 124(Pt 4), pp. 501-13.

Appendix 1

Strain	Genotype[1,2]	Background
TBR310	*hop2::ADE2*	BR1919
TBR2065	wild type	BR1919
TBR2434	*zip1-4LA*	BR1919
TBR2780	*zip2::kanMX4 zip3::hphMX4*	BR1919
TBR3451	*a* wild type	SK1
TBR4711	*hop2::ADE2 rad17::LEU2*	BR1919
TBR5188	*sae2::kanMX4 tel1::natMX4*	SK1
TBR5514	*sae2::kanMX4*	SK1
TBR5515	*sae2::kanMX4 pch2::hphMX4*	SK1
TBR5696	*a rad17::natMX4*	SK1
TBR5697	α *rad17::natMX4*	SK1
TBR6396	*rad51::hisGURA3hisG dmc1::natMX4 ndt80::LEU2 spo11-HA-kanMX4*	SK1
TBR6448	*hop2::ADE2 dbf4-E86K*	BR1919
TBR6449	*hop2::ADE2 dbf4-R83E*	BR1919
TBR6450	*hop2::ADE2 dbf4-E86V*	BR1919
TBR6451	*zip1-4LA dbf4-E86K*	BR1919
TBR6505	*zip1-4LA dbf4-R83E*	BR1919
TBR6506	*zip1-4LA dbf4-E86V*	BR1919
TBR6507	*zip2::LEU2 zip3::URA3 dbf4-E86K*	BR1919
TBR6508	*zip2::LEU2 zip3::URA3 dbf4-R83E*	BR1919
TBR6557	*zip2::LEU2 zip3::URA3 dbf4-E86V*	BR1919
TBR6618	*sae2::kanMX4 ndt80::LEU2*	SK1
TBR6619	*sae2::kanMX4 ndt80::LEU2 pch2::hphMX4*	SK1
TBR6620	*sae2::kanMX4 ndt80::LEU2 tel1::natMX4*	SK1
TBR6621	wild type	SK1
TBR6730	*a kanMX4-*P_{CLB2}*-HA-RAD17*	SK1
TBR6742	*rad51::hisGURA3hisG dmc1::natMX4 kanMX4-*P_{CLB2}*-HA-RAD17*	SK1
TBR6749	*kanMX4-*P_{CLB2}*-HA-RAD17*	SK1
TBR6862	*rad51::hisGURA3hisG dmc1::natMX4 ndt80::LEU2 kanMX4-*P_{CLB2}*-HA-RAD17 pch2::hphMX4*	SK1
TBR6864	*rad51::hisGURA3hisG dmc1::natMX4 kanMX4-*P_{CLB2}*-HA-RAD17 pch2::hphMX4*	SK1
TBR6884	*rad51::hisGURA3hisG dmc1::natMX4 ndt80::LEU2 kanMX4-*P_{CLB2}*-HA-RAD17*	SK1
TBR6887	*dmc1::natMX4*	SK1
TBR6888	*rad51::hisGURA3hisG dmc1::natMX4 ndt80::LEU2 kanMX4-*P_{CLB2}*-HA-RAD17 spo11-HA-kanMX4*	SK1
TBR6904	*rad51::hisGURA3hisG dmc1::natMX4 kanMX4-*P_{CLB2}*-HA-RAD17 spo11-HA-kanMX4*	SK1
TBR6906	*rad51::hisGURA3hisG dmc1::natMX4 ndt80::LEU2 pch2::hphMX4*	SK1
TBR6908	*rad51::hisGURA3hisG dmc1::natMX4*	SK1

	pch2::hphMX4	
TBR6918	*rad51::hisGURA3hisG dmc1::natMX4 ndt80::LEU2*	SK1
TBR6920	*rad51::hisGURA3hisG dmc1::natMX4*	SK1
TBR6939	*rad51::hisGURA3hisG dmc1::natMX4 spo11-HA-kanMX4*	SK1
TBR7464	*dbf4-E86V*	SK1
TBR7483	*dmc1::natMX4 dbf4-E86V*	SK1
TBR7552	*dmc1::natMX4 dbf4-E86K*	SK1
TBR7553	*dmc1::natMX4 dbf4-R83E*	SK1
TBR8372	*dmc1::natMX4 P_{DBF4}-CDC5-DBF4-URA3 dbf4-R83E*	SK1
TBR8450	*dmc1::natMX4 P_{DBF4}-CDC5-URA3 dbf4-R83E*	SK1
TBR8454	*dmc1::natMX4 P_{DBF4}-CDC5-URA3*	SK1
TBR8672	*dmc1::natMX4 dbf4-E86V dbf4-E86V-URA3*	SK1
TBR8673	*ndt80::LEU2 ER-GAL-URA3/ura3-1*	BR1919
TBR8674	*ndt80::LEU2 ER-GAL-URA3/P_{GAL}-CDC5-URA3*	BR1919
TBR8764	*ndt80::LEU2 ER-GAL-URA3/P_{GAL}-CDC5-URA3 dbf4-E86K*	BR1919
TBR8765	*ndt80::LEU2 ER-GAL-URA3/P_{GAL}-CDC5-URA3 dbf4-R83E*	BR1919
TBR9107	*ndt80::LEU2 ER-GAL-URA3/P_{GAL}-CDC5-URA3 dbf4-E86V*	BR1919
TBR9121	*dmc1::natMX4 P_{DBF4}-CDC5-dbf4-R83E-URA3 dbf4-R83E*	SK1
TBR9175	*dmc1::natMX4 rad51::hisGURA3hisG dbf4-E86V*	SK1
TBR9176	*dmc1::natMX4 P_{DBF4}-CDC5-dbf4-R83E-URA3*	SK1
TBR9237	*dmc1::natMX4 rad51::kanMX4 dbf4-E86V dbf4-E86V-URA3*	SK1
TBR9367	*NDT80-6HA*	BR1919
TBR9488	*dbf4-R83E*	SK1
TBR9533	*NDT80-6HA dbf4-R83E*	BR1919
TBR9693	*ndt80::LEU2 ER-GAL-URA3/ P_{GAL}-CDC5-URA3*	SK1
TBR9695	*ndt80::LEU2 ER-GAL-URA3/ura3*	SK1
TBR9697	*ndt80::LEU2 ER-GAL-URA3/ P_{GAL}-CDC5-URA3 dbf4-E86K*	SK1
TBR9699	*ndt80::LEU2 ER-GAL-URA3/ P_{GAL}-CDC5-URA3 dbf4-R83E*	SK1
TBR9701	*ndt80::LEU2 ER-GAL-URA3/ P_{GAL}-CDC5-URA3 dbf4-E86V*	SK1
TBR9747	*NDT80-6HA DBF4/dbf4::kanMX4 CDC5/cdc5::natMX4*	BR1919
TBR9749	*NDT80-6HA dbf4-R83E/dbf4::kanMX4 CDC5/cdc5::natMX4*	BR1919
TBR10060	*ndt80::LEU2 dmc1::natMX4 ER-GAL-URA3/ura3*	SK1
TBR10062	*ndt80::LEU2 dmc1::natMX4 ER-GAL-URA3/P_{GAL}-CDC5-URA3*	SK1
TBR10076	*ndt80::LEU2 dmc1::natMX4 ER-GAL-URA3/P_{GAL}-CDC5-URA3 dbf4-E86V*	SK1

TBR10078	*ndt80::LEU2 dmc1::natMX4 ER-GAL-URA3/P_{GAL}-CDC5-URA3 dbf4-R83E*	SK1
TBR10080	*ndt80::LEU2 dmc1::natMX4 ER-GAL-URA3/P_{GAL}-CDC5-URA3 dbf4-E86K*	SK1
TBR10101	*α tor1-1::HIS3 fpr1::hphMX4 RPL13A-2xFKBP12::TRP1 dmc1::natMX4 CDC7-FRB*	SK1
TBR10105	*α tor1-1::HIS3 fpr1::hphMX4 RPL13A-2xFKBP12::TRP1 dmc1::natMX4 DBF4-FRB*	SK1
TBR10119	*α tor1-1::HIS3 fpr1::hphMX4 RPL13A-2xFKBP12::TRP1 dmc1::natMX4*	SK1
TBR10129	*ndt80::LEU2 tor1-1::HIS3 fpr1::hphMX4 RPL13A-2xFKBP12::TRP1 ER-GAL-URA3/P_{GAL}-CDC5-URA3 DBF4-FRB-kanMX4*	SK1
TBR10131	*ndt80::LEU2 tor1-1::HIS3 fpr1::hphMX4 RPL13A-2xFKBP12::TRP1 ER-GAL-URA3/P_{GAL}-CDC5-URA3 CDC7-FRB-kanMX4*	SK1
TBR10190	*ndt80::LEU2 dmc1::natMX4 ER-GAL-URA3/P_{GAL}-cdc5-N209A-URA3*	SK1
TBR10192	*ndt80::LEU2 dmc1::natMX4 ER-GAL-URA3/P_{GAL}-cdc5-N209A-URA3 dbf4-E86K*	SK1
TBR10541	*ndt80::LEU2 rad51::hisGURA3hisG dmc1::natMX4 ER-GAL-URA3/P_{GAL}-CDC5-URA3 red1::hphMX4*	SK1
TBR10575	*ndt80::LEU2 rad51::hisGURA3hisG dmc1::natMX4 ER-GAL-URA3/P_{GAL}-CDC5-URA3*	SK1
TBR10576	*ndt80::LEU2 rad51::hisGURA3hisG dmc1::natMX4 ER-GAL-URA3/P_{GAL}-CDC5-URA3 dbf4-R83E*	SK1
TBR10670	*ndt80::LEU2 rad51::kanMX4/rad51::hisGURA3hisG dmc1::natMX4 ER-GAL-URA3/P_{GAL}-CDC5-URA3 dbf4-R83E red1::hphMX4*	SK1
TBR10718	*ndt80::LEU2 tor1-1::HIS3 fpr1::hphMX4 RPL13A-2xFKBP12::TRP1 ER-GAL-URA3/P_{GAL}-CDC5-URA3*	SK1
TBR10798	*ndt80::LEU2 ER-GAL-URA3/ P_{GAL}-CDC5-URA3 P_{CLB2}-dbf4*	SK1
TBR10800	*ER-GAL-URA3/ P_{GAL}-CDC5-URA3 P_{CLB2}-dbf4*	
TBR10816	*ER-GAL-URA3/ P_{GAL}-CDC5-URA3*	SK1
TBR10840	*ndt80::LEU2 ER-GAL-URA3/ P_{GAL}-CDC5-URA3 P_{CLB2}-dbf4 MCM5-bob1*	SK1
TBR10842	*ER-GAL-URA3/ P_{GAL}-CDC5-URA3 P_{CLB2}-dbf4 MCM5-bob1*	SK1
TBR10843	*ndt80::LEU2 ER-GAL-URA3-DBF4-TRP1/ P_{GAL}-CDC5-URA3-DBF4-TRP1 P_{CLB2}-dbf4*	SK1
TBR10967	*ndt80::LEU2 ER-GAL-URA3-dbf4-10A-TRP1/ P_{GAL}-CDC5-URA3-dbf4-10A-TRP1 P_{CLB2}-dbf4*	SK1
TBR10968	*ndt80::LEU2 ER-GAL-URA3-dbf4-4A-TRP1/*	SK1

	P_{GAL}-CDC5-URA3-dbf4-4A-TRP1 P_{CLB2}-dbf4	

All listed strains are isogenic diploids, unless indicated otherwise by the presence of *a* or α, derived from either BR1919 or SK1. All loci are homozygous unless indicated otherwise by a forward slash symbol (/), in which case heterozygosity is described.

[1]BR1919 strains are in the following genetic background:
ho leu2-3, 112 his4-260 ura3-1 ade2-1 thr1-4 trp1-289 lys2

[2]SK1 strains are in the following genetic background:
ho::LYS2 lys2 ura3 leu2::hisG his3::hisG trp1::hisG

CLB2 is not expressed in meiotic cells. P_{CLB2} denotes that a gene was placed under the control of the *CLB2* promoter. This is the equivalent of a meiotic null mutant (i.e., *mn*), as confirmed by immunoblotting.